Synthesis, *In Silico* and *In Vitro* Studies of Cuminaldehyde–Thiazolidinedione Hybrids as α-Glucosidase Inhibitors

The thesis submitted in partial fulfillment of the requirement of the

Degree of Master of Pharmacy

Faculty of Engineering and Technology

by

SAI SATYAPRAKASH MISHRA

Class Roll No.: 002211402005

Examination Roll No.: M4PHB24001

Reg. No.: 163649 of 2022-23

Under the Guidance of

Prof. (Dr.) Tapan Kumar Maity

Synthetic and Natural Products Research Laboratory

Department of Pharmaceutical Technology

Faculty Council of Engineering and Technology

Department of Pharmaceutical Technology

Jadavpur University

Kolkata – 700032

2024

Certificate of Approval

This is to certify that **Sai Satyaprakash Mishra** (Examination Roll No: **M4PHB24001** Registration No: **163649 of 2022-23**) has carried out the project work on the subject entitled " ***Synthesis, In Silico and In Vitro Studies of Cuminaldehyde–Thiazolidinedione Hybrids as α-Glucosidase Inhibitors***" under the supervision of **Prof. (Dr.) Tapan Kumar Maity**, Professor, Department of Pharmaceutical Technology, Jadavpur University. This project work is submitted by him in partial fulfillment of the requirements for the degree of **Master of Pharmacy (Pharmaceutical Chemistry)** of Jadavpur University. He has carried out his work independently and with proper care and attention to our entire satisfaction.

Supervised by:

T Maity 28/08/24

Prof. (Dr.) Tapan Kumar Maity
Synthetic and Natural Product Research Laboratory,
Department of Pharmaceutical Technology,
Jadavpur University,
Kolkata-700032

Dr. Tapan Kr. Maity
M. Pharm., Ph.D.
Professor
Dept. of Pharmaceutical Technology
Jadavpur University, Kolkata - 700 032

28/8/24.

Prof. (Dr.) Amalesh Samanta
Head of the Department,
Department of Pharmaceutical Technology,
Jadavpur University,
Kolkata-700032

Dept. of Pharmaceutical Technology
Jadavpur University
Kolkata - 700 032, W.B. India

Dipak Laha 29.8.24

Prof. Dipak Laha
Dean
Faculty of Engineering and Technology,
Jadavpur University,
Kolkata-700032

DEAN
Faculty of Engineering & Technology
JADAVPUR UNIVERSITY
KOLKATA-700 032

Declaration of the Originality and Compliance of Academic Ethics

I hereby declare that this thesis contains a literature survey and original research part of my work on " **Synthesis, *In Silico* and *In Vitro* Studies of Cuminaldehyde–Thiazolidinedione Hybrids as α-Glucosidase Inhibitors".**

All the information in this document has been obtained and presented in accordance with academic rules and ethical conduct.

I also declare that as required by these rules and conduct, I have fully cited and referred all the information and results that are not original to this work.

Name:	Sai Satyaprakash Mishra
Class Roll No.	002211402005
Examination Roll No.	M4PHB24001
Registration No.	163649 of 2022-23
Thesis Title:	" Synthesis, *In Silico* and *In Vitro* Studies of Cuminaldehyde–Thiazolidinedione Hybrids as α-Glucosidase Inhibitors "
Signature:	Sai Satyaprakash Mishra

PREFACE

Research is carried out to design and develop newer drugs in academic institutions and the pharmaceutical industry. The new drug design involves in modifying the existing bioactive drugs to change their therapeutic effects along with developing new bioactive chemical molecules.

Cuminaldehyde (CUM) is a bioactive compound majorly present in the seeds of *Cuminum cyminum*. The plant *C. cyminum* is the hub of numerous bioactive compounds that have various pharmacological significance, and Cuminaldehyde is one of them. There are several bioactive secondary metabolites discovered in *C. cyminum* seeds, which have been shown to have antibacterial, anti-inflammatory, antioxidant, anti-cancer, and anti-diabetic effects. The composition of essential oil components has been studied using GC-MS, and the analytical result indicates that cuminaldehyde is a prominent chemical in essential oil components. As a result, scientists believe cuminaldehyde has potential benefits as an antioxidant, antibacterial, and anti-diabetic agent.

The heterocyclic compounds display various biological activity. Among the heterocyclic Thiazolidine-2,4-diones, a significant class of heterocyclic compounds, have garnered considerable interest due to their potent biological actions, including antidiabetic, anticancer, antioxidative, and anti-inflammatory effects. Thiazolidine-2,4-dione presents potential α-glucosidase inhibitory activity but also can bind with the residues of the -glucosidase active pockets.

The present work entitled **" Synthesis, *In Silico* and *In Vitro* Studies of Cuminaldehyde-Thiazolidinedione Hybrids as α-Glucosidase Inhibitors"** was undertaken with an aim to synthesize a suitable lead compound with α-glucosidase inhibitory activity, which can be exploited to develop novel antidiabetic agents.

Acknowledgement

First and foremost, I feel immense pleasure in expressing my sincere and deep sense of gratitude to my supervising guide, ***Prof. (Dr.) Tapan Kumar Maity, Professor, Department of Pharmaceutical Technology, Jadavpur University,*** *for giving me such a progressive & unconventional topic for my thesis work and, of course for the patience and support in overcoming numerous obstacles I have faced through my research. This work would have been impossible without his exemplary guidance, sustained interest, creative suggestions & motivation.*

I want to express my sincere gratitude to ***Prof. (Dr.) Amalesh Samanta, Head of the Department,*** *for rendering me valuable help and necessary facilities to carry out this work.*

I offer humble gratitude to ***Prof. (Dr.) Sanmoy Karmakar, Department of Pharmaceutical Technology, Jadavpur University,*** *for the affection and kindness rendered to me throughout my work.*

*I would also like to express my thanks to all of my respected teachers, laboratory seniors (****Mr. Abhik Paul, Mrs. Ajeya Samanta,*** *and* ***Mr. Avik Maji)*** *& juniors (****Mr. Sourav Mondal*** *and* ***Mr. Rajesh Khan****) for their help and support in each step of work.*

I would also like to thank ***Mr. Arnab Sarkar, Mr. Rudranil Bhowmik, Mr. Akash De, Mr. Totan Das,*** *and* ***Mr. Rajarshi Ray*** *for helping me perform my research work.*

I would like to express my deepest gratitude to my parents, ***Mr. Shashikanta Mishra*** *&* ***Mrs. Sarita Mishra*** *whose steadfast support and encouragement have been the foundation of my educational voyage. This thesis is a testament to your love and dedication. I am forever grateful for everything you have done for me.*

Special thanks to my friends ***Ms. Saismita Mishra, Ms. Tejaswini Mishra, Ms. Rinki Prasad Bhagat, Mr. Abhisek Samal,*** *and* ***Mr. Shubham Kumar Pandey*** *for their constant support throughout the M. Pharm journey.*

I also thank my friends and all the others who have extended their cooperation and helped me immensely during the entire project work.

Sai Satyaprakash Mishra

Sai Satyaprakash Mishra
Class Roll No.: 002211402005
Examination Roll No.: M4PHB24001

Dedicated to
my guide, family and well wishers

INDEX

List of Figures

List of Tables

List of Schemes

CHAPTER: 1

INTRODUCTION

1. Introduction:

Heterocyclic compounds that include nitrogen and sulfur, particularly those in the thiazole family, have drawn significant attention in synthetic chemistry due to their pharmacological activities and potency as agrochemicals and pharmaceuticals [1]. For the purpose of creating novel drugs to treat a variety of pathological conditions, such as melanoma, type-II diabetes and its complications, cancer, arthritis, and inflammation-related illnesses; the heterocyclic nucleus thiazolidine-2,4-dione (TZD) has been the subject of extensive research. Aside from pharmaceuticals, TZD is used as a brightener in the electroplating industry, a highly sensitive reagent for heavy metals, and for preventing the corrosion of mild steels [2,3]. The well-studied anti-hyperglycemic effect of TZD derivatives is one of them; this effect has also prompted the creation of therapeutically used "glitazone" drugs, including rosiglitazone, pioglitazone, lobeglitazone, troglitazone, etc. (**Figure 1**) [4].

Diabetes is a metabolic disease that can be deadly and is typified by ongoing hyperglycemia. Type 2 diabetes mellitus (T2DM) is brought on by insulin's inability to reach its target tissues, whereas Type 1 diabetes mellitus (T1DM) is brought on by a partial or complete lack of insulin secretion. Diabetes increases the risk of serious, life-threatening consequences, which degrade quality of life, increase medical costs, and shorten life expectancy. Some diabetics are not diagnosed until they experience consequences including kidney failure, foot ulcers, or visual abnormalities [5]. As of right now, 537 million people worldwide suffer from diabetes, by 2045, that number is expected to rise to 783 million, based on the statistics released by the International Diabetes Federation (IDF). About 90% of all cases of diabetes are currently caused by type 2 diabetes (T2DM), whose incidence has increased dramatically over the past three decades. Effective anti-diabetic medications that don't have harmful side effects are therefore necessary [6].

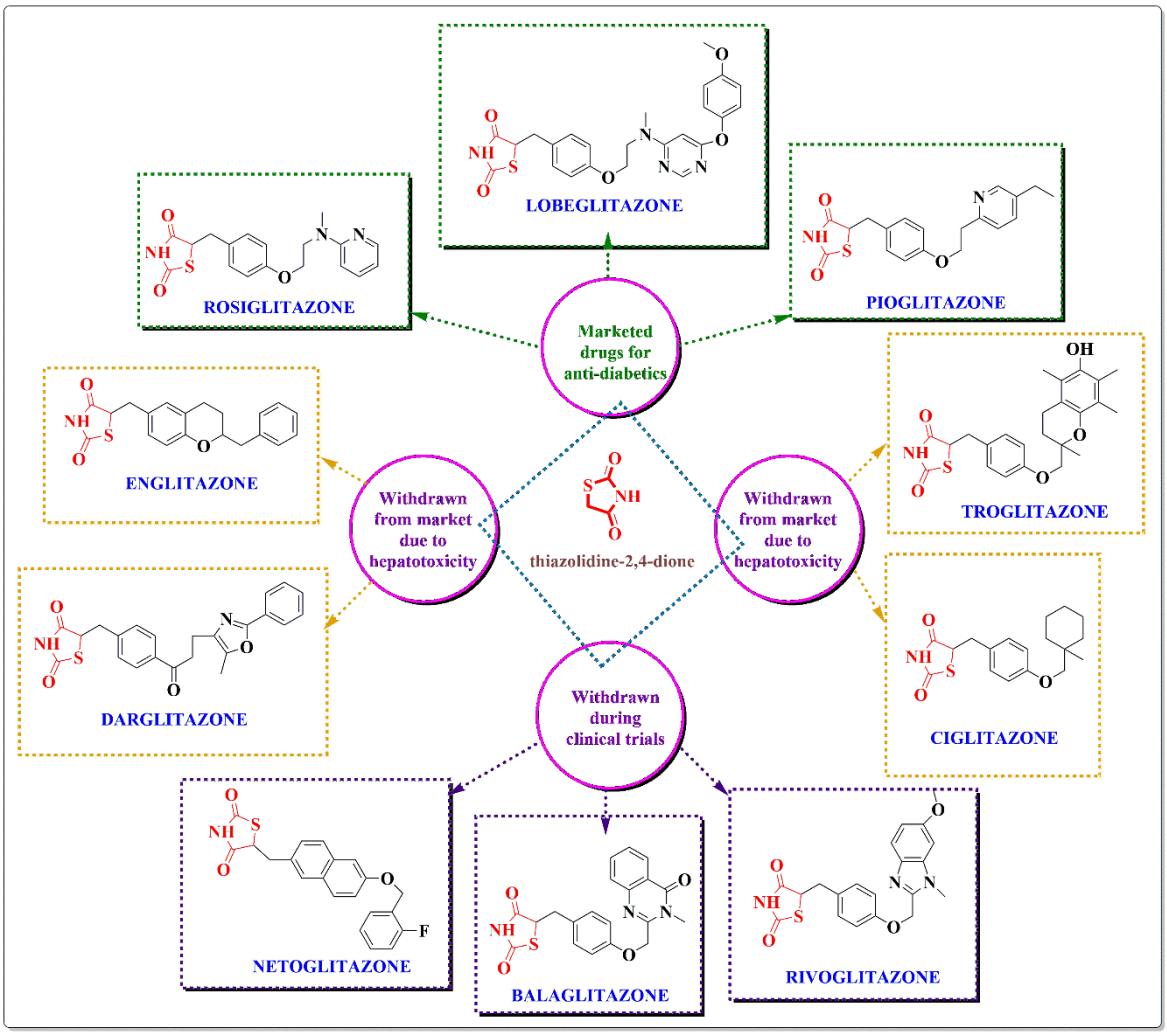

Figure 1: Examples of antidiabetic medications containing TZD moiety.

Metformin is the primary line therapy for high blood sugar; however, it should not be used if lactic acidosis is present. Alpha-glucosidase inhibitors, DPP4 inhibitors, thiazolidinediones, and meglitinides are further classes of antihyperglycemic drugs that are frequently prescribed. These drugs can be taken either on their own or in addition to metformin. Recently, a number of new and unique pharmaceutical targets have been discovered for the treatment of type 2 diabetes (T2D). These targets include glycogen synthase kinase 3, fructose-1, 6-bisphosphatase, glucagonlike peptide-1, glucokinase, G protein-coupled receptor 119, PTP1B, SGLT2, and many others [7].

In the current study, I developed derivatives of cuminaldehyde–thiazolidinedione hybrids and assessed them *in vitro* for their ability to inhibit the α-glucosidase enzyme. In addition, I carried out *in silico* studies of synthesized compounds (molecular docking and ADMET) for its identification of protein-inhibitor interactions, safety profile, and drug-likeness characteristics.

1.1. Brief history of thiazolidine-2,4-dione (TZD) scaffold:

In 1954, an Italian scientist named "Vistentini" presented the first pharmacological assessment, or anti-TB activity, of any TZD derivative. This discovery brought attention to the pentacyclic moiety known as thiazolidine-2,4-dione. Several TZD derivatives' anti-convulsant effects were documented by Marshall and Vallance that same year. Further studies of the pharmacological and toxicological effects of TZD compounds were conducted in the 1960s and 1970s by additional research groups [2]. Ciglitazone was the first anti-diabetic medication to be commercialized; however, it was later removed due to hepatotoxicity. Following that, in 1988, the Shankyo Company created troglitazone, a medication that also induced hepatotoxicity and had a TZD scaffold. Two pharmaceutical companies, Pfizer and Takeda, created pioglitazone and englitazone, respectively, in 1999. These compounds were comparable to one another. Pioglitazone established itself in the market since it showed no signs of liver damage. However, the same unfavorable events led to the withdrawal of englitazone from the market. Fortunately, Pfizer and SmithKline created two additional medications in that same year that belong to the same class: rosiglitazone and darglitazone. While rosiglitazone was promptly taken off the market in 1999, darglitazone was not. In 2001, the Food and Drug Administration (FDA) reported certain cases of heart failure and fluid retention, which led to restrictions. in 2010. However, the FDA eventually removed the limits as a result of a lack of evidence (**Figure 2**) [8].

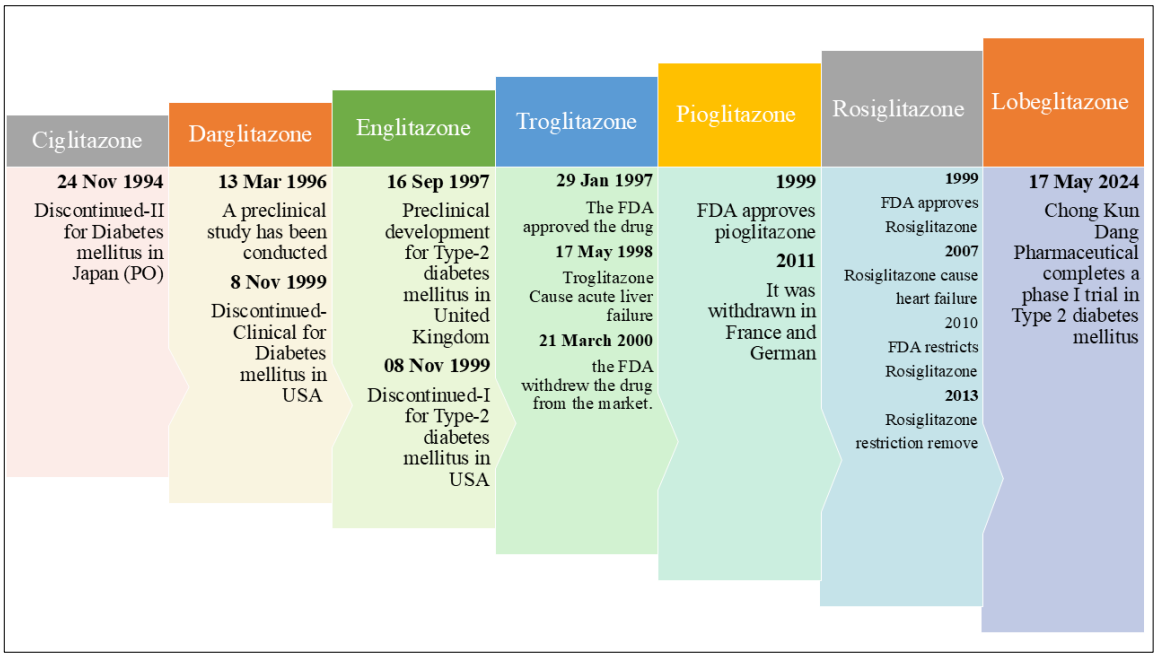

Figure 2: The historical background of Thiazolidinediones (TZDs).

1.2. Chemistry and reactivity of thiazolidine-2,4-dione (TZD):

1.2.1. Chemistry of TZDs:

Thiazolidine-2,4-dione is a five-member heterocyclic ring bearing one sulfur, nitrogen, methylene, and carbonyl groups. The molecular formula of thiazolidine-2,4-dione is $C_3H_3NO_2S$. The pharmacological properties of thiazolidine-2,4-dione make it an appealing scaffold that has attracted a lot of interest and been the subject of substantial investigation. The thiazolidine-2,4-dione nucleus can be synthesized from thiosemicarbazone, thiourea, or thiocarbamate as starting chemicals. Nonetheless, the most popular method of synthesizing thiazolidinedione is to reflux thiourea and α-chloroacetic acid for 12 hours. An additional benefit of this approach is its ability to expedite the rate of reaction through the adoption of a microwave-assisted technique (**Figure 3**) [9].

The nucleus of thiazolidinedione was found to have a pKa value of 6.82 and a melting point range of 120–122 °C. The thiazolidine-2,4-dione core has one α hydrogen and two

carbonyl groups [3]. Thiazolidine-2,4-dione experiences distinct tautomerism as a result, which includes amide-imidol and keto-enol (**Figure 4**).

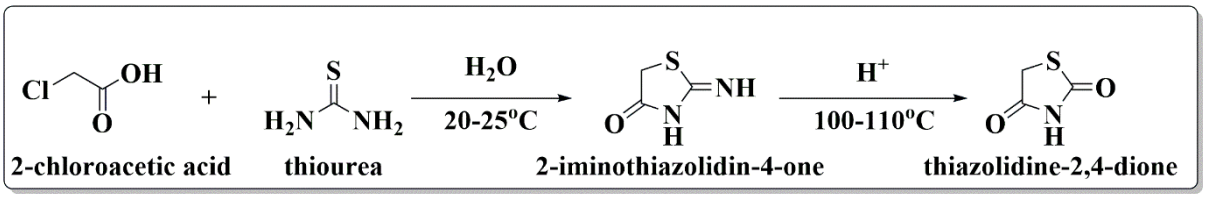

Figure 3: Synthesis of thiazolidine-2,4-dione (TZD) using thiourea and α-chloroacetic acids.

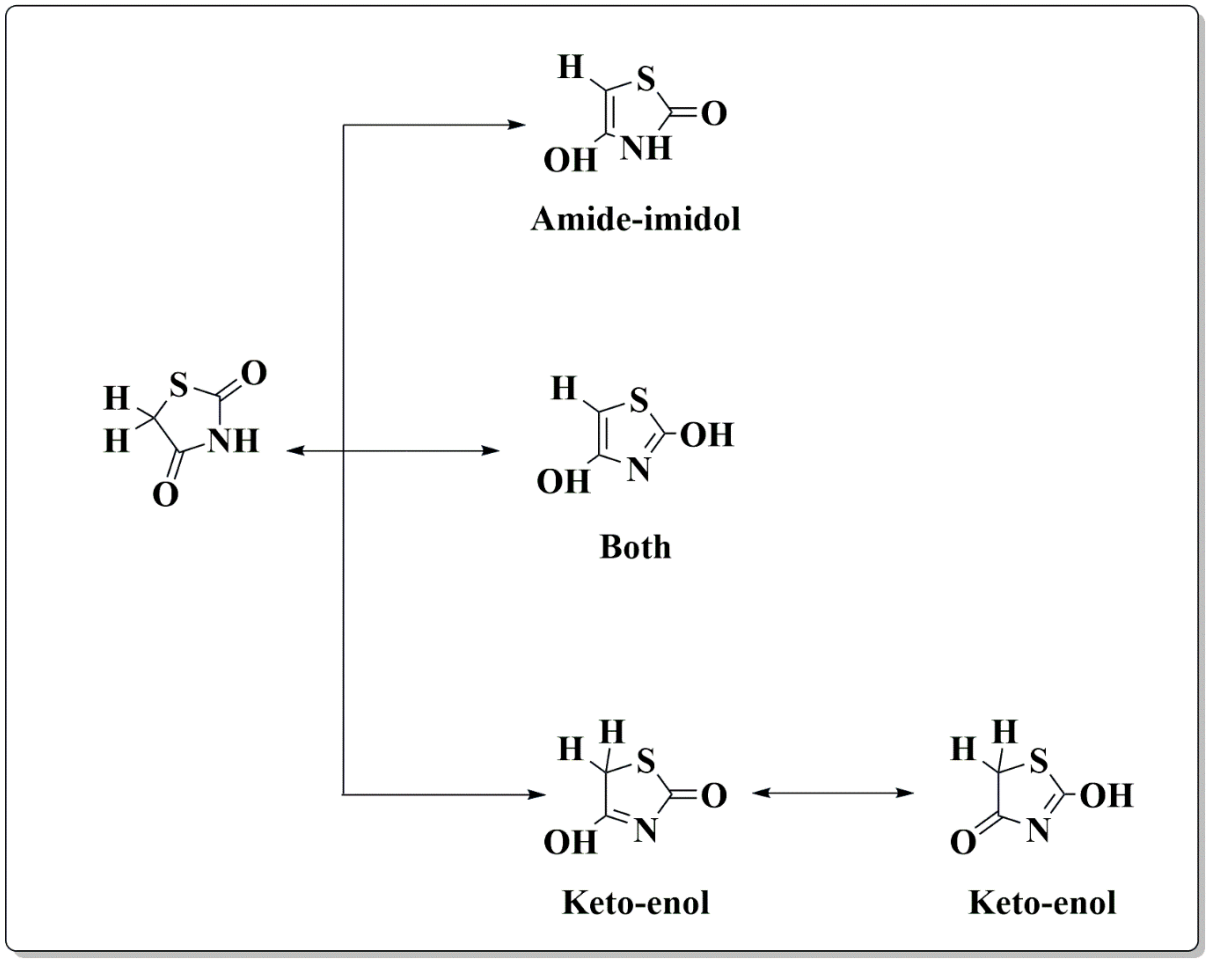

Figure 4: Tautomeric structure of TZD.

1.2.2. Reactivity of TZDs:

The substantial number of recorded substitutions on the central TZD structure can result in alterations in chemical properties, the formation of novel compounds, and the

possible development of bioactive candidates. Modifications at the nitrogen site N-3, the C-2 carbonyl, and the methylene group have been detected. The carbonyl group positioned at C-4 is regarded as extremely unreactive [10]. In conclusion, the thiazolidinedione core has two potential sites for substitution.

1.2.2.1. Reactivity at the -NH group of TZD core:

Substitution at NH- group can be done by aryl or alkyl halides, in the presence of a base and a solvent. Extensive studies have been conducted to explore the N-alkylation of TZD frameworks, resulting in the screening of several bases. Currently, it is widely acknowledged that various appropriate bases, such as potassium carbonate, tetrabutylammonium iodide, NEt_3, or even sodium hydride, are considered acceptable. Additionally, it has been established that appropriate solvents for this purpose are acetone and DMF [10].

1.2.2.2. Reactivity at the -CH_2 moiety of TZD core:

The methylene moiety can be substituted by aromatic aldehydes or ketones and the formation of arylidene derivative of thiazolidinedione. The process described is commonly referred to as the 'Knoevenagel condensation'. This specific condensation reaction can be conducted under many conditions. The reagents most frequently employed are piperidine (as a base) and either ethanol or methanol as solvents. Similarly, the use of anhydrous sodium acetate in glacial acetic acid presented an alternative method for the condensation of TZD with aldehyde. For the condensation reaction involving a ketone, either ammonium acetate or piperidinium acetate was employed in toluene or ethyl acetate as the solvent (**Figure 5**) [2].

The most significant structural and physical changes in thiazolidine-2,4-dione are caused by replacement at position 2, while dynamic variations occur at positions 3 and 5. Rhodanine derivatives are formed when sulfur replaces oxygen at position 2, while

oxazolidinedione derivatives are formed when oxygen removes sulfur at position 1(**Figure 6**) [11].

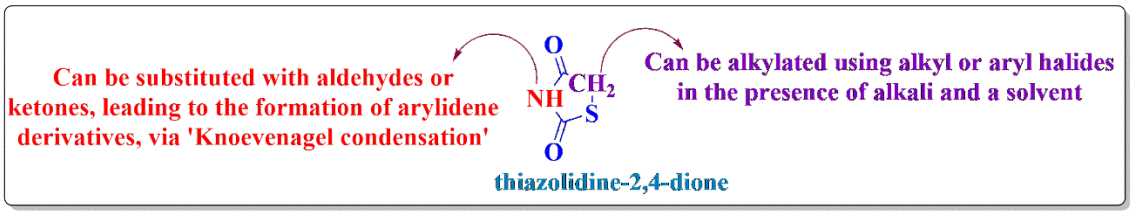

Figure 5: Reactivity of TZD at -CH_2 and -NH.

Figure 6: Dynamic alterations of TZD.

1.3. Therapeutic targets in the management of type 2 diabetes mellitus:

1.3.1. Role of alpha-glucosidase as a target in diabetes:

α-glucosidase (EC 3.2.1.20) is an enzyme that is part of the glycoside hydrolase family. It is found chiefly at the intestinal brush border and breaks down polysaccharides into monosaccharides. The process of breakdown of disaccharide and polysaccharide into easily absorbed monosaccharide units is carried out by α-Glucosidase, which regulates the amount of glucose available after meals and the severity of postprandial hyperglycemia. It works by cleaving the α-glucopyranoside linkage (**Figure 7**) [12]. Alpha-glucosidase inhibitors have a structure similar to saccharides and have the ability to attach to α-active glucosidase's site, generating complexes with a higher affinity than

the complex formed by carbohydrates and α-glucosidase. This causes a competitive inhibition of the enzyme, which in turn reduces the rate at which carbohydrates are hydrolyzed and delays the absorption of glucose. Studies also show that α-glucosidase stimulates L cells in the intestine, which suppresses glucagon secretion while enhancing insulin secretion [13]. However, α-glucosidase inhibitors have an insulin-independent hypoglycemic effect. As a result, they are used as monotherapy in moderate cases of diabetes and are regarded as first-line oral sugar-reducing medications. In contrast, they are used in combination therapy with insulin or other drugs in cases of acute diabetic complications [14].

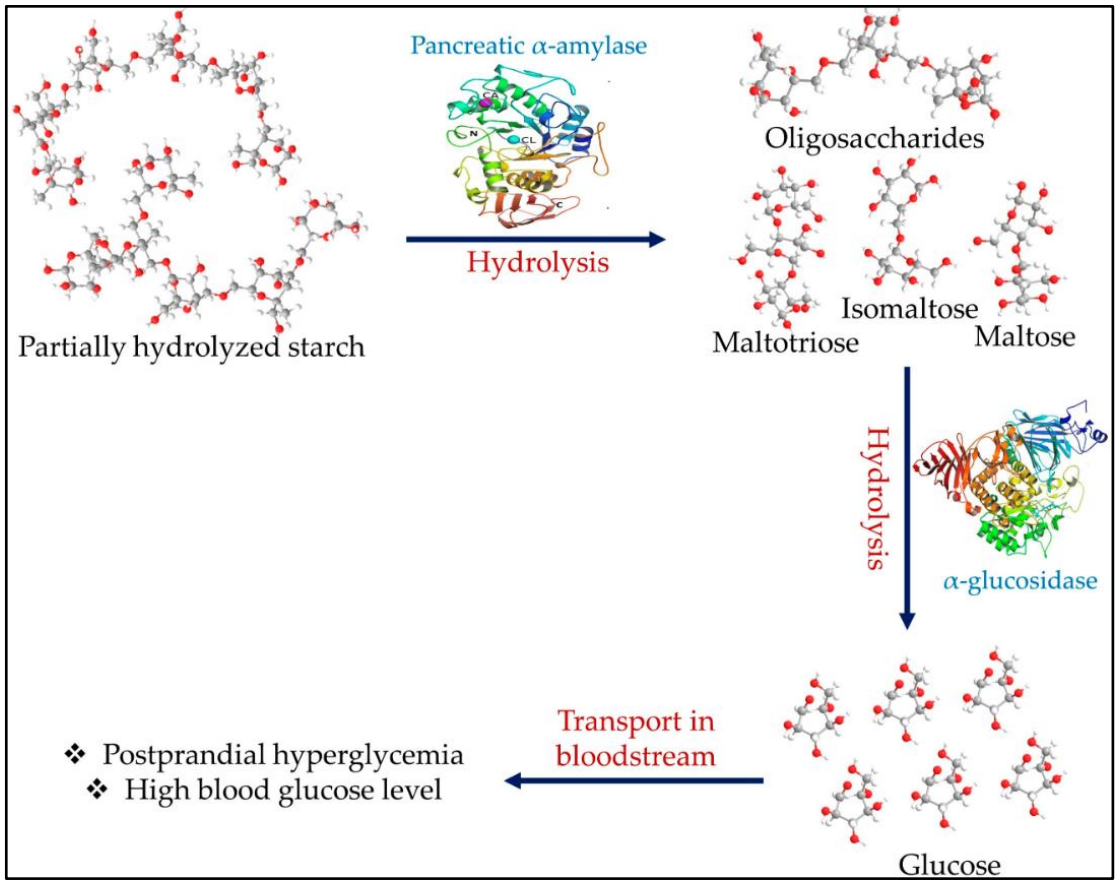

Figure 7: Role of alpha-glucosidase and alpha-amylase in diabetes.

1.3.2. Role of alpha-amylase as a target in diabetes:

One of the most important digestive enzymes in humans is pancreatic alpha-amylase (EC 3.2.1.1), which catalyzes the reaction that breaks down starch, amylopectin, amylose, glycogen, and numerous maltodextrins through the hydrolysis of their alpha-1,4 glycosidic linkages (**Figure 7**). Taka-amylase A is another name for -amylase, honoring its discoverer Takamine. The main digesting enzyme found in saliva is amylase. Amylase becomes inactive in the stomach due to gastric acid. Because of this, the optimal pH for -amylase is slightly alkaline. Since glucose must travel to the brain, big molecules like starch are unable to penetrate the blood-brain barrier. To solve this issue, alpha-amylase breaks the giant starch molecules down into smaller sugar pieces. The job of insulin is to direct cells to metabolize the extra sugar moieties and store them as energy sources, such as glycogen if there is an excessive amount of starch conversion to sugars, which raises the blood sugar level. But in some circumstances, the amylase enzyme over-activates, there is a lack of insulin, or there is insulin resistance, and this can cause blood sugar levels to rise and lead to hyperglycemia. Thus, by inhibiting the enzyme we can control diabetes [15,16,17].

1.4. References:

1) Kumar, H., Aggarwal, N., Marwaha, M. G., Deep, A., Chopra, H., Matin, M. M., Roy, A., Emran, T. B., Mohanta, Y. K., Ahmed, R., Mohanta, T. K., Saravanan, M., Marwaha, R. K., & Al-Harrasi, A. (2022). Thiazolidin-2,4-Dione Scaffold: An Insight into Recent Advances as Antimicrobial, Antioxidant, and Hypoglycemic Agents. *Molecules (Basel, Switzerland)*, *27*(19), 6763. https://doi.org/10.3390/molecules27196763
2) Chadha, N., Bahia, M. S., Kaur, M., & Silakari, O. (2015). Thiazolidine-2,4-dione derivatives: programmed chemical weapons for key protein targets of various pathological conditions. *Bioorganic & medicinal chemistry*, *23*(13), 2953–2974. https://doi.org/10.1016/j.bmc.2015.03.071
3) Jain, V. S., Vora, D. K., & Ramaa, C. S. (2013). Thiazolidine-2,4-diones: progress towards multifarious applications. *Bioorganic & medicinal chemistry*, *21*(7), 1599–1620. https://doi.org/10.1016/j.bmc.2013.01.029
4) Singh, G., Kumar, R., D.S., D., Chaudhary, M., Kaur, C., & Khurrana, N. (2024). Thiazolidinedione as a Promising Medicinal Scaffold for the Treatment of Type 2 Diabetes. In Current Diabetes Reviews (Vol. 20, Issue 6). Bentham Science Publishers Ltd. https://doi.org/10.2174/0115733998254798231005095627
5) Kharyal, A., Ranjan, S., Jaswal, S., Parveen, D., Gupta, G. D., Thareja, S., & Verma, S. K. (2022). Research progress on 2,4-thiazolidinedione and 2-thioxo-4-thiazolidinone analogues as aldose reductase inhibitors. In Journal of Molecular Structure (Vol. 1269, p. 133742). Elsevier BV. https://doi.org/10.1016/j.molstruc.2022.133742
6) Paul, A., Nahar, S., Nahata, P., Sarkar, A., Maji, A., Samanta, A., Karmakar, S., & Maity, T. K. (2024). Synthetic GPR40/FFAR1 agonists: An exhaustive survey on the most recent chemical classes and their structure-activity relationships. In European Journal of Medicinal

Chemistry (Vol. 264, p. 115990). Elsevier BV. https://doi.org/10.1016/j.ejmech.2023.115990

7) Rochester CD, Akiyode O. Novel and emerging diabetes mellitus drug therapies for the type 2 diabetes patient. World J Diabetes. 2014 Jun 15;5(3):305-15. doi: 10.4239/wjd. v5.i3.305. PMID: 24936252; PMCID: PMC4058735.
8) Bansal, G., Thanikachalam, P. V., Maurya, R. K., Chawla, P., & Ramamurthy, S. (2020). An overview on medicinal perspective of thiazolidine-2,4-dione: A remarkable scaffold in the treatment of type 2 diabetes. *Journal of advanced research*, *23*, 163–205. https://doi.org/10.1016/j.jare.2020.01.008
9) Bhat, A. R., Najar, M. H., Dongre, R. S., & Akhter, M. S. (2020). Microwave assisted synthesis of Knoevenagel Derivatives using water as green solvent. In Current Research in Green and Sustainable Chemistry (Vol. 3, p. 100008). Elsevier BV. https://doi.org/10.1016/j.crgsc.2020.06.001
10) Long, N., Le Gresley, A., & Wren, S. P. (2021). Thiazolidinediones: An In-Depth Study of Their Synthesis and Application to Medicinal Chemistry in the Treatment of Diabetes Mellitus. ChemMedChem, 16(11), 1716–1735. https://doi.org/10.1002/cmdc.202100177
11) Naim, M. J., Alam, M. J., Ahmad, S., Nawaz, F., Shrivastava, N., Sahu, M., & Alam, O. (2017). Therapeutic journey of 2,4-thiazolidinediones as a versatile scaffold: An insight into structure activity relationship. *European journal of medicinal chemistry*, *129*, 218–250. https://doi.org/10.1016/j.ejmech.2017.02.031
12) Singh, A., Singh, K., Sharma, A., Kaur, K., Kaur, K., Chadha, R., & Bedi, P. M. S. (2023). Recent developments in synthetic α-glucosidase inhibitors: A comprehensive review with structural and molecular insight. Journal of Molecular Structure, 1281, 135115. https://doi.org/10.1016/j.molstruc.2023.135115

13) Hossain, U., Das, A. K., Ghosh, S., & Sil, P. C. (2020). An overview on the role of bioactive α-glucosidase inhibitors in ameliorating diabetic complications. Food and Chemical Toxicology, 145(S3), 111738. https://doi.org/10.1016/j.fct.2020.111738

14) Mushtaq, A., Azam, U., Mehreen, S., & Naseer, M. M. (2023). Synthetic α-glucosidase inhibitors as promising anti-diabetic agents: Recent developments and future challenges. In European Journal of Medicinal Chemistry (Vol. 249). https://doi.org/10.1016/j.ejmech.2023.115119

15) Kaur, N., Kumar, V., Nayak, S. K., Wadhwa, P., Kaur, P., & Sahu, S. K. (2021). Alpha-amylase as molecular target for treatment of diabetes mellitus: A comprehensive review. *Chemical biology & drug design*, *98*(4), 539–560. https://doi.org/10.1111/cbdd.13909

16) Horii, S., Fukase, H., Matsuo, T., Kameda, Y., Asano, N., & Matsui, K. (1986). Synthesis and alpha-D-glucosidase inhibitory activity of N-substituted valiolamine derivatives as potential oral antidiabetic agents. *Journal of medicinal chemistry*, *29*(6), 1038–1046. https://doi.org/10.1021/jm00156a023

17) Kashtoh, H., & Baek, K.-H. (2023). New Insights into the Latest Advancement in α-Amylase Inhibitors of Plant Origin with Anti-Diabetic Effects. In Plants (Vol. 12, Issue 16, p. 2944). MDPI AG. https://doi.org/10.3390/plants12162944

CHAPTER: 2

LITERATURE REVIEW

2. Literature review:

2.1. Cuminaldehyde:

Cuminaldehyde (CUM; CAS Registry Number: 122-03-2 and PubChem CID: 326; (**Figure 8**) is a terpenoid class of compounds isolated from essential oil components and is found in cumin (*C. cyminum*) seeds and other plants [1]. Structurally, CUM is a member of the benzaldehyde class, where the isopropyl group is attached at position 4. The structure, chemical formula, molecular weight, melting point, log P, and tPSA of CUM is depicted in **Figure 8**. Traditionally, fruits and seeds of *C. cyminum* were used for the treatment of cough, inflammation, ulcers, and boils. Recent research studies revealed that CUM has also been demonstrated to have phytotoxic action, preventing the growth of a variety of plant species and promoting the generation of reactive oxygen species (ROS) and programmed cell death in the roots of onions [2]. Furthermore, against *Pseudomonas aeruginosa*, CUM has shown antibiofilm efficacy by preventing ROS buildup, which prevents biofilm development [3].

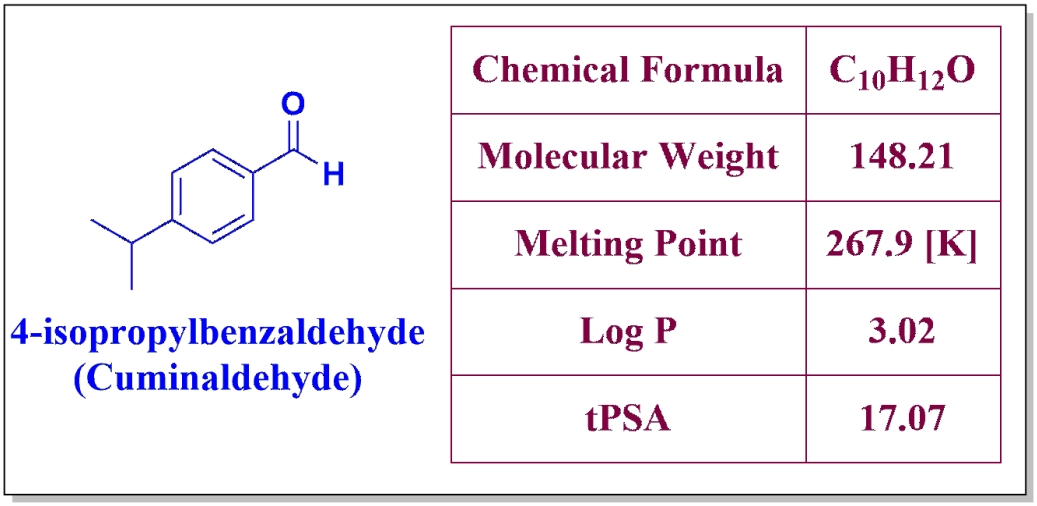

Figure 8: Structure, chemical formula, molecular weight, melting point, log P, and tPSA of CUM calculated from ChemBioDraw Ultra 12.0.

Figure 9 illustrates the various pharmacological effects that CUM provides, together with their mechanisms of action.

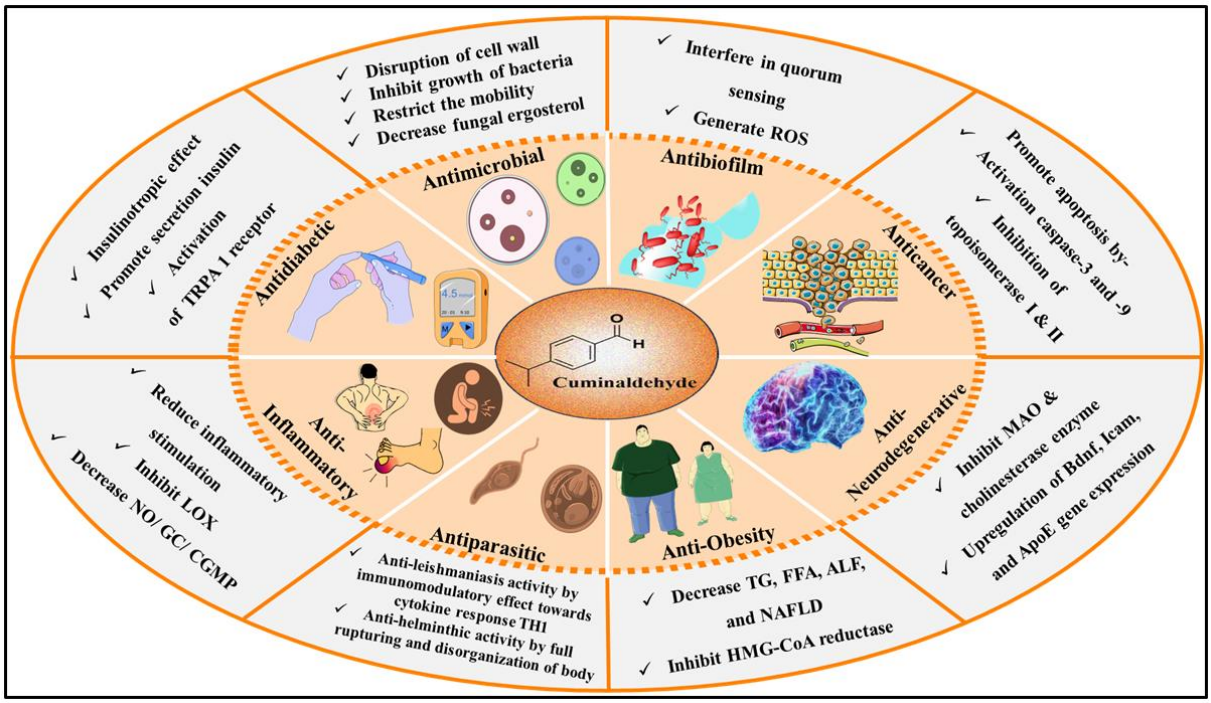

Figure 9: Therapeutic potential of CUM with its schematic mode of action.

2.2. Synthetic analogues of Cuminaldehyde:

Meenatchi *et al.* synthesized cuminaldehyde-3-hydroxy-2-napthoichydrazone (**Compound 1**) (**Figure 10**), a new essential oil component derivative, using the ultrasonication method. The CUM derivatives have been evaluated for antibacterial activity using the agar-well diffusion method, which showed a significant growth inhibition zone against *B. subtilis* (21 ± 0.2 mm) and *E. coli* (18 ± 0.3 mm). These bactericidal effects may be attributed to the disruption of the cell wall and cytoplasmic membranes, as well as the release of pathogen cytoplasm. In addition, it has been determined that the biological activity of an essential oil component, CUM was retained even if its derivative was synthesized by condensation with polycyclic aryl hydrazide. This novel CUM derivative has also shown remarkable promise as an antioxidant with nonlinear optical activity [4].

By modifying the natural scaffold CUM, a series of oxadiazoles were designed, synthesized by Hamdy *et al.*, and evaluated for antifungal activity. At sub-micromolar MIC_{50}

concentrations, the novel series inhibited *Candida albicans* and *Candida auris*, with **compound 2** (**Figure 10**) being the most potent analogue that did not exhibit toxicity on normal mammalian cells. Additionally, they carried out molecular dynamics simulations of the *C. auris* CYP51 enzyme using molecular docking and homology modeling, demonstrating the stability and effectiveness of **compound 2**. Furthermore, a 70% decrease in the fungal ergosterol content was shown by **compound 2**, and the ADME prediction suggested that **compound 2** meets the requirements for drug resemblance as a potential antifungal medication [5].

Zhang *et al*. planned and created two sets of new CUM derivatives, which include pyrazoline and isoxazoline components. They assessed their antifungal activity against six plant-pathogenic fungal strains. **Compounds 3** and **4** (**Figure 10**) with potent antifungal properties should undergo further assessment *in vivo* and field conditions, as reported. Remarkably, **compound 3**, which has a fluorine atom, exhibited significant antifungal properties, surpassing those of commercially available fungicides. The CUM derivatives in this research showed notable antifungal activity against the fungi that were examined. Compared to CUM alone, around half of the reported compounds showed more potent inhibitory effects. Specifically, **compound 3** outperformed CUM by 3.5 times in activities against *Ph. Piricola* (7.25 vs. 25.50 μg·mL−1), while **compound 4** outperformed CUM by around five times in potential against *S. sclerotiorum* (12.75 vs. 63.62 μg·mL−1) [6].

Francesca and his fellow researchers have effectively synthesized semi-carbazone, a compound derived from CUM thiosemicarbazone (**compound 5**; **Figure 10**), in which the sulfur atom has been replaced with an oxygen atom. This modification aimed to investigate the role of sulfur and oxygen in forming hydrogen bonds of varying strength, as well as their redox potentials. Typically, sulfur has weaker hydrogen bonds compared to oxygen because of its lower electronegativity. Additionally, sulfur is more prone to oxidation by

creating disulfide bridges. Thiosemicarbazones may function as reducers due to their ability to undergo thione-thiol tautomerism in their thiolic form. As a result, they can also operate as producers of ROS or scavengers of radicals. The selection of the ortho-Htcum and meta-Htcum isopropyl derivatives of Htcum is determined by the similarity in hydrophobicity to CUM while exhibiting distinct geometries. This study seeks to determine if the position of the isopropyl group serves as a general hydrophobic segment that enables the molecule to enter the cell or whether its placement is part of a more specialized molecule recognition process [7].

Regarding the biochemical characterization of hydrazide with thiophene moiety produced from CUM, no research has been done until Rajavel *et al.* reported a synthesis of **compound 6**; [(E)-N-(4-isopropyl benzylidene) thiophene-2-carbohydrazide] (**Figure 10**). CUM and 2-thiophenecarboxylic acid hydrazide were condensed to create **compound 6**. The findings indicate that **compound 6** exhibits lower activity against the tested microorganisms in comparison to the standards. In addition, **compound 6** has modest efficacy against two bacterial strains (*P. aeruginosa* and *E. coli*) and two fungus strains (*Mucor sp.* and *Rhizopus sp.*), as seen by the minimum inhibitory concentration values. The **compound 6** also exhibited a mild antioxidant property. The compound's notable activity may be attributed to the existence of the thiophene ring [8].

Witold and his colleagues researched the stereoisomers of CUM derivatives. They showed trans-lactones with a (4S,5R,6S)-framework more activity than other compounds. The trans-lactone and cis-lactone enantiomers with a 1,3-benzodioxole substituent (**compound 7**; **Figure 10**) showed a moderate variation (IC_{50} = 34.75 and 14.48 vs. 38.93 and 20.28 for the Jurkat and GL-1 cancer lines, respectively). The observed relationship in the case of cis-isomers was dependent on an aryl substituent and tested cancer line [9].

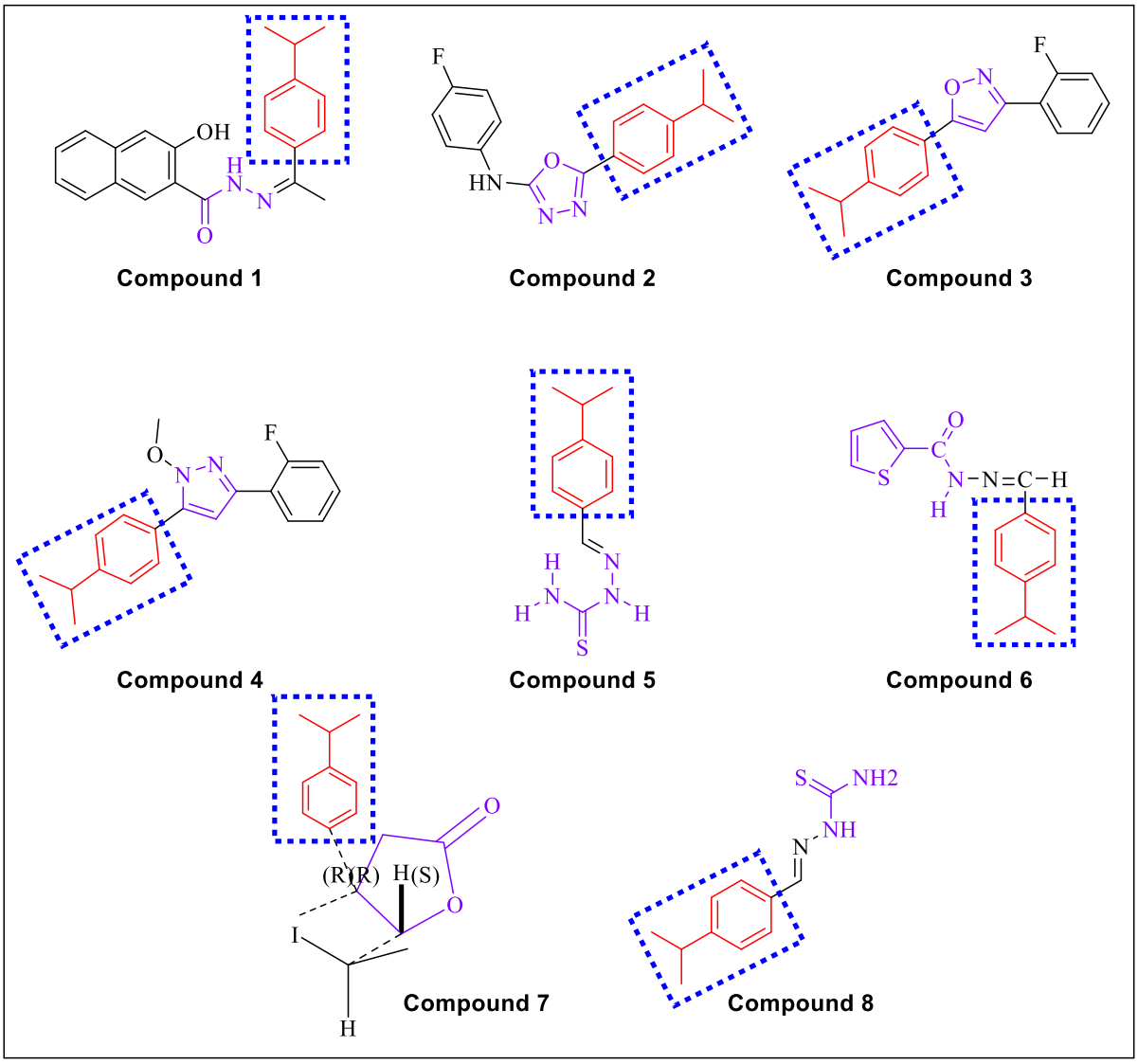

Figure 10: Structure of potential Cuminaldehyde analogues.

Arish *et al.* developed a Schiff base (L) by the condensation of CUM and L-histidine as antimicrobial agents. This Schiff-base ligand is synthesized and characterized by elemental analysis, molar conductance, mass, IR, electronic spectra, magnetic moment, electron spin resonance (ESR), CV, TG/DTA, granular XRD, and SEM. The complexes of Co (II), Ni (II), Cu (II), and Zn (II) are also involved. The Schiff base is a tridentate monobasic donor, as IR data indicates. It coordinates through carboxylate oxygen, imidazole nitrogen, and azomethine nitrogen. The crystalline nature of the Co (II), Cu (II), and Zn (II) complexes is demonstrated by XRD and SEM. In contrast, the Ni (II) complex is amorphous, and the

particles are in the nanocrystalline phase. The disc diffusion method was employed to evaluate the *in vitro* biological activities of the synthesized compounds against the bacterial species. The biological investigation suggests complexes demonstrate more significant activity than their ligand counterparts. In the presence and absence of H_2O_2, the nuclease activity of the ligand and its complexes is evaluated on CT DNA using gel electrophoresis. Experiments on CT-DNA cleavage and antimicrobial activity indicate that the complex (**Compound 8**; **Figure 10**) exhibits more significant activity than the ligand [10].

2.3. TZD as alpha-glucosidase inhibitors:

Patil *et al.* developed 32 molecules of 5-benzylidine-2,4-thiazolidinedione derivatives to investigate their α-glucosidase inhibitory activity. From *in vitro* studies, it was confirmed that **compound 9 (Figure 11)** is the most potent among others. **compound 9** has a chloro group at the 4^{th} position of the phenyl ring and two methyl groups at the 5th and 6th position of benzothiazole moiety. Out of 32 compounds, **compound 9** satisfactorily inhibits the α-glucosidase enzyme when compared with standard acarbose. Docking studies were performed to defend *in vitro* results through which it was found that binding energy was between -7.9 to -9.2 kcal/mol of all ligand-enzyme complexes [11].

Thiazolidinedione, rhodanine, hydantoin, and thiohydantoin-containing novel chemical entities that are connected to benzoxazolyl via meta- and para substitution were developed by Singh and co-workers. Compounds were tested for alpha-glucosidase inhibitory activity and **compound 10 (Figure 11)** which is a rhodanine moiety substituted at the meta-position of phenyl ring was found to be the most potent inhibitor of α-glucosidase. Further, *in vitro* results were confirmed by correlating with docking results which showed a good correlation (R^2= 0.883) [12].

Hussain *et al.* synthesized molecules containing thiazolidine-2,4-dione and dihydropyrimidine. Compounds were screened for alpha-glucosidase inhibition properties

and from the results it was found that **compound 11** (**Figure 11**) showed the highest potency with IC_{50} of 0.98 µM. *In vivo*, studies on alloxan-induced diabetic mice model confirmed the anti-diabetic potential of the compound. Moreover, toxicity studies ensured the safety of these compounds. SAR studies revealed that N-phenyl, C-phenyl, and ethoxy substitution showed better inhibition [13].

Wang *et al.* developed new series of thiazolidine-2,4-dione or rhodanine moieties. Compounds were screened for α-glucosidase inhibitory potential and **compound 12 (Figure 11)** (IC_{50} = 5.44 µM) was found to be most active. Other compounds in the series showed moderate to high inhibitory activity when compared to acarbose (IC_{50} = 817.38 µM). SAR studies revealed that TZD or rhodanine at the 4-position and electron-withdrawing group at the 2-position of phenyl enhances activity [14].

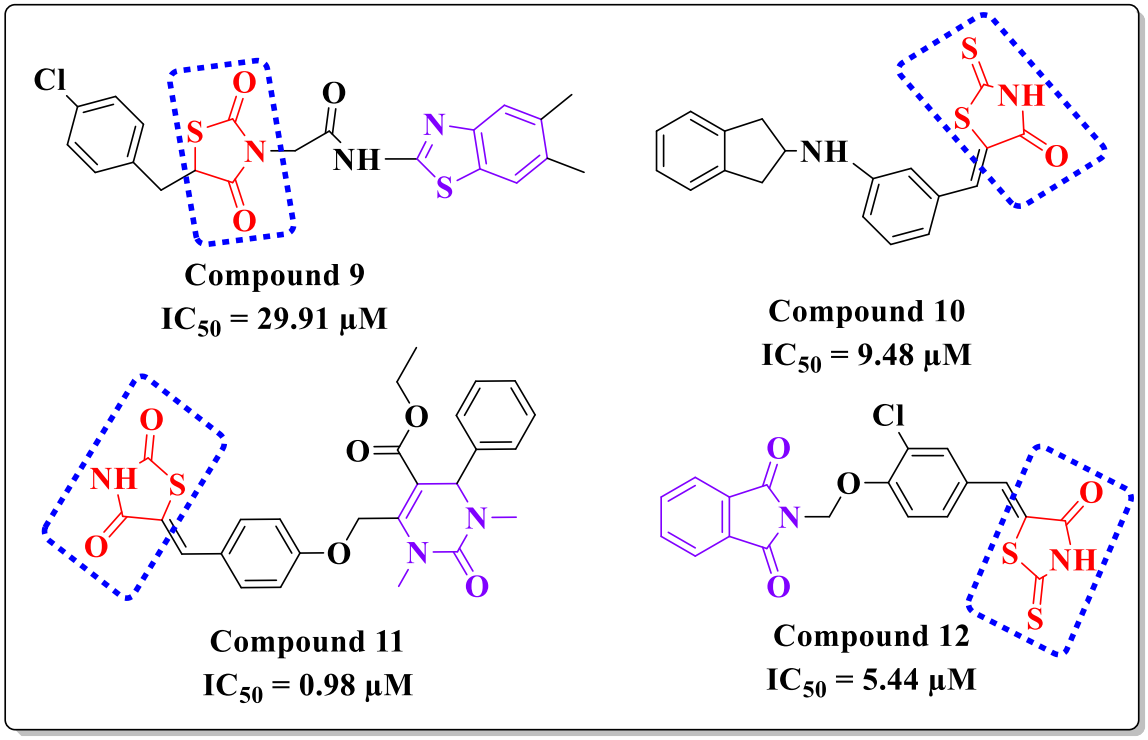

Figure 11: Compounds inhibiting α-glucosidase.

2.4. TZD as alpha-amylase inhibitors:

Manasa and co-workers synthesized a series of 20 compounds of 2,4-thiazolidinedione-phenothiazine moiety. Compounds were tested for alpha-amylase and glucose uptake activity by taking acarbose and metronidazole as positive controls respectively. After testing the compounds for amylase inhibition with the 3,5, di-nitro salicylic acid (DNS) method it was found that four compounds with electron-withdrawing groups on phenylene moiety of thiazolidinedione enhance inhibition activity reporting IC_{50} of 83.7-60.8 μM which were more than acarbose (101.7 μM) with **compound 13 (Figure 12)** being the most potent inhibitor. Glucose uptake studies revealed that the electron-releasing group increases glucose uptake activity in yeast. The role of the 3-nitro, 2-chloro-6-fluoro, 4-nitro, and 2,3-dichloro groups on the phenylene moiety of thiazolidinedione in the inhibition of -amylase enzymes was demonstrated by docking experiments [15].

Addanki *et al*. designed some phosphorylated derivatives of a thiazolidinedione and *in silico* ADMET and molecular docking, results showed drug likeliness and good oral bioavailability. Molecules were subjected to *in-vitro* α-amylase inhibition activity taking acarbose as standard (IC_{50} = 110.5 μg/ml) and **compound 14 (Figure 12)** was found to be the most potent inhibitor (IC_{50} = 113.1 μg/ml). It was also reported that synthesized compounds are poorly absorbed through the GI tract and unable to cross the BBB, making them unsuitable as P-glycoprotein substrates [16].

Chirag *et al.* developed a series of 10 compounds of biphenyl carbonitrile-thiazolidinedione moiety by using a combination technique by combining two privileged scaffolds one being a glitazone scaffold and other with PPAR α/γ agonist and PDF inhibition property. It was speculated that the N-atom of biphenyl carbonitrile-thiazolidinedione moiety comes up with a better spatial arrangement to bind with the α-amylase active site. From the results of in-vitro α-amylase studies, it was revealed that **compound 15 and 16 (Figure 12)** showed high

potency with an IC_{50} value of 0.13 µM. SAR studies revealed that methoxy and phenoxy were most potent and the electron-withdrawing nitro group is least potent [17].

Thiazolidinedione-containing compounds were created and synthesized by Sameeh and co-workers. Compounds demonstrated low to moderate anti-hyperglycemic potency, with **compound 17 (Figure 12)** being the most potent in contrast to standard, according to an evaluation of their radical scavenging and α-amylase inhibitory capabilities. *In vivo* tests using an alloxan-induced diabetic rat model were carried out, and **compound 17** showed a 69.55% reduction in blood glucose levels. Compounds also demonstrated good results when measured against several biological indicators. (CH, LDL, and HDL) [18].

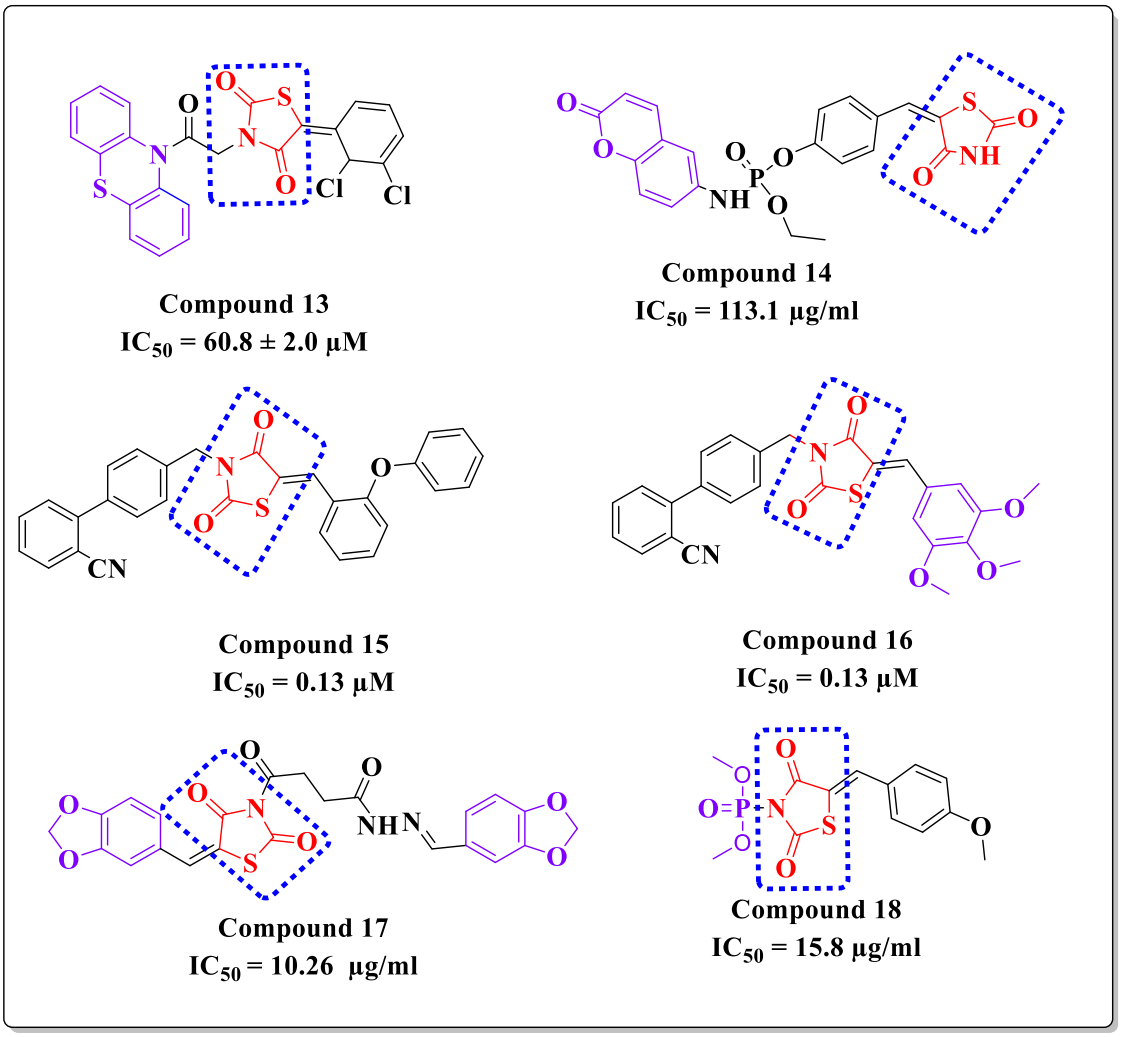

Figure 12: Compounds inhibiting α-amylase.

Phosphonates containing thiazolidinedione moiety were formed by Sujatha and co-workers. Docking studies revealed that compounds showed better binding in comparison to standard rosiglitazone against PPARγ. Compounds were subjected to *in-vitro* α-amylase inhibition activity and **compound 18 (Figure 12)** was found to be most potent among others with IC_{50} = 15.8 µg/ml which is much less than standard acarbose (47.8 µg/ml) [19].

2.5. TZD as dual alpha-glucosidase and alpha-amylase inhibitors:

Arineitwe *et al*. developed four compounds using a pharmacophore hybridization technique based on N-aryl pyrrole and TZD. Compounds were then evaluated for anti-diabetic properties by inhibiting various enzymes viz. α-amylase, α-glucosidase, aldose reductase, dipeptidyl peptidase-4(DPP4), and PTP1B. It was revealed that **Compound 19 (Figure 13)** was most potent for α-amylase inhibition (18.24 µg/ml) and **Compound 20 (Figure 13)** was most potent for α-glucosidase inhibition (56.82 µg/ml). Furthermore, molecules were docked with PPAR-γ and they showed good binding much like rosiglitazone [20].

Huneif *et al.* continued their study on a multitarget inhibitor of a thiazolidine-vanillin hybrid molecule by replacing vanillin with a succinimide-based substitute. They developed five molecules by substituting moieties on the N-atom of succinimide. Compounds were tested for α-amylase, α-glucosidase, aldose reductase, and DPP4, and **compound 21 (Figure 13)** was found to be the most effective anti-diabetic agent. Furthermore, *in silico*, *in vivo,* and docking results gave promising results after which it was concluded that benzyl group containing **compound 21** can be further substituted [21].

Srinivasa *et al*. synthesized some hybrid molecules containing thiazolidinediones and oxadiazoles that can inhibit α-amylase and α-glucosidase. The compounds were subjected to *in vitro* α-amylase and α-glucosidase inhibitory assays and *in vivo* anti-hyperglycemic activity study. The results showed the good inhibitory potential of the compounds out of which **compound 22 (Figure 13)** (α-amylase; IC_{50} = 18.42 µM and α-glucosidase; IC_{50} =

17.21 µM) showed the highest potency. *In vivo* studies, also revealed a considerable reduction of blood glucose levels after treatment with the compounds on *Drosophila melanogaster*. SAR studies revealed that methylene linker between thiazolidinedione and oxadiazole enhances activity. It was also found that withdrawing groups at ortho and para positions and the presence of electronegative groups increase activity whereas activity decreases because of electron-donating and phenyl groups at the para position [22].

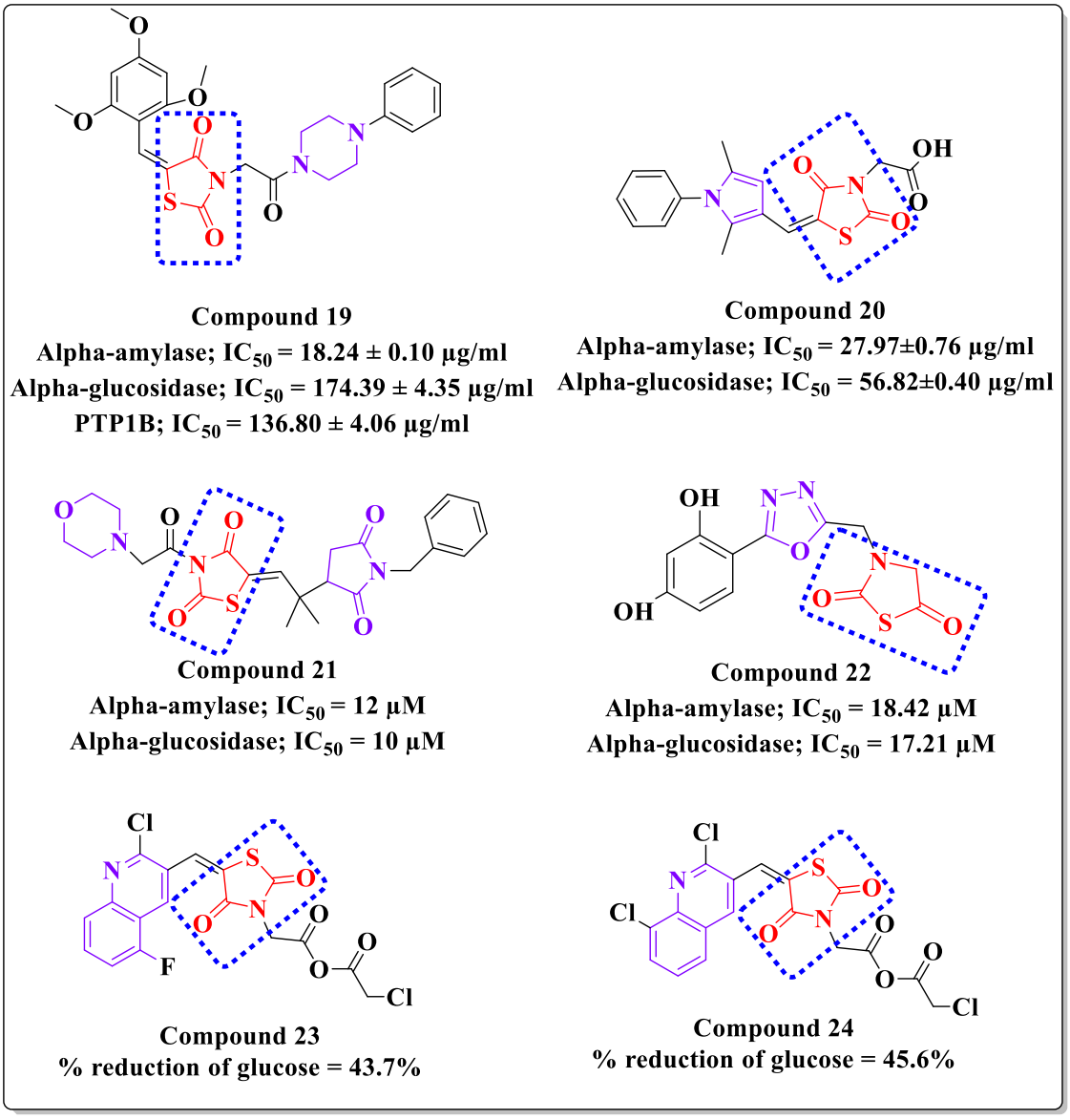

Figure 13: Compounds having dual α-glucosidase and α-amylase inhibitory activity.

A series of compounds containing thiazolidinedione and quinoline were designed and synthesized by Angajala *et al.* by Knoevenagel condensation and N-alkylation, a novel one-pot three-component technique was used and catalyzed by ANAP (*Aspergillus niger* from alkaline protease). After performing *in vitro* α-amylase and α-glucosidase inhibitory assays and *in vivo* evaluation of hypoglycemic activity it was found that **compound 23 and 24 (Figure 13)** showed better hypoglycemic activity in comparison to the standard pioglitazone [23].

2.6. References:

1) Singh, N., Yadav, S. S., Kumar, S., & Narashiman, B. (2021). A review on traditional uses, phytochemistry, pharmacology, and clinical research of dietary spice <scp>Cuminum cyminum</scp> L. In Phytotherapy Research (Vol. 35, Issue 9, pp. 5007–5030). Wiley. https://doi.org/10.1002/ptr.7133
2) Singh, R. P., H.V., G., & K, M. (2017). Cuminum cyminum – A Popular Spice: An Updated Review. In Pharmacognosy Journal (Vol. 9, Issue 3, pp. 292–301). EManuscript Technologies. https://doi.org/10.5530/pj.2017.3.51
3) Chatterjee, S., Paul, P., Chakraborty, P., Das, S., Sarker, R. K., Sarkar, S., Das, A., & Tribedi, P. (2021). Cuminaldehyde exhibits potential antibiofilm activity against Pseudomonas aeruginosa involving reactive oxygen species (ROS) accumulation: a way forward towards sustainable biofilm management. In 3 Biotech (Vol. 11, Issue 11). Springer Science and Business Media LLC. https://doi.org/10.1007/s13205-021-03013-1
4) Meenatchi, V., Zo, S. M., Won, S. Y., Nam, J.-W., Cheng, L., & Han, S. S. (2023). Cuminaldehyde-3-hydroxy-2-napthoichydrazone: Synthesis, effect of solvents, nonlinear optical activity, antioxidant activity, antimicrobial activity, and DFT analysis. In Spectrochimica Acta Part A: Molecular and Biomolecular Spectroscopy (Vol. 302, p. 123071). Elsevier BV. https://doi.org/10.1016/j.saa.2023.123071
5) Hamdy, R., Hamoda, A. M., Al-Khalifa, M., Menon, V., El-Awady, R., & Soliman, S. S. M. (2022). Efficient selective targeting of Candida CYP51 by oxadiazole derivatives designed from plant cuminaldehyde. In RSC Medicinal Chemistry (Vol. 13, Issue 11, pp. 1322–1340). Royal Society of Chemistry (RSC). https://doi.org/10.1039/d2md00196a
6) Zhang, T., Dong, M., Zhao, J., Zhang, X., & Mei, X. (2019). Synthesis and antifungal activity of novel pyrazolines and isoxazolines derived from cuminaldehyde. In Journal of Pesticide Science (Vol. 44, Issue 3, pp. 181–185). Pesticide Science Society of Japan. https://doi.org/10.1584/jpestics.d19-028
7) Degola, F., Bisceglie, F., Pioli, M., Palmano, S., Elviri, L., Pelosi, G., Lodi, T., & Restivo, F. M. (2017). Structural modification of cuminaldehyde thiosemicarbazone increases inhibition specificity toward aflatoxin biosynthesis and sclerotia development in Aspergillus flavus. In Applied Microbiology and Biotechnology (Vol. 101, Issue 17,

pp. 6683–6696). Springer Science and Business Media LLC. https://doi.org/10.1007/s00253-017-8426-y

8) Rajavel, A., Jeyakumar, T., Sundararajan, M. L., Srinivasan, T., & Velmurugan, D. (2016). Synthesis, crystal structure, characterization, and microbial evaluation of (E)-N-(4-isopropylbenzylidene)thiophene-2-carbohydrazide. In Molecular Crystals and Liquid Crystals (Vol. 631, Issue 1, pp. 176–186). Informa UK Limited. https://doi.org/10.1080/15421406.2016.1170285
9) Gładkowski, W., Skrobiszewski, A., Mazur, M., Gliszczyńska, A., Czarnecka, M., Pawlak, A., Obmińska-Mrukowicz, B., Maciejewska, G., & Białońska, A. (2016). Chiral δ-iodo-γ-lactones derived from cuminaldehyde, 2,5-dimethylbenzaldehyde and piperonal: chemoenzymatic synthesis and antiproliferative activity. In Tetrahedron: Asymmetry (Vol. 27, Issue 6, pp. 227–237). Elsevier BV. https://doi.org/10.1016/j.tetasy.2016.02.003
10) Arish, D., & Sivasankaran Nair, M. (2010). Synthesis, characterization, antimicrobial, and nuclease activity studies of some metal Schiff-base complexes. In Journal of Coordination Chemistry (Vol. 63, Issue 9, pp. 1619–1628). Informa UK Limited. https://doi.org/10.1080/00958972.2010.483729
11) Patil, V. M., Tilekar, K. N., Upadhyay, N. M., & Ramaa, C. S. (2022). Synthesis, In-Vitro Evaluation and Molecular Docking Study of N-Substituted Thiazolidinediones as α-Glucosidase Inhibitors. In ChemistrySelect (Vol. 7, Issue 1). Wiley. https://doi.org/10.1002/slct.202103848
12) Singh, V., Singh, A., Singh, G., Verma, R. K., & Mall, R. (2021). Benzoxazolyl linked benzylidene based rhodanine and analogs as novel antidiabetic agents: synthesis, molecular docking, and *in vitro* studies. In Medicinal Chemistry Research (Vol. 30, Issue 10, pp. 1905–1914). Springer Science and Business Media LLC. https://doi.org/10.1007/s00044-021-02781-y
13) Hussain, F., Khan, Z., Jan, M. S., Ahmad, S., Ahmad, A., Rashid, U., Ullah, F., Ayaz, M., & Sadiq, A. (2019). Synthesis, in-vitro α-glucosidase inhibition, antioxidant, in-vivo antidiabetic and molecular docking studies of pyrrolidine-2,5-dione and thiazolidine-2,4-dione derivatives. *Bioorganic chemistry*, *91*, 103128. https://doi.org/10.1016/j.bioorg.2019.103128
14) Wang, G. C., Peng, Y. P., Xie, Z. Z., Wang, J., & Chen, M. (2017). Synthesis, α-glucosidase inhibition and molecular docking studies of novel thiazolidine-2,4-dione or

rhodanine derivatives. *MedChemComm*, *8*(7), 1477–1484. https://doi.org/10.1039/c7md00173h

15) Doddagaddavalli, M. A., Kalalbandi, V. K. A., & Seetharamappa, J. (2023). Synthesis, characterization, crystallographic, binding, *in silico* and antidiabetic studies of novel 2,4-thiazolidinedione-phenothiazine molecular hybrids. In Journal of Molecular Structure (Vol. 1276, p. 134625). Elsevier BV. https://doi.org/10.1016/j.molstruc.2022.134625
16) Addanki, H. R., Vallabhaneni, M. R., Chennamsetty, S., Pullagura, P., Sagurthi, S. R., & Pasupuleti, V. R. (2022). An *in silico* ADMET, molecular docking study and microwave-assisted synthesis of new phosphorylated derivatives of thiazolidinedione as potential anti-diabetic agents. In Synthetic Communications (Vol. 52, Issue 2, pp. 300–315). Informa UK Limited. https://doi.org/10.1080/00397911.2021.2024574
17) Rathod, C. H., Nariya, P. B., Maliwal, D., Pissurlenkar, R. R. S., Kapuriya, N. P., & Patel, A. S. (2021). Design, Synthesis and Antidiabetic Activity of Biphenylcarbonitrile-Thiazolidinedione Conjugates as Potential α-Amylase Inhibitors. In ChemistrySelect (Vol. 6, Issue 9, pp. 2464–2469). Wiley. https://doi.org/10.1002/slct.202004362
18) Sameeh, M. Y., Khowdiary, M. M., Nassar, H. S., Abdelall, M. M., Alderhami, S. A., & Elhenawy, A. A. (2021). Discovery Potent of Thiazolidinedione Derivatives as Antioxidant, α-Amylase Inhibitor, and Antidiabetic Agent. *Biomedicines*, *10*(1), 24. https://doi.org/10.3390/biomedicines10010024
19) Sujatha, B., Chennamsetty, S., Chintha, V., Wudayagiri, R., & Prasada Rao, K. (2020). Synthesis and anti-diabetic activity evaluation of phosphonates containing thiazolidinedione moiety. In Phosphorus, Sulfur, and Silicon and the Related Elements (Vol. 195, Issue 7, pp. 586–591). Informa UK Limited. https://doi.org/10.1080/10426507.2020.1737061
20) Arineitwe, C., Oderinlo, O., Tukulula, M., Khanye, S., Khathi, A., & Sibiya, N. (2023). Discovery of Novel Thiazolidinedione-Derivatives with Multi-Modal Antidiabetic Activities *In Vitro* and In Silico. *International journal of molecular sciences*, *24*(3), 3024. https://doi.org/10.3390/ijms24033024
21) Huneif, M. A., Mahnashi, M. H., Jan, M. S., Shah, M., Almedhesh, S. A., Alqahtani, S. M., Alzahrani, M. J., Ayaz, M., Ullah, F., Rashid, U., & Sadiq, A. (2023). New Succinimide-Thiazolidinedione Hybrids as Multitarget Antidiabetic Agents: Design,

Synthesis, Bioevaluation, and Molecular Modelling Studies. *Molecules (Basel, Switzerland)*, *28*(3), 1207. https://doi.org/10.3390/molecules28031207

22) Srinivasa, M. G., Paithankar, J. G., Saheb Birangal, S. R., Pai, A., Pai, V., Deshpande, S. N., & Revanasiddappa, B. C. (2023). Novel hybrids of thiazolidinedione-1,3,4-oxadiazole derivatives: synthesis, molecular docking, MD simulations, ADMET study, *in vitro*, and *in vivo* anti-diabetic assessment. *RSC advances*, *13*(3), 1567–1579. https://doi.org/10.1039/d2ra07247e

23) Angajala, G., Aruna, V., Pavan, P., & Guruprasad Reddy, P. (2022). Biocatalytic one pot three component approach: Facile synthesis, characterization, molecular modelling and hypoglycemic studies of new thiazolidinedione festooned quinoline analogues catalyzed by alkaline protease from Aspergillus niger. *Bioorganic chemistry*, *119*, 105533. https://doi.org/10.1016/j.bioorg.2021.105533

CHAPTER: 3

MATERIALS AND METHODS

3. Materials and Methods:

3.1. General:

All reagents and solvents used were of laboratory (LR) grade, obtained from Sisco Research Laboratories Pvt. Ltd. (Mumbai, India) and Merck Limited (Mumbai, India), Avra Research Laboratories Pvt. Ltd. (Hyderabad, India) and were used without further purification. The progress of the reaction and purity of the synthesized compounds were checked on the precoated silica gel F_{254} plates obtained from Merck (Mumbai, India) using hexane and ethyl acetate (1:4) as mobile phase. The iodine chamber and UV lamp (λ = 254 nm) were used for visualization of the spots. Melting points were determined in an open capillary tube on the VEEGO VMP-DS melting point apparatus and were uncorrected. IR spectra were recorded on a Bruker, FT-IR spectrophotometer using KBr optics. ^{1}H NMR and 13C NMR spectra were recorded on a Bruker FT-NMR Spectrometer (400 MHz) in $CDCl_3$. Chemical shifts (δ) are given in ppm relative to TMS and coupling constants (J) are expressed in Hz. Mass spectra (m/z) were recorded using an LC-MS ESI (Q-TOF and Orbitrap, positive ion mode) mass spectrometry instrument (Applied Biosystems, MDS SCIEX).

3.2. Rationale of design:

In 2005, Hoi-Seon Lee isolated *Cuminum cyminum* seed and tested it for α-glucosidase inhibitory activity. The active component of *C. cyminum* seed oil was reported as cuminaldehyde. The IC_{50} value was reported as 0.5 mg/ml. cuminaldehyde was 1.8 times less active than standard acarbose. Simultaneously, it was also evaluated for aldose reductase inhibition and gave satisfactory results. Finally, it can be concluded that cuminaldehyde can be a lead compound and a new agent for the treatment of diabetes [1].

Garg *et al.* synthesized a group of compounds named 5-substituted-arylidene-3-substituted benzyl-thiazolidine-2, 4-dione derivatives. These compounds were created via a chemical reaction called Knoevenagel condensation. The researchers then tested the compounds on

rats with diabetes induced by alloxan to see if they could lower glucose levels and found that some substances had significant antidiabetic action that was similar to the standard drug rosiglitazone [2].

Saima and her colleagues have effectively created a collection of 18 Schiff base derivatives by combining isatin with ibuprofen and mefenamic pharmaceuticals. They have then studied the effectiveness of these derivatives as inhibitors of both α–glucosidase and urease. Their findings demonstrated that those substances exhibited significant α-glucosidase inhibitory activity. The synthesized compounds may have a synergistic effect in controlling glucose levels and lowering gastrointestinal illnesses by simultaneously inhibiting α-glucosidase and urease enzymes [3].

After a thorough search using Sci-Finder, we have designed ten derivatives of cuminaldehyde-thiazolidine-2,4-dione hybrid and the rational design for the target compounds has been presented in **Figure 14.**

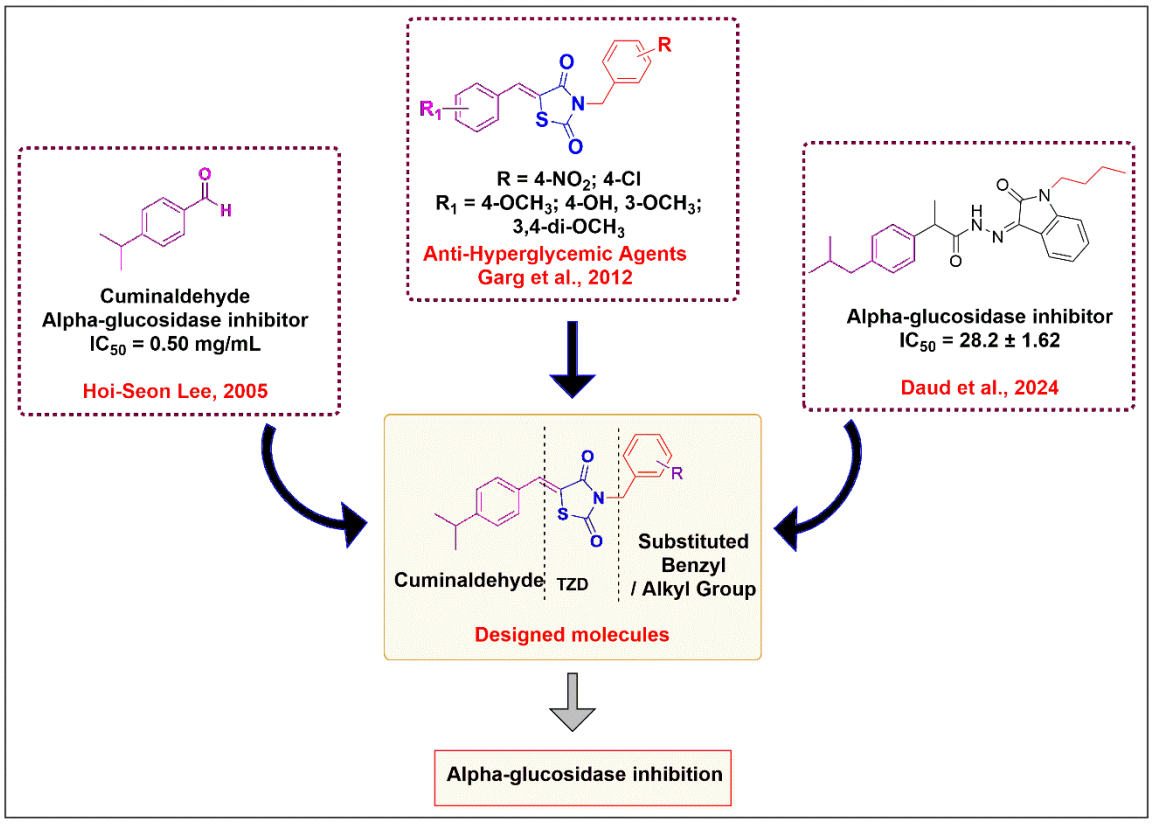

Figure 14: The rationale behind the designing of compounds.

3.3. Synthetic scheme:

The synthesis of derivatives of cuminaldehyde-thiazolidine-2,4-dione hybrid was achieved through a three-step reaction in good yields. **Scheme 1** showed the original synthetic route to prepare the final compound, starting from the chloroacetic acid and thiourea to form TZD, then hybridization of TZD with Cuminaldehyde, and then finally substituting it with various side chains.

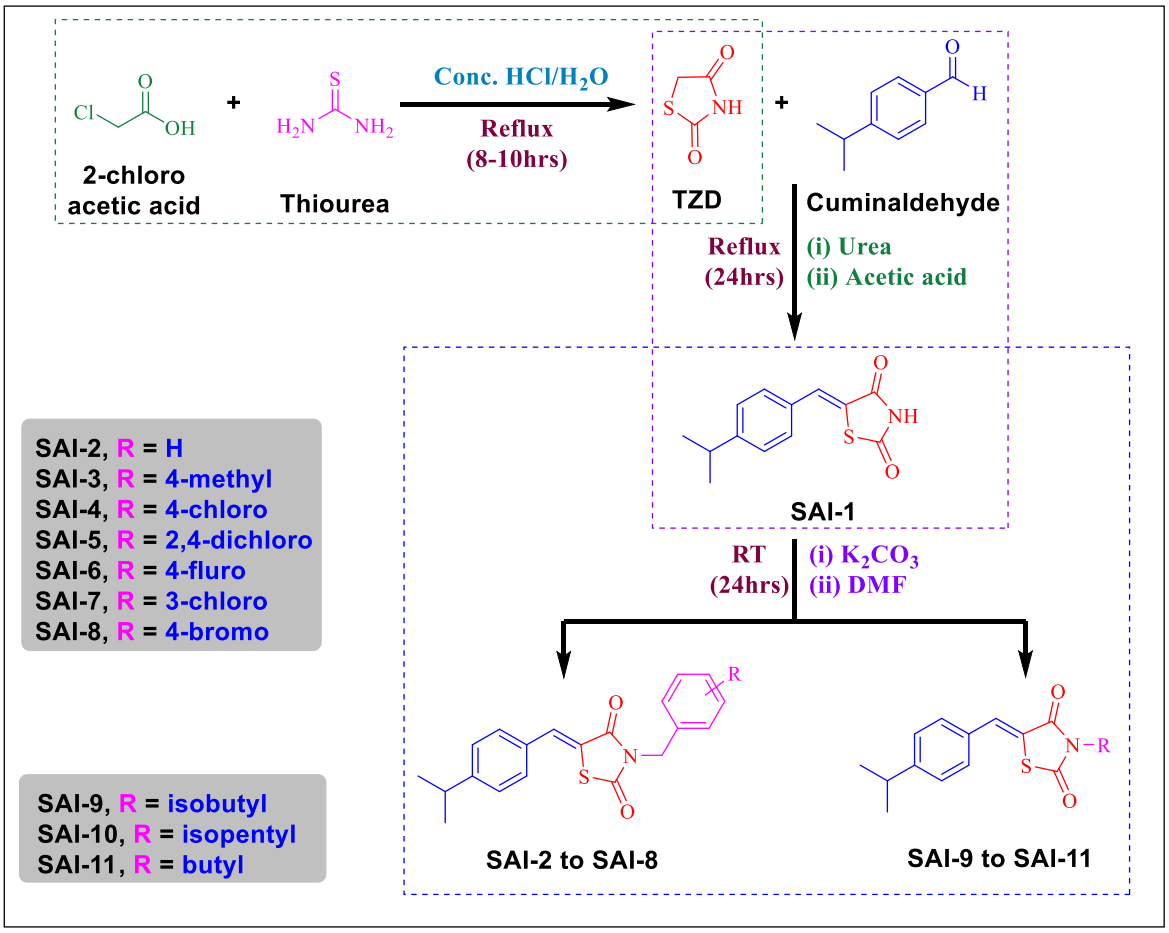

Scheme 1: Synthetic scheme for SAI-1 to SAI-11.

3.4. Novelty search:

Every synthesized compound was searched in sci finder (**Figure 15**) for their novelty and reported activity which is compiled in **Table 1**:

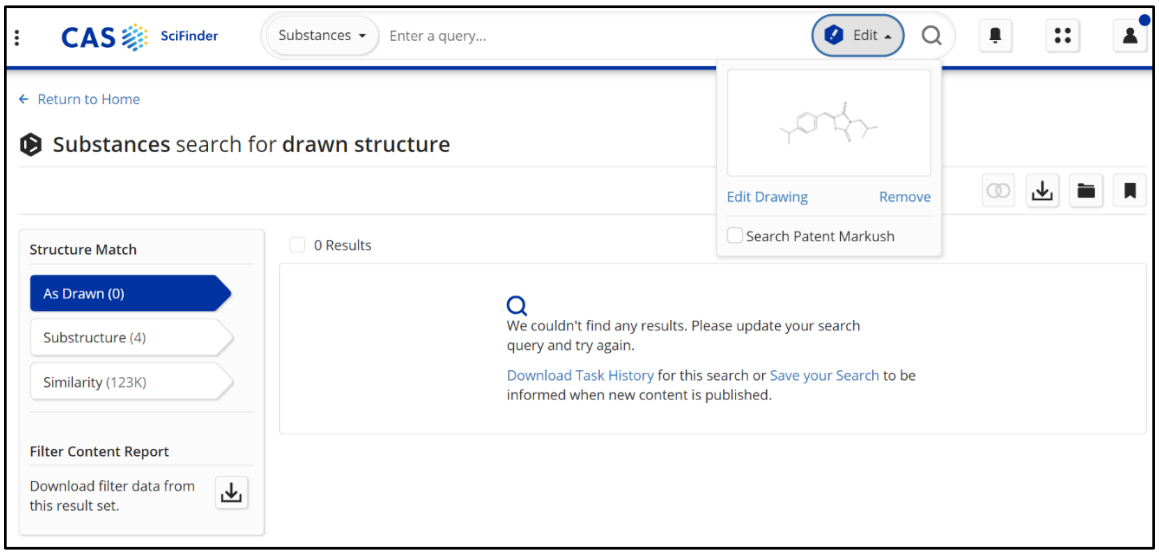

Figure 15: Figure showing novelty report of **SAI-9** in Sci-Finder.

Table 1: Sci-Finder novelty report of designed compounds with activity status.

Sl. No.	Compound name	Structure	Status in Sci Finder	Reported activity
1	SAI-1	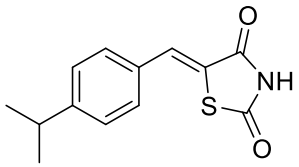 **Chemical Formula: $C_{13}H_{13}NO_2S$ Molecular Weight: 247.31**	Present	Antimicrobial
2	SAI-2	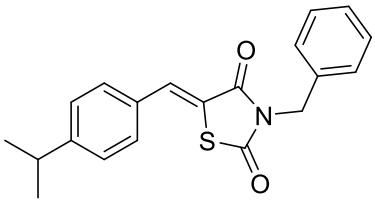 **Chemical Formula: $C_{20}H_{19}NO_2S$ Molecular Weight: 337.44**	Present	No activity reported
3	SAI-3	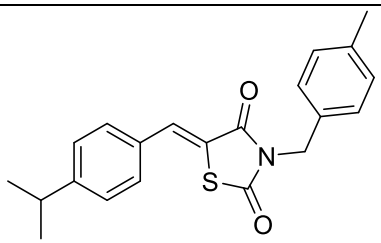 **Chemical Formula: $C_{21}H_{21}NO_2S$ Molecular Weight: 351.46**	Present	No activity reported

4	SAI-4	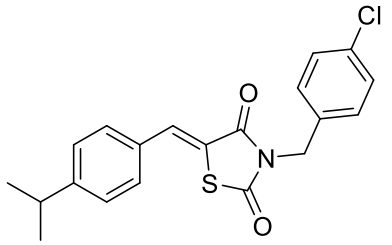 **Chemical Formula: $C_{20}H_{18}ClNO_2S$** **Molecular Weight: 371.88**	Present	No activity reported
5	SAI-5	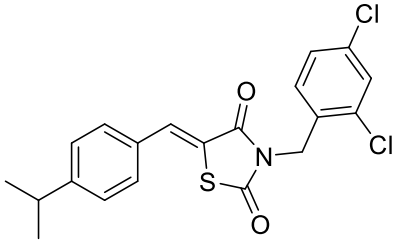 **Chemical Formula: $C_{20}H_{17}Cl_2NO_2S$** **Molecular Weight: 406.32**	Present	No activity reported
6	SAI-6	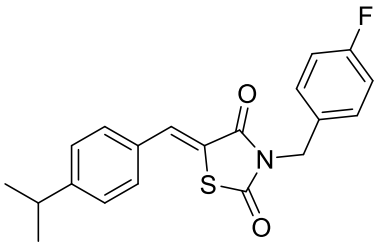 **Chemical Formula: $C_{20}H_{18}FNO_2S$** **Molecular Weight: 355.43**	Present	No activity reported
7	SAI-7	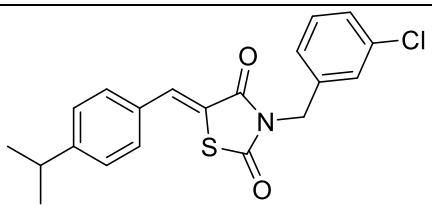 **Chemical Formula: $C_{20}H_{18}ClNO_2S$** **Molecular Weight: 371.88**	Present	No activity reported
8	SAI-8	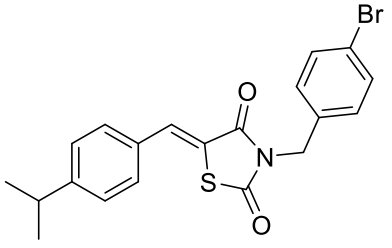 **Chemical Formula: $C_{20}H_{18}BrNO_2S$** **Molecular Weight: 416.33**	Present	No activity reported

9	SAI-9	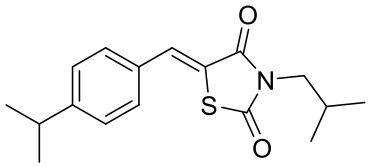 **Chemical Formula: $C_{17}H_{21}NO_2S$ Molecular Weight: 303.42**	Not Present	No activity reported
10	SAI-10	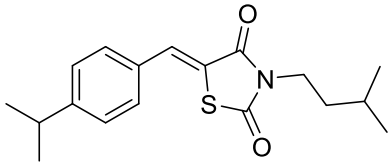 **Chemical Formula: $C_{18}H_{23}NO_2S$ Molecular Weight: 317.45**	Not Present	No activity reported
11	SAI-11	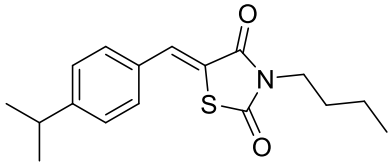 **Chemical Formula: $C_{17}H_{21}NO_2S$ Molecular Weight: 303.42**	Present	Antimicrobial Antifungal

3.5. Chemistry:

In this work, I have synthesized a series of 4-isopropylbenzaldehyde containing TZD hybrids in high yields with simple chemistry.

3.5.1. Methodology:

Step 1: An equimolar amount of chloroacetic acid and thiourea will be reacted to carry out the cyclization of chloroacetic acid and it will give the parent scaffold thiazolidine-2,4-dione.

Step 2: The methylene group (-CH_2-) of thiazolidine-2,4-dione is substituted with 4-isopropylbenzaldehyde using urea as catalyst and acetic acid as solvent to form (Z)-5-(4-isopropylbenzylidene) thiazolidine-2,4-dione.

Step 3: N-3 position of compounds will be substituted by ten different side chains in the presence of DMF and K_2CO_3 to obtain the target compounds.

3.5.1.1. Synthesis of thiazolidine-2,4-dione (TZD):

In a 150 mL round-bottomed flask, 28.35 g chloroacetic acid (0.3 mol) and 22.83 g thiourea (0.3 mol) were dissolved in 35 mL of water. The mixture was stirred for 1 h to form a white precipitate, accompanied by considerable cooling. To the contents of the flask, 18mL of concentrated hydrochloric acid was then added slowly from a dropping funnel, the flask was then connected with a reflux condenser, and gentle heat was applied to effect a complete solution, after which the reaction mixture was stirred and refluxed for 8–10 hrs. at 100–110 ℃. The progress of the reaction was monitored by using TLC using n-hexane/ethyl acetate 3:2 as an eluent. On cooling the contents of the flask solidified to a cluster of white needles, the product was filtered and washed with double distilled water to remove traces of hydrochloric acid and dried. It was purified by recrystallization from ethyl alcohol.

3.5.1.2. Synthesis of 5-(4-isopropylbenzylidene) thiazolidine-2,4-dione:

Acetic acid (50 ml) and 3.04 g urea (0.051 mol) were taken in a 250 ml round-bottomed flask and stirred for 15 mins. To the same flask 3.95 g 2,4-thiazolidinedione (0.034 mol) was added and again stirred for 15 mins. 5 g of 4-isopropyl benzaldehyde (0.034 mol) was added and kept for reflux at 100 ºC for 24 hrs (**Figure 16**). The reaction mixture was then cooled to room temperature (RT) and then poured into ice-cold water and the beige color precipitate was recovered by filtering under a vacuum, washing with water several times, and drying at RT.

Figure 16: Reaction setup of 5-(4-isopropylbenzylidene) thiazolidine-2,4-dione.

3.5.1.3. Synthesis of 3-substituted-5-(4-isopropyl benzylidene) thiazolidine-2,4-dione:

1.12g of potassium carbonate (0.008 mol) and 15 ml of dimethylformamide was taken in a 50 ml round bottom flask and stirred for 15 mins. 1 g of (Z)-5-(4-isopropylbenzylidene) thiazolidine-2,4-dione (0.004 mol) was added and stirred for 20-30 mins. The calculated amount of substituted compound was added dropwise at an interval of 5 mins. The reaction mixture was left steering for 24 hrs at RT (**Figure 17**). After completion of the reaction, the reaction mixture was extracted with Ethyl Acetate and Water using a separating funnel, followed by evaporation of the solvent under vacuum using a rotary evaporator. The crude material was air dried at RT and then purified by recrystallization using methanol as solvent, to achieve a shiny needle-shaped crystal.

Figure 17: Reaction setup of 3-substituted-5-(4-isopropylbenzylidene) thiazolidine-2,4-dione.

3.6. *In vitro* assay of α-glucosidase inhibitory activity:

The study on α-glucosidase inhibition was conducted using 96-well plates, with minor modifications to the methodology used in past methods [4,5]. The α-glucosidase (Maltase) enzyme extracted from Yeast was purchased from Sisco Research Laboratories Pvt. Ltd, while the substrate employed was p-nitrophenyl-α-d-glucopyranoside (pNPG), and acarbose served as the positive control. For the experiment, 20 µL of various concentrations

of test samples or acarbose which were made by dissolving it in MeOH, were placed in 96-well plates. Additionally, 10 µL of α-glucosidase solution (0.1 U/mL) in 0.1 mM phosphate buffer (pH 6.8) was added to each well. The plates were then incubated at 37 °C for 10 minutes. Following pre-incubation, 20 µL of PNPG substrate solution (1.25 mM) in potassium phosphate buffer (pH 6.8) was introduced into each well and subjected to incubation at 37 °C for 30 minutes. In the end, the alteration in the absorbance was assessed at a wavelength of 405 nm using a microplate reader (Spectramax M5, Molecular Devices, USA). The percentage of inhibition for the target molecules, control, and positive control was computed and reported as a percentage of inhibition. The calculation method used was as follows:

$$\%Inhibition = \frac{(Abs_{\ control} - Abs_{samples})}{Abs_{\ control}} \times 100$$

Using the Logit approach, the IC_{50} values of the samples under study or positive control were determined from the linear regression curve.

3.7. Molecular docking studies:

Predicting the potential orientation and binding affinity analysis of a ligand against a receptor (target) to create a stable complex is a common use of molecular docking. The LeDock software was used to carry out docking studies. LeDock is a GUI-based docking program that is accurate, user-friendly, and semi-flexible (ligand complexes attach flexibly towards the active site whereas proteins are considered stiff). The maltase-glucoamylase protein was chosen from the LeDock "LePro" module, and the grid box parameters were automatically chosen by overlapping the geometric pattern in the PDB ID: 3AXH crystal structure that the prototype in-bound ligand occupied. (Where Xmin =-23.758, Xmax =-11.956, Ymin = -13.772, Ymax = -2.695, Zmin = -26.123, Zmax =-12.612; with an RMSD cut-off range of 1.0 to reduce the redundancy of docking poses), and then started the

docking [6]. In addition to reporting the final docking findings with the docking score expressed in terms of binding affinity (kcal/mol), PyMOL allowed for the visual inspection of the compounds' docked postures and Discovery Studio Visualiser version 3.0 produced 2D binding interaction graphs.

3.8. *In silico* ADMET predictions:

Pharmacokinetic (pK) and pharmacodynamic (pD) profiles of any compounds provide confidence for the development of the clinics in the indication of various diseases. In drug discovery and development, the absorption, distribution, metabolism, excretion, and toxicity (ADMET) profiles of compounds have a significant role [7]. Orally accessible molecules are more likely to have drug-like characteristics and satisfy the Lipinski and Veber criteria. Because of their drug-like characteristics, molecules may be as good as or even better than commercially available drugs. The compound must adhere to all Lipinski parameters since drug bioavailability drops with increasing parameter violations. It is essential to conduct *in silico* research before performing the pK-pD properties in an *in vivo* model [8,9,10].

So, we have forecasted the ADMET profiles of all the synthesized compounds using the *in silico* SwissADME [11] and Deep-PK [12] webserver.

3.9.References:

1) Lee, H.-S. (2005). Cuminaldehyde: Aldose Reductase and α-Glucosidase Inhibitor Derived from Cuminum cyminum L. Seeds. In Journal of Agricultural and Food Chemistry (Vol. 53, Issue 7, pp. 2446–2450). American Chemical Society (ACS). https://doi.org/10.1021/jf048451g
2) Ankush, G., Pooja, C., & Shubhini, S. A. (2012). Syntheses of some novel 5-substituted-arylidene-3-substituted-benzyl-thiazolidine-2, 4-dione analogues as anti-Hyperglycemic agents. *Int. J. Drug Dev. & Res*, *4*(3), 141-146.
3) Daud, S., Abid, O., Saadullah, M., Fakhar-e-Alam, M., Carradori, S., Sardar, A., Niaz, B., Atif, M., Zara, S., & Rashad, M. (2024). Isatin-based ibuprofen and mefenamic acid Schiff base derivatives as dual inhibitors against urease and α–glucosidase: In vitro, in silico and cytotoxicity studies. In Journal of Saudi Chemical Society (Vol. 28, Issue 5, p. 101905). Elsevier BV. https://doi.org/10.1016/j.jscs.2024.101905
4) , G., Peng, Z., Wang, J., Li, X., & Li, J. (2017). Synthesis, in vitro evaluation and molecular docking studies of novel triazine-triazole derivatives as potential α-glucosidase inhibitors. In European Journal of Medicinal Chemistry (Vol. 125, pp. 423–429). Elsevier BV. https://doi.org/10.1016/j.ejmech.2016.09.067
5) Fan, M., Zhong, X., Huang, Y., Peng, Z., & Wang, G. (2023). Synthesis, biological evaluation and molecular docking studies of chromone derivatives as potential α-glucosidase inhibitors. In Journal of Molecular Structure (Vol. 1274, p. 134575). Elsevier BV. https://doi.org/10.1016/j.molstruc.2022.134575
6) Das, T., Bhattacharya, A., Jha, T., & Gayen, S. (2024). Exploration of Fingerprints and Data Mining-based Prediction of Some Bioactive Compounds from Allium sativum as Histone Deacetylase 9 (HDAC9) Inhibitors. In Current Computer-Aided Drug Design

(Vol. 20). Bentham Science Publishers Ltd. https://doi.org/10.2174/0115734099282303240126061624

7) van de Waterbeemd, H., & Gifford, E. (2003). ADMET in silico modelling: towards prediction paradise? In Nature Reviews Drug Discovery (Vol. 2, Issue 3, pp. 192–204). Springer Science and Business Media LLC. https://doi.org/10.1038/nrd1032
8) Lipinski C. A. (2016). Rule of five in 2015 and beyond: Target and ligand structural limitations, ligand chemistry structure and drug discovery project decisions. *Advanced drug delivery reviews*, *101*, 34–41. https://doi.org/10.1016/j.addr.2016.04.029
9) Lohit, N., Singh, A. K., Kumar, A., Singh, H., Yadav, J. P., Singh, K., & Kumar, P. (2024). Description and In silico ADME Studies of US-FDA Approved Drugs or Drugs under Clinical Trial which Violate the Lipinski's Rule of 5. In Letters in Drug Design & Discovery (Vol. 21, Issue 8, pp. 1334–1358). Bentham Science Publishers Ltd. https://doi.org/10.2174/1570180820666230224112505
10) Hassan, J., Saeed, S. M., Deka, L., Uddin, M. J., & Das, D. B. (2024). Applications of Machine Learning (ML) and Mathematical Modeling (MM) in Healthcare with Special Focus on Cancer Prognosis and Anticancer Therapy: Current Status and Challenges. Pharmaceutics, 16(2), 260. https://doi.org/10.3390/pharmaceutics16020260
11) Daina, A., Michielin, O., & Zoete, V. (2017). SwissADME: a free web tool to evaluate pharmacokinetics, drug-likeness and medicinal chemistry friendliness of small molecules. In Scientific Reports (Vol. 7, Issue 1). Springer Science and Business Media LLC. https://doi.org/10.1038/srep42717
12) Myung, Y., de Sá, A. G. C., & Ascher, D. B. (2024). Deep-PK: deep learning for small molecule pharmacokinetic and toxicity prediction. In Nucleic Acids Research (Vol. 52, Issue W1, pp. W469–W475). Oxford University Press (OUP). https://doi.org/10.1093/nar/gkae254

CHAPTER: 4

RESULTS AND DISCUSSION

4. Results and discussion:

4.1. Structure, physicochemical properties and physical appearance of synthesized compounds:

1) Thiazolidine-2,4-dione (TZD):

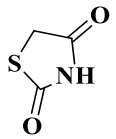

Thiazolidine-2,4-dione

TLC	Solubility		Melting Point	Recrystallization Solvent	Color	Percentage of yield
Hexane: Ethyl acetate (4:1) Rf= 0.6	$CHCl_3$	Soluble	113-120 ℃	EtOH	White	65%
	DMSO	Soluble				
	EtOH	Slightly Soluble				
	MeOH	Slightly Soluble				

2) SAI-1

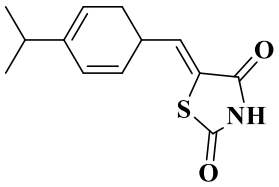

(*Z*)-5-((4-isopropylcyclohexa-2,4-dien-1-yl)methylene)thiazolidine-2,4-dione

TLC	Solubility		Melting Point	Recrystallization Solvent	Color	Percentage of yield
Hexane: Ethyl acetate (4:1) Rf= 0.7	$CHCl_3$	Soluble	160-162 ℃	MeOH	Cream color powder	98.32%
	EtOAc	Soluble				
	EtOH	Soluble				
	MeOH	Slightly Soluble				

3) SAI-2

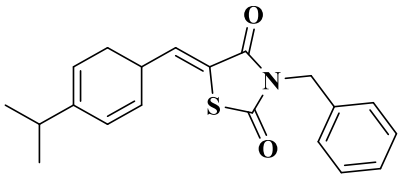

(*Z*)-3-benzyl-5-((4-isopropylcyclohexa-2,4-dien-1-yl)methylene) thiazolidine-2,4-dione

TLC	Solubility		Melting Point	Recrystallization Solvent	Color	Percentage of yield
Hexane: Ethyl acetate (4:1) Rf= 0.6	$CHCl_3$	Soluble	138-140 °C	MeOH	White Needle shaped crystal	79.12%
	EtOAc	Soluble				
	EtOH	Soluble				
	MeOH	Slightly Soluble				

4) SAI-3

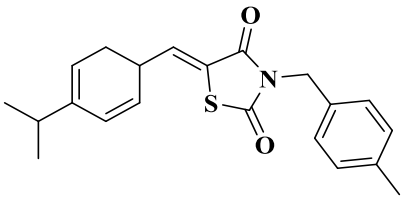

(*Z*)-5-((4-isopropylcyclohexa-2,4-dien-1-yl)methylene)-3-(4-methylbenzyl)thiazolidine-2,4-dione

TLC	Solubility		Melting Point	Recrystallization Solvent	Color	Percentage of yield
Hexane: Ethyl acetate (4:1) Rf= 0.5	$CHCl_3$	Soluble	130-132 °C	MeOH	White Needle shaped crystal	76.82%
	EtOAc	Soluble				
	EtOH	Soluble				
	MeOH	Slightly Soluble				

5) SAI-4

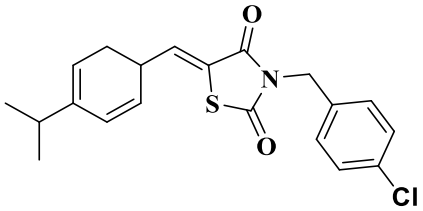

(*Z*)-3-(4-chlorobenzyl)-5-((4-isopropylcyclohexa-2,4-dien-1-yl)methylene)thiazolidine-2,4-dione

TLC	Solubility		Melting Point	Recrystallization Solvent	Color	Percentage of yield
Hexane: Ethyl acetate (4:1) Rf= 0.6	$CHCl_3$	Soluble	158-160 °C	MeOH	White Needle shaped crystal	77.22%
	EtOAc	Soluble				
	EtOH	Soluble				
	MeOH	Slightly Soluble				

6) SAI-5

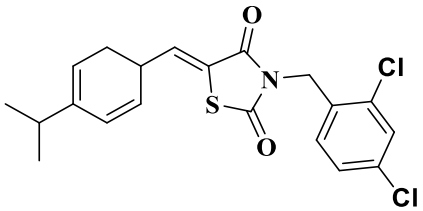

(*Z*)-3-(2,4-dichlorobenzyl)-5-((4-isopropylcyclohexa-2,4-dien-1-yl)methylene)thiazolidine-2,4-dione

TLC	Solubility		Melting Point	Recrystallization Solvent	Color	Percentage of yield
Hexane: Ethyl acetate (4:1) Rf= 0.7	$CHCl_3$	Soluble	142-144 °C	MeOH	White Needle shaped crystal	75.81%
	EtOAc	Soluble				
	EtOH	Soluble				
	MeOH	Slightly Soluble				

7) SAI-6

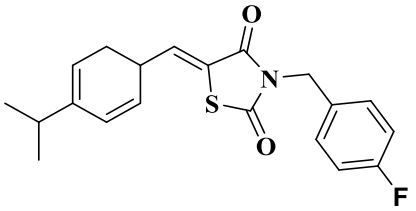

(*Z*)-3-(4-fluorobenzyl)-5-((4-isopropylcyclohexa-2,4-dien-1-yl)methylene)thiazolidine-2,4-dione

TLC	Solubility		Melting Point	Recrystallization Solvent	Color	Percentage of yield
Hexane: Ethyl acetate (4:1) Rf= 0.6	$CHCl_3$	Soluble	125-127 ℃	MeOH	White Needle shaped crystal	72.35%
	EtOAc	Soluble				
	EtOH	Soluble				
	MeOH	Slightly Soluble				

8) SAI-7

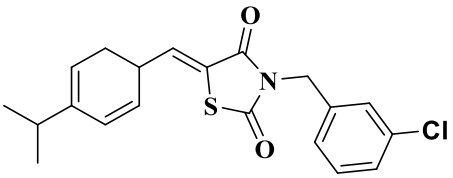

(*Z*)-3-(3-chlorobenzyl)-5-((4-isopropylcyclohexa-2,4-dien-1-yl)methylene)thiazolidine-2,4-dione

TLC	Solubility		Melting Point	Recrystallization Solvent	Color	Percentage of yield
Hexane: Ethyl acetate (4:1) Rf= 0.6	$CHCl_3$	Soluble	118-120 ℃	MeOH	White Needle shaped crystal	74.71%
	EtOAc	Soluble				
	EtOH	Soluble				
	MeOH	Slightly Soluble				

9) SAI-8

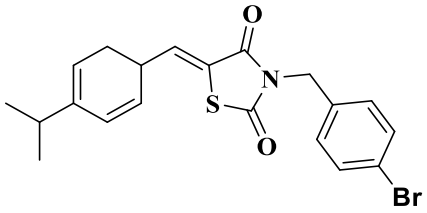

(*Z*)-3-(4-bromobenzyl)-5-((4-isopropylcyclohexa-2,4-dien-1-yl)methylene)thiazolidine-2,4-dione

TLC	Solubility		Melting Point	Recrystallization Solvent	Color	Percentage of yield
Hexane: Ethyl acetate (4:1) Rf= 0.7	$CHCl_3$	Soluble	158-160 °C	MeOH	White Needle shaped crystal	77.42%
	EtOAc	Soluble				
	EtOH	Soluble				
	MeOH	Slightly Soluble				

10) SAI-9

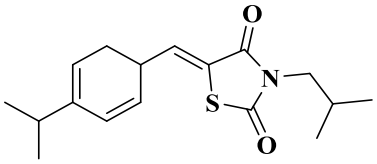

(*Z*)-3-isobutyl-5-((4-isopropylcyclohexa-2,4-dien-1-yl)methylene) thiazolidine-2,4-dione

TLC	Solubility		Melting Point	Recrystallization Solvent	Color	Percentage of yield
Hexane: Ethyl acetate (4:1) Rf= 0.6	$CHCl_3$	Soluble	104-106 °C	MeOH	White Needle shaped crystal	75.34%
	EtOAc	Soluble				
	EtOH	Soluble				
	MeOH	Slightly Soluble				

11) SAI-10

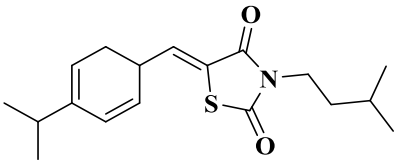

(*Z*)-3-isopentyl-5-((4-isopropylcyclohexa-2,4-dien-1-yl)methylene)thiazolidine-2,4-dione

TLC	Solubility		Melting Point	Recrystallization Solvent	Color	Percentage of yield
Hexane: Ethyl acetate (4:1) Rf= 0.5	$CHCl_3$	Soluble	109-111 °C	MeOH	White Needle shaped crystal	72.41%
	EtOAc	Soluble				
	EtOH	Soluble				
	MeOH	Slightly Soluble				

12) SAI-11

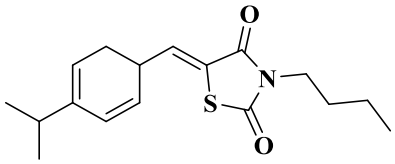

(*Z*)-3-butyl-5-((4-isopropylcyclohexa-2,4-dien-1-yl)methylene) thiazolidine-2,4-dione

TLC	Solubility		Melting Point	Recrystallization Solvent	Color	Percentage of yield
Hexane: Ethyl acetate (4:1) Rf= 0.6	$CHCl_3$	Soluble	80-82 °C	MeOH	White Needle shaped crystal	73.58%
	EtOAc	Soluble				
	EtOH	Soluble				
	MeOH	Slightly Soluble				

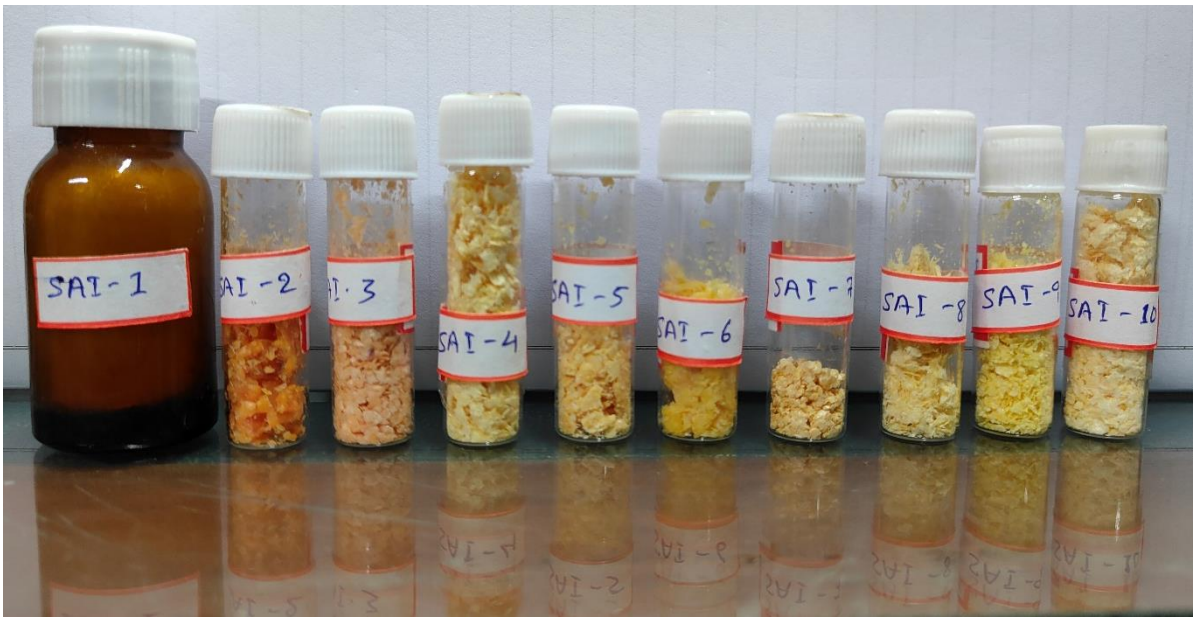

Figure 18: Picture of synthesized crude compounds.

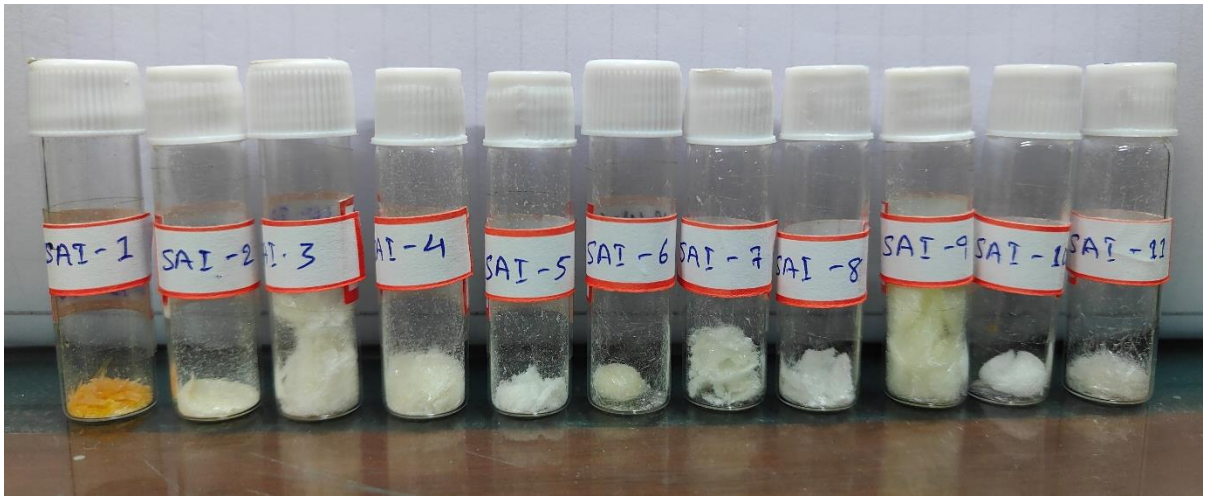

Figure 19: Picture of recrystallized compounds.

4.2. Characterization of synthesized compounds via NMR, FT-IR spectra, and Mass spectrometry:

1) Thiazolidine-2,4-dione (TZD):

^{1}H NMR (DMSO-d6) δ_H: 4.01 (2H, d, J = 12.3 Hz) 8.68 (1H, s). **FTIR** (cm-1); 2978.35,2885.66 (Ar-H), 3543.28 (-NH), 1808.99 (-C=O). FT-IR (ATR) υmax/cm^{-1}: 2978.35, 2885.66 (CH_2 str.), 3543.28 (-NH str.), 1736.51, 1808.99 (-C=O str.)

2) **SAI-1:**

^{1}H NMR (300 MHz, $CDCl_3$) δ 9.48 (s, 1H), 7.87 (s, 1H), 7.47 – 7.42 (m, 2H), 7.37 – 7.32 (m, 2H), 2.96 (p, *J* = 6.9 Hz, 1H), 1.27 (d, *J* = 6.9 Hz, 6H). **^{13}C NMR** (101 MHz, $CDCl_3$) δ 167.60, 167.02, 152.44, 134.70, 130.61, 130.54, 127.48, 121.09, 34.22, 29.72, 23.67. **FT-IR** (ATR) υmax/cm^{-1}: 3739.49 (-NH str.), 2385.53, 2312.26 (C-H str.), 1694.79, 1516.27 (CH_3-CH_3 str.)

3) **SAI-2:**

^{1}H NMR (400 MHz, $CDCl_3$) δ 7.89 (s, 1H), 7.45 (d, *J* = 1.8 Hz, 1H), 7.44 (s, 1H), 7.43 (s, 1H), 7.42 (s, 1H), 7.36 (d, *J* = 1.9 Hz, 1H), 7.34 (s, 1H), 7.32 (s, 1H), 7.29 (d, *J* = 7.8 Hz, 1H), 4.90 (s, 2H), 2.95 (p, *J* = 6.9 Hz, 1H), 1.27 (d, *J* = 6.9 Hz, 6H). **^{13}C NMR** (101 MHz, $CDCl_3$) δ 168.01, 166.33, 152.15, 145.38, 135.22, 134.24, 130.81, 130.50, 128.90, 128.76, 128.26, 127.43, 120.19, 45.24, 34.19, 23.68, 22.72. **FT-IR** (ATR) υmax/cm^{-1}: 3850.88, 3739.03, 3600.03 (Benzyl C-H str.), 2810.88 (CH_2 str.), 2312.29 (C-H str.), 1643.35 (C=O str.), 1513.07, 1378.21 (CH_3-CH_3 str.), 1169.35 (Benzyl C-H str.), 833.83 (Benzyl C-H str.)

4) **SAI-3:**

^{1}H NMR (400 MHz, $CDCl_3$) δ 7.88 (s, 1H), 7.44 (s, 1H), 7.42 (s, 1H), 7.35 (s, 1H), 7.33 (s, 1H), 7.31 (s, 1H), 7.15 (s, 1H), 7.13 (s, 1H), 4.86 (s, 2H), 2.95 (p, *J* = 7.0 Hz, 1H), 2.32 (s, 3H), 1.27 (d, *J* = 6.9 Hz, 6H). **^{13}C NMR** (101 MHz, $CDCl_3$) δ 167.99, 166.34, 152.08, 138.07, 134.09, 132.29, 130.86, 130.48, 129.40, 128.92, 127.41, 120.31, 45.02, 34.19, 23.68, 21.18. **FT-IR** (ATR) υmax/cm^{-1}: 3862.36, 3735.88 (Benzyl C-H str.), 3390.32 (CH_2 str.), 2311.48 (C-H str.), 1660.63 (C=O str.), 1516.37, 1375.09 (CH_3-CH_3 str.), 1160.64 (Benzyl C-H str.), 829.02 (Benzyl C-H str.)

5) SAI-4:

^{1}H NMR (400 MHz, $CDCl_3$) δ 7.89 (s, 1H), 7.43 (d, *J* = 7.9 Hz, 2H), 7.38 (d, *J* = 8.0 Hz, 2H), 7.31 (t, *J* = 9.3 Hz, 4H), 4.86 (s, 2H), 2.95 (p, *J* = 7.0 Hz, 1H), 1.27 (s, 3H), 1.26 (s, 3H). **^{13}C NMR** (101 MHz, $CDCl_3$) δ 167.96, 166.21, 152.28, 134.51, 134.28, 133.65, 130.73, 130.52, 130.40, 128.94, 127.45, 119.97, 60.43, 44.50, 34.20, 29.72, 23.67, 22.71, 21.07. **FT-IR** (ATR) υmax/cm-1: 3863.32, 3736.45 (Benzyl C-H str.), 3613.06 (CH2 str.), 2384.68, 2311.68 (C-H str.), 1667.07 (C=O str.), 1517.55, 1376.96 (CH3-CH3 str.), 1153.29 (Benzyl C-H str.), 698.46 (Benzyl C-H str.).

6) SAI-5:

^{1}H NMR (400 MHz, $CDCl_3$) δ 7.92 (d, *J* = 1.9 Hz, 1H), 7.48 – 7.43 (m, 2H), 7.41 (d, *J* = 2.7 Hz, 1H), 7.37 – 7.33 (m, 2H), 7.21 (d, *J* = 8.3 Hz, 1H), 7.16 (d, *J* = 1.9 Hz, 1H), 5.00 (d, *J* = 2.0 Hz, 2H), 3.00 – 2.92 (m, 1H), 1.29 – 1.28 (m, 3H), 1.26 (d, *J* = 2.1 Hz, 3H). **^{13}C NMR** (101 MHz, $CDCl_3$) δ 167.67, 166.06, 152.42, 134.84, 134.45, 133.97, 130.96, 130.67, 130.59, 129.75, 129.65, 127.49, 127.35, 119.63, 42.39, 37.11, 34.22, 29.72, 23.67, 22.72. **FT-IR** (ATR) υmax/cm^{-1}: 3850.82, 3736.94 (Benzyl C-H str.), 3598.64 (CH_2 str.), 2385.05, 2311.75 (C-H str.), 1696.13 (C=O str.), 1516.40, 1378.58 (CH_3-CH_3 str.), 704.09 (Benzyl C-H str.).

7) SAI-6:

^{1}H NMR (400 MHz, $CDCl_3$) δ 7.89 (s, 1H), 7.45 (d, *J* = 5.8 Hz, 2H), 7.42 (d, *J* = 1.7 Hz, 2H), 7.33 (d, *J* = 7.3 Hz, 2H), 7.05 – 6.98 (m, 2H), 4.86 (s, 2H), 2.95 (p, *J* = 6.8 Hz, 1H), 1.27 (s, 3H), 1.26 (d, *J* = 1.6 Hz, 3H). **^{13}C NMR** (101 MHz, $CDCl_3$) δ 167.99, 166.26, 163.87, 161.42, 152.23, 134.41, 131.11, 131.08, 130.97, 130.88, 130.75, 130.51, 127.44, 120.06, 115.75, 115.54, 44.47, 34.19, 23.67, 22.71. **FT-IR** (ATR) υmax/cm^{-1}: 3859.39, 3736.35 (Benzyl C-H str.), 3609.23 (CH_2 str.), 2387.81, 2309.36

(C-H str.), 1689.27 (C=O str.), 1513.01, 1378.06 (CH_3-CH_3 str.), 1158.86 (Benzyl C-H str.), 704.74 (Benzyl C-H str.).

8) **SAI-7:**

^{1}H NMR (400 MHz, $CDCl_3$) δ 7.90 (s, 1H), 7.45 (s, 1H), 7.43 (s, 2H), 7.33 (d, *J* = 8.1 Hz, 3H), 7.28 (s, 2H), 4.86 (s, 2H), 2.95 (p, *J* = 6.9 Hz, 1H), 1.28 (s, 3H), 1.26 (s, 3H). **^{13}C NMR** (101 MHz, $CDCl_3$) δ 167.92, 166.16, 152.29, 137.01, 134.60, 134.59, 130.73, 130.53, 130.04, 128.96, 128.53, 127.46, 127.06, 119.93, 44.57, 34.20, 31.95, 30.95, 23.67, 22.72. **FT-IR** (ATR) υmax/cm^{-1}: 3851.20, 3736.95 (Benzyl C-H str.), 3598.85 (CH_2 str.), 2311.78 (C-H str.), 1697.32 (C=O str.), 1516.57, 1378.48 (CH_3-CH_3 str.), 1168.88 (Benzyl C-H str.), 705.13 (Benzyl C-H str.).

9) **SAI-8:**

^{1}H NMR (400 MHz, $CDCl_3$) δ 7.89 (s, 1H), 7.46 (d, *J* = 8.2 Hz, 2H), 7.43 (d, *J* = 7.8 Hz, 2H), 7.32 (dd, *J* = 8.3, 3.2 Hz, 3H), 4.84 (s, 2H), 3.00 – 2.88 (m, 1H), 1.27 (d, *J* = 7.0 Hz, 6H). **^{13}C NMR** (101 MHz, $CDCl_3$) δ 167.95, 166.20, 162.08, 156.98, 152.29, 138.62, 134.88, 134.54, 134.15, 131.91, 130.71, 130.52, 127.45, 122.45, 119.95, 118.03, 44.55, 34.20, 23.66, 22.71. **FT-IR** (ATR) υmax/cm^{-1}: 3864.50, 3736.83 (Benzyl C-H str.), 3613.69 (CH_2 str.), 2385.16, 2311.72 (C-H str.), 1674.27 (C=O str.), 1516.47, 1378.20 (CH_3-CH_3 str.), 1161.49 (Benzyl C-H str.), 697.62 (Benzyl C-H str.).

10) **SAI-9:**

^{1}H NMR (400 MHz, $CDCl_3$) δ 7.87 (s, 1H), 7.45 (d, *J* = 7.9 Hz, 2H), 7.33 (d, *J* = 7.9 Hz, 2H), 3.58 (dd, *J* = 7.5, 1.3 Hz, 2H), 2.95 (p, *J* = 7.0 Hz, 1H), 2.18 – 2.10 (m, 1H), 1.27 (dd, *J* = 7.0, 1.3 Hz, 6H), 0.94 (dd, *J* = 6.7, 1.2 Hz, 6H). **^{13}C NMR** (101 MHz, $CDCl_3$) δ 168.33, 166.80, 152.02, 133.82, 130.92, 130.47, 127.40, 120.28, 114.92, 94.17, 49.04, 34.18, 30.94, 29.72, 27.24, 23.69, 19.98. **FT-IR** (ATR) υmax/cm^{-1}: 3864.47, 3736.81 (Benzyl C-H str.), 3391.67 (CH_2 str.), 2311.75 (C-H str.), 1696.46

(C=O str.), 1516.36, 1376.79 (CH_3-CH_3 str.), 1166.91 (CH-CH_3-CH_3 C-H str.), 830.57 (C-H str.).

11) SAI-10:

^{1}H NMR (400 MHz, $CDCl_3$) δ 7.87 (d, *J* = 2.0 Hz, 1H), 7.45 (dd, *J* = 8.3, 2.1 Hz, 2H), 7.33 (dd, *J* = 8.3, 2.1 Hz, 2H), 3.80 – 3.73 (m, 2H), 2.94 (dt, *J* = 13.1, 6.4 Hz, 1H), 1.62 (s, 1H), 1.59 – 1.51 (m, 2H), 1.27 (dd, *J* = 7.0, 2.0 Hz, 6H), 0.96 (dd, *J* = 6.4, 2.0 Hz, 6H). **^{13}C NMR** (101 MHz, $CDCl_3$) δ 168.08, 166.54, 152.01, 133.73, 130.91, 130.47, 127.40, 120.42, 86.66, 40.57, 36.47, 34.19, 25.97, 23.70, 22.37. **FT-IR** (ATR) υmax/cm^{-1}: 3864.23, 3736.39 (Benzyl C-H str.), 3598.58 (CH_2 str.), 2311.45 (C-H str.), 1696.27 (C=O str.), 1516.65, 1377.66 (CH_3-CH_3 str.), 1167.76 (CH-CH_3-CH_3 C-H str.), 831.40 (C-H str.).

12) SAI-11:

^{1}H NMR (400 MHz, $CDCl_3$) δ 7.81 (s, 1H), 7.40 – 7.36 (m, 2H), 7.27 (d, *J* = 7.1 Hz, 2H), 3.69 (t, *J* = 7.3 Hz, 2H), 2.89 (p, *J* = 6.7 Hz, 1H), 1.64 – 1.57 (m, 2H), 1.30 (h, *J* = 7.7 Hz, 2H), 1.23 – 1.18 (m, 6H), 0.89 (t, *J* = 7.3 Hz, 3H). **^{13}C NMR** (101 MHz, $CDCl_3$) δ 168.16, 166.60, 152.02, 133.76, 130.91, 130.47, 127.40, 120.40, 41.82, 34.19, 29.84, 29.73, 23.70, 20.00, 13.65. **FT-IR** (ATR) υmax/cm^{-1}: 3850.85, 3736.24 (Benzyl C-H str.), 3391.53 (CH_2 str.), 2311.70 (C-H str.), 1641.03 (C=O str.), 1375.72 (CH_3-CH_3 str.), 1259.77, 1166.60 (CH_2-CH_2-CH_2-CH_3 C-H str.), 830.04 (C-H str.).

4.2.1. ^{1}H NMR spectra of the synthesized compounds:

1) Thiazolidine-2,4-dione (TZD):

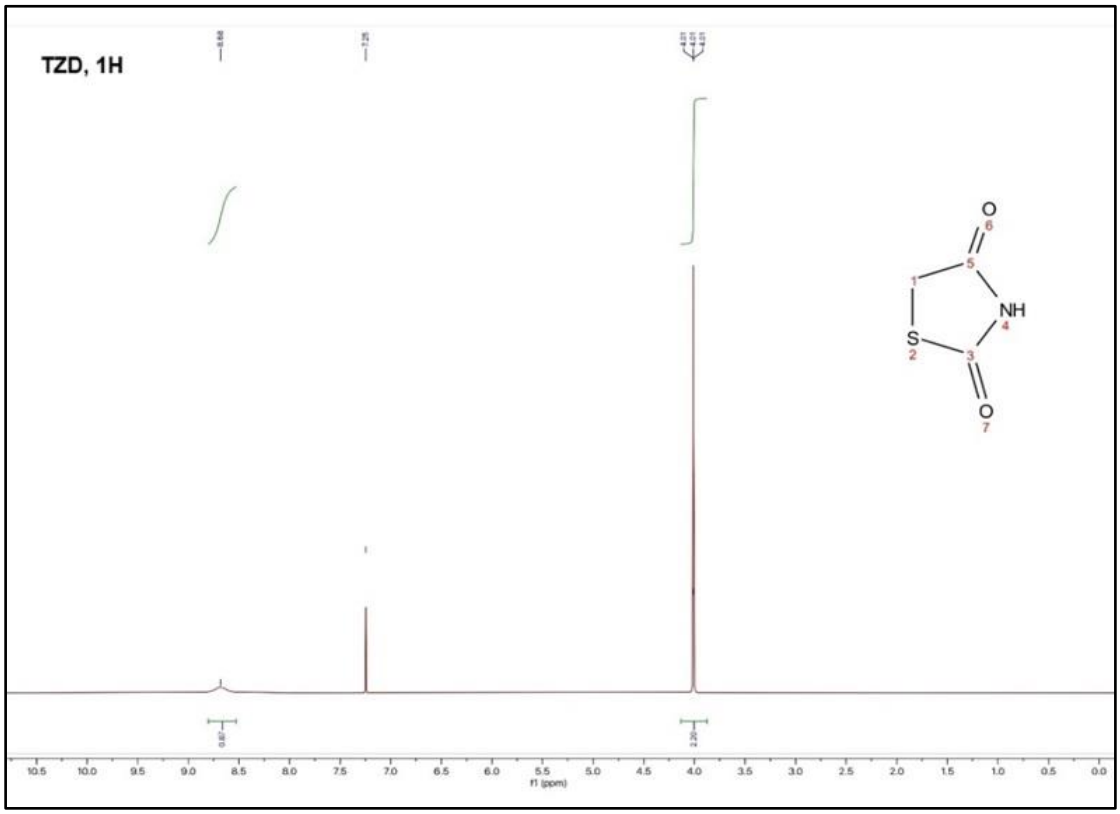

Figure 20: ^{1}H NMR spectra of Thiazolidine-2,4-dione.

2) SAI-1:

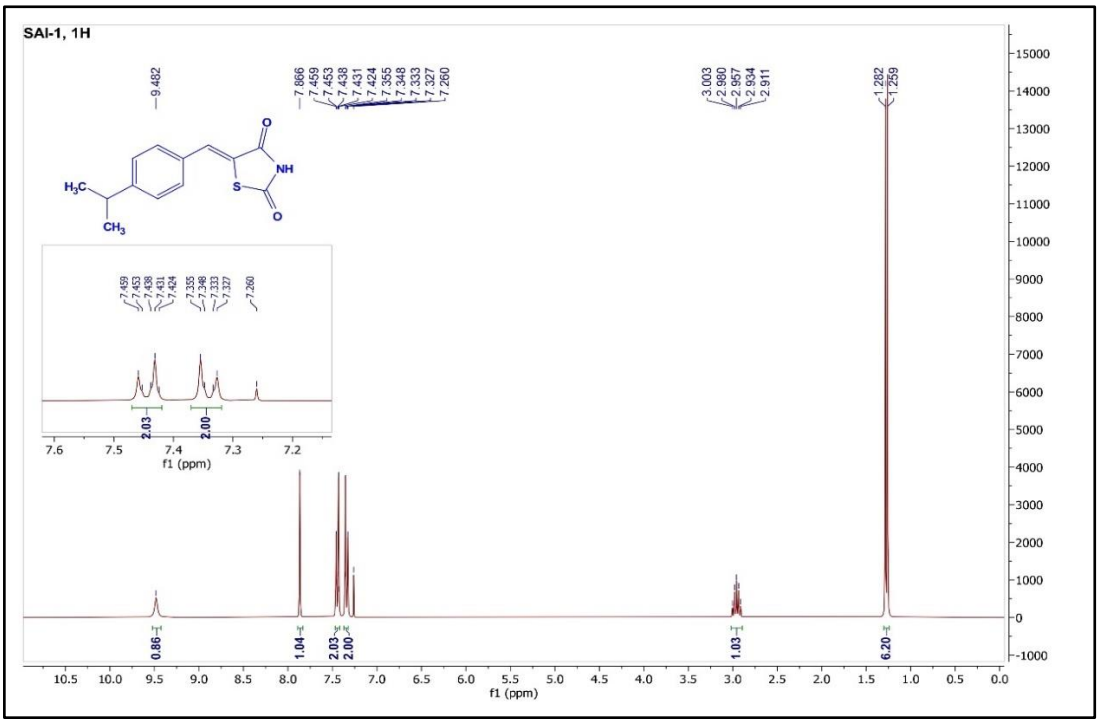

Figure 21: ^{1}H NMR spectra of SAI-1.

3) SAI-2:

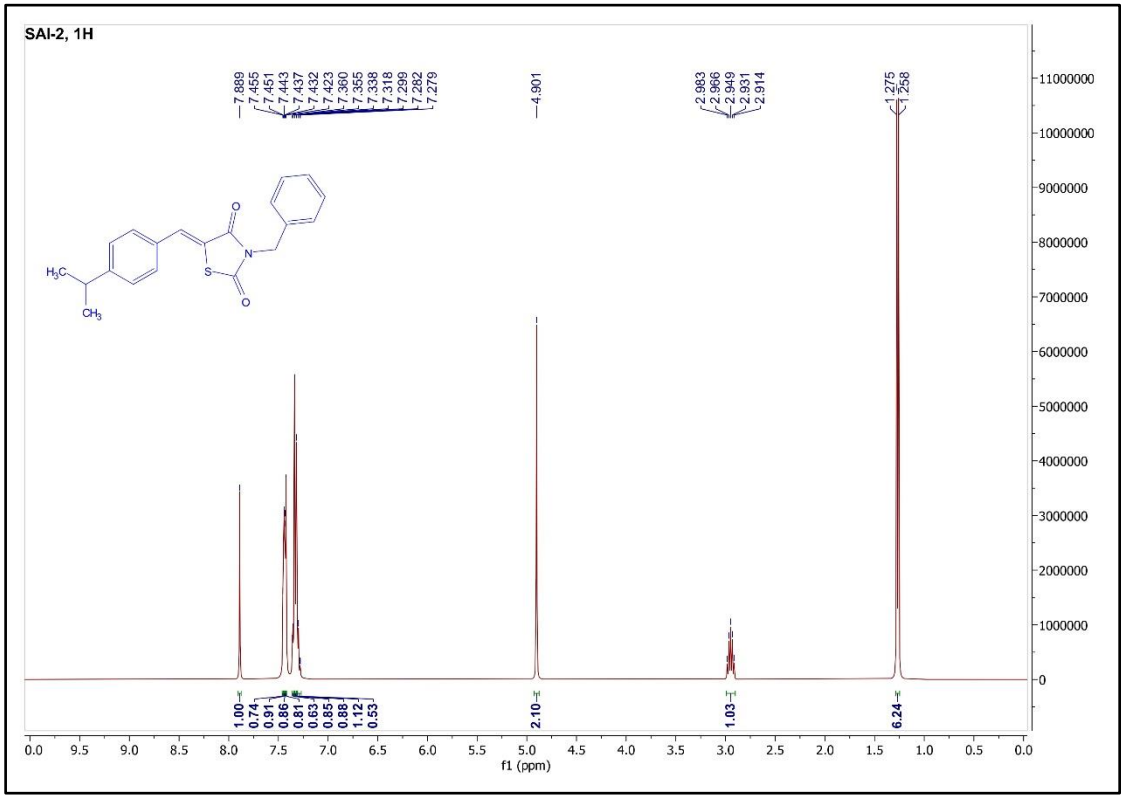

Figure 22: ^{1}H NMR spectra of SAI-2.

4) SAI-3:

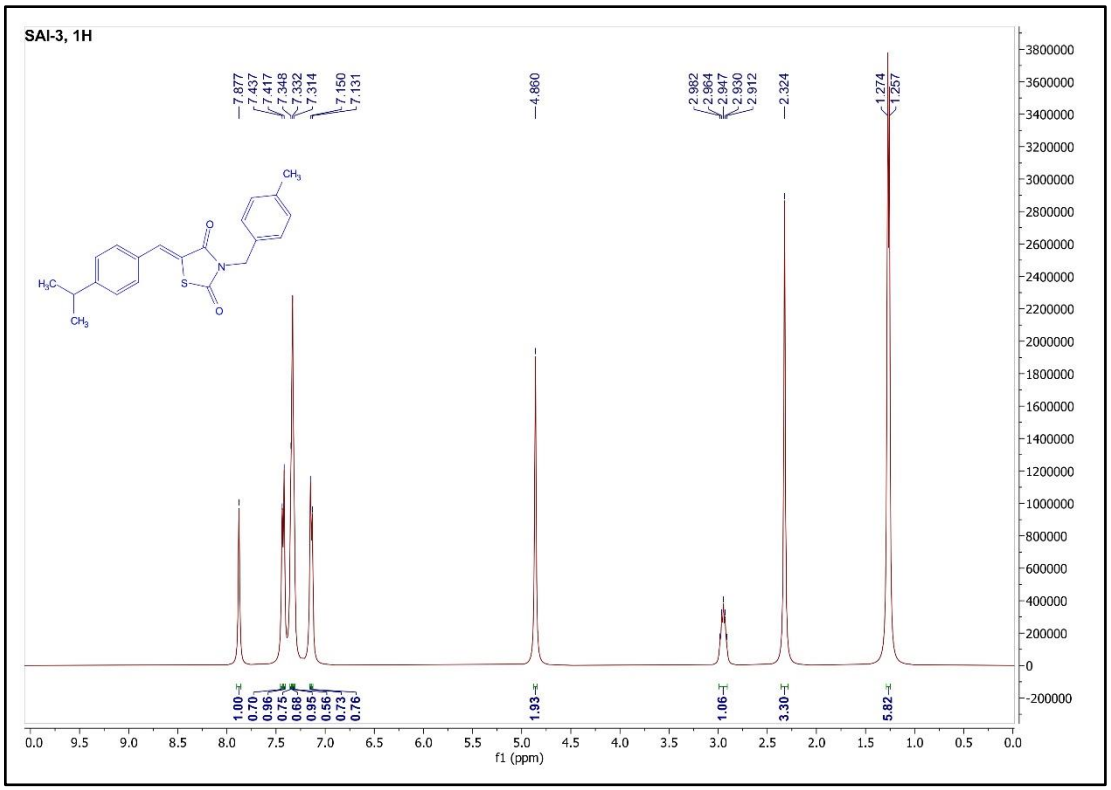

Figure 23: ^{1}H NMR spectra of SAI-3.

5) SAI-4:

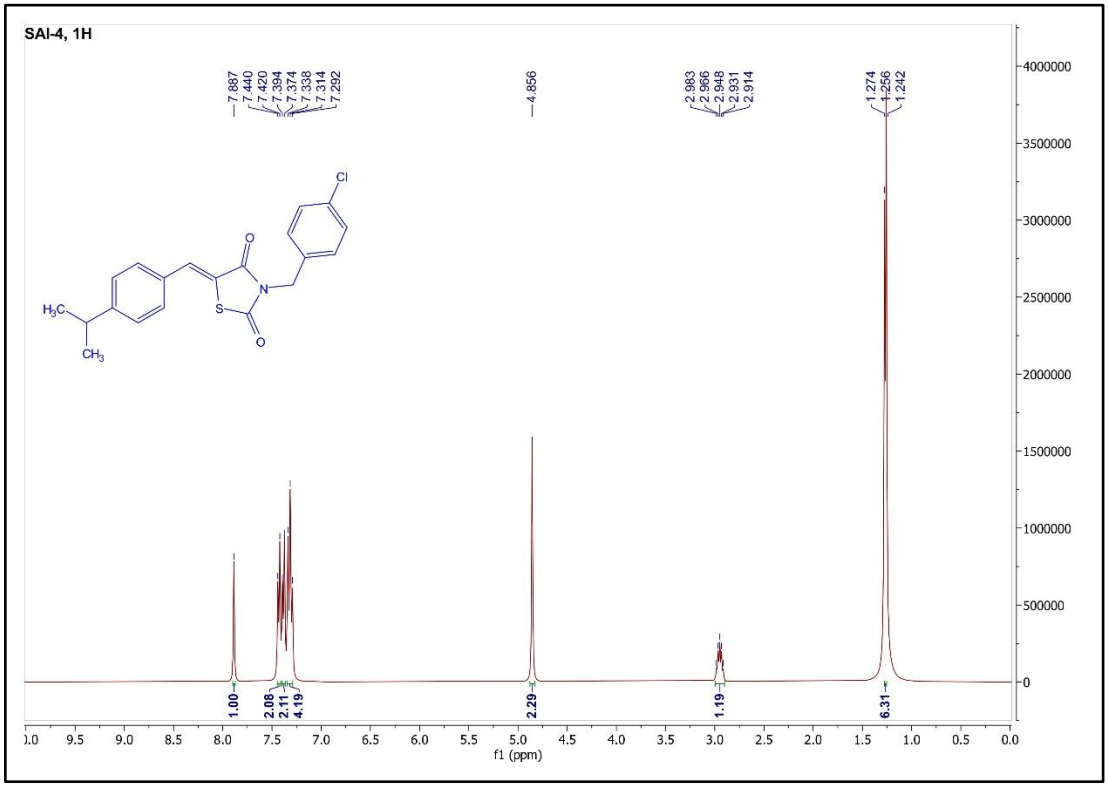

Figure 24: ^{1}H NMR spectra of SAI-4.

6) SAI-5:

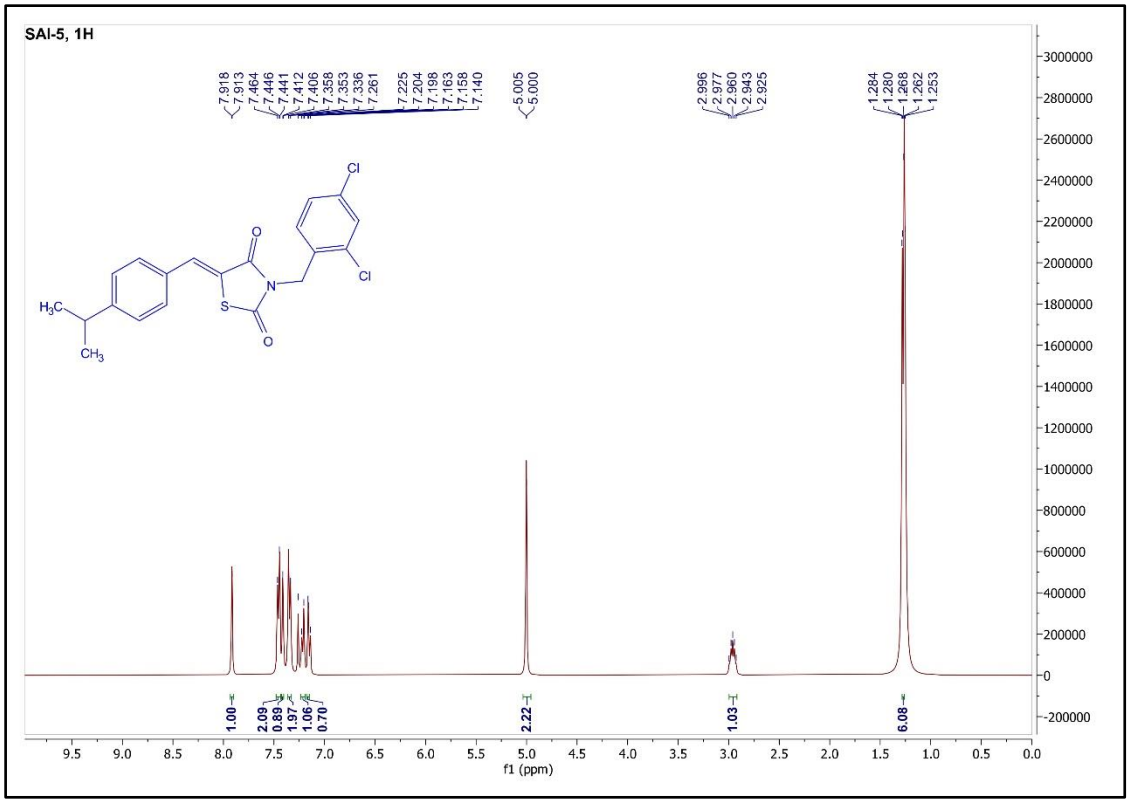

Figure 25: ^{1}H NMR spectra of SAI-5.

7) SAI-6:

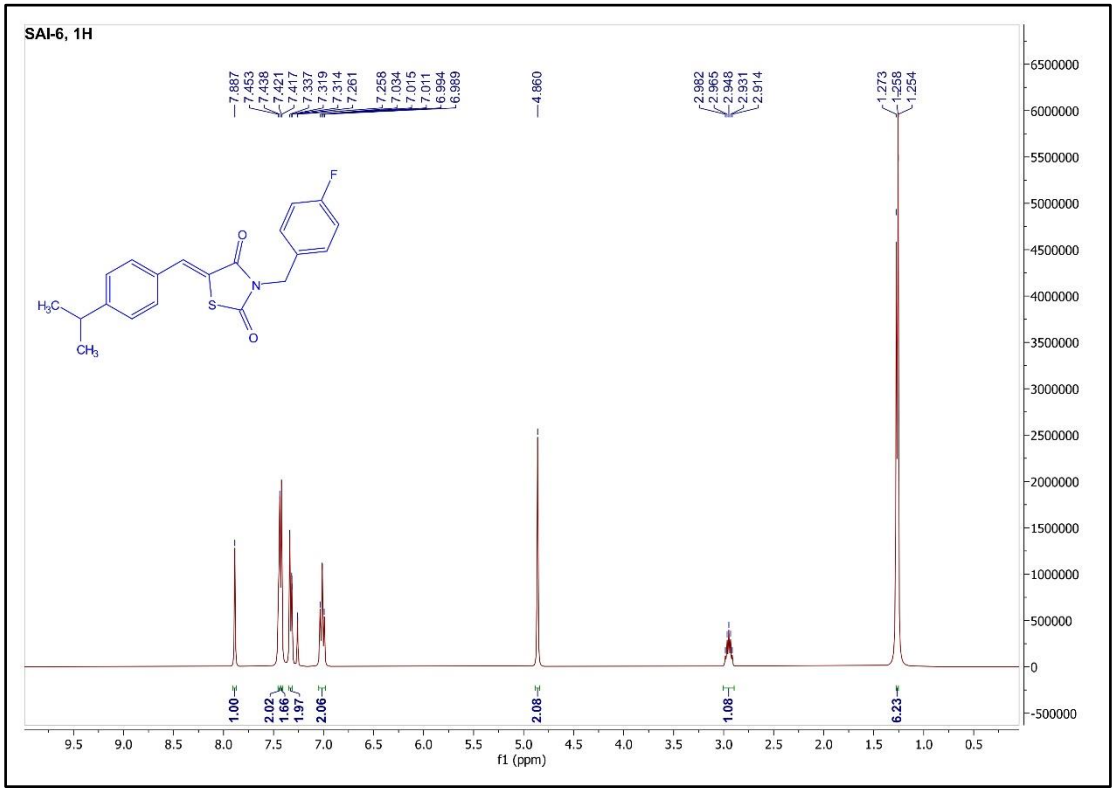

Figure 26: ^{1}H NMR spectra of SAI-6.

8) SAI-7:

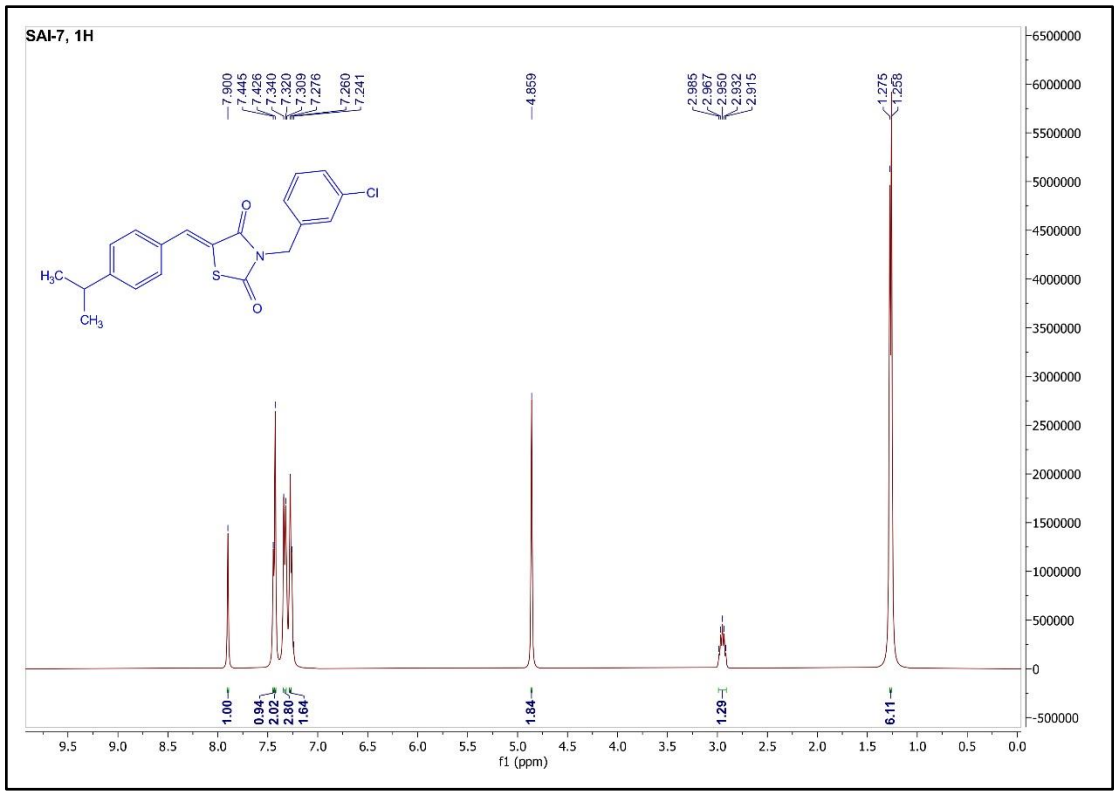

Figure 27: ^{1}H NMR spectra of SAI-7.

9) SAI-8:

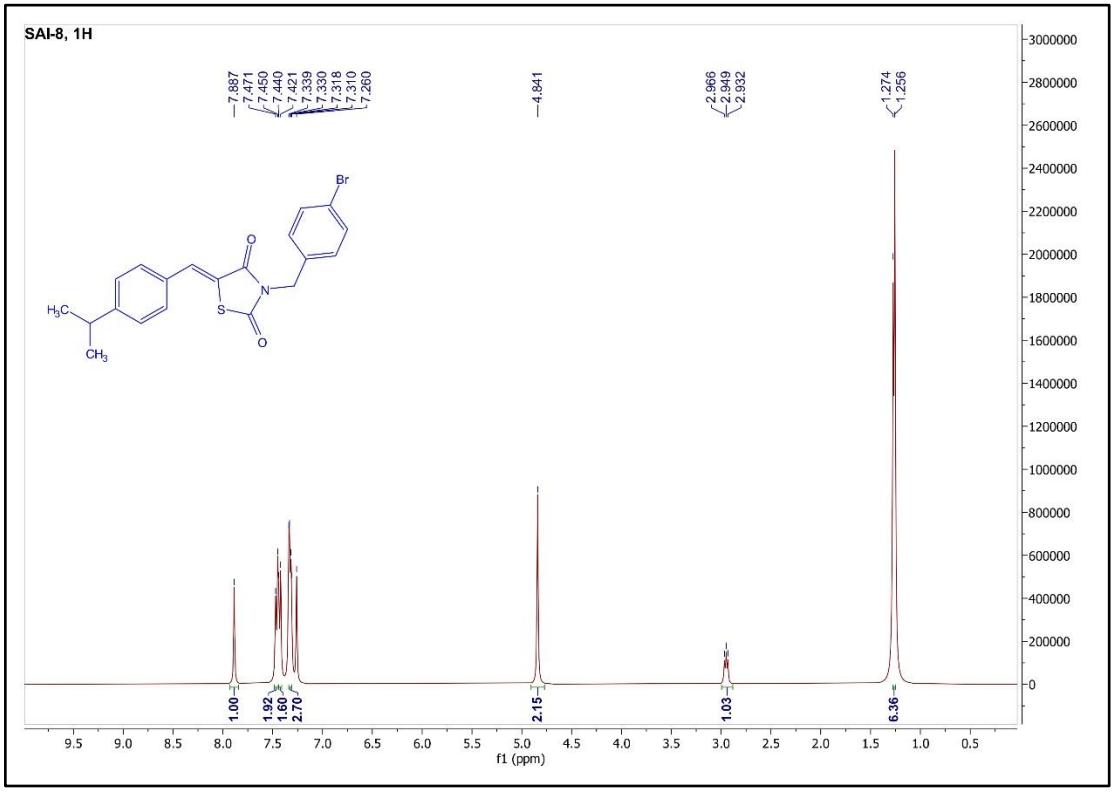

Figure 28: ^{1}H NMR spectra of SAI-8.

10) SAI-9:

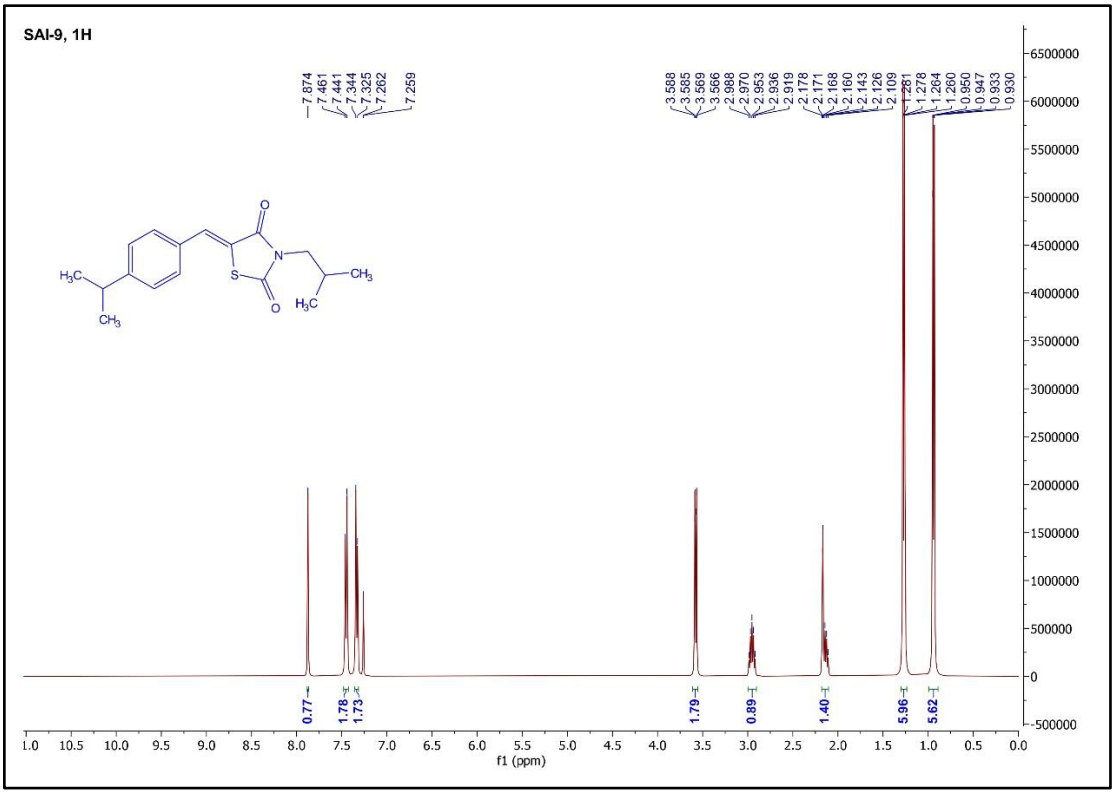

Figure 29: ^{1}H NMR spectra of SAI-9.

11) SAI-10:

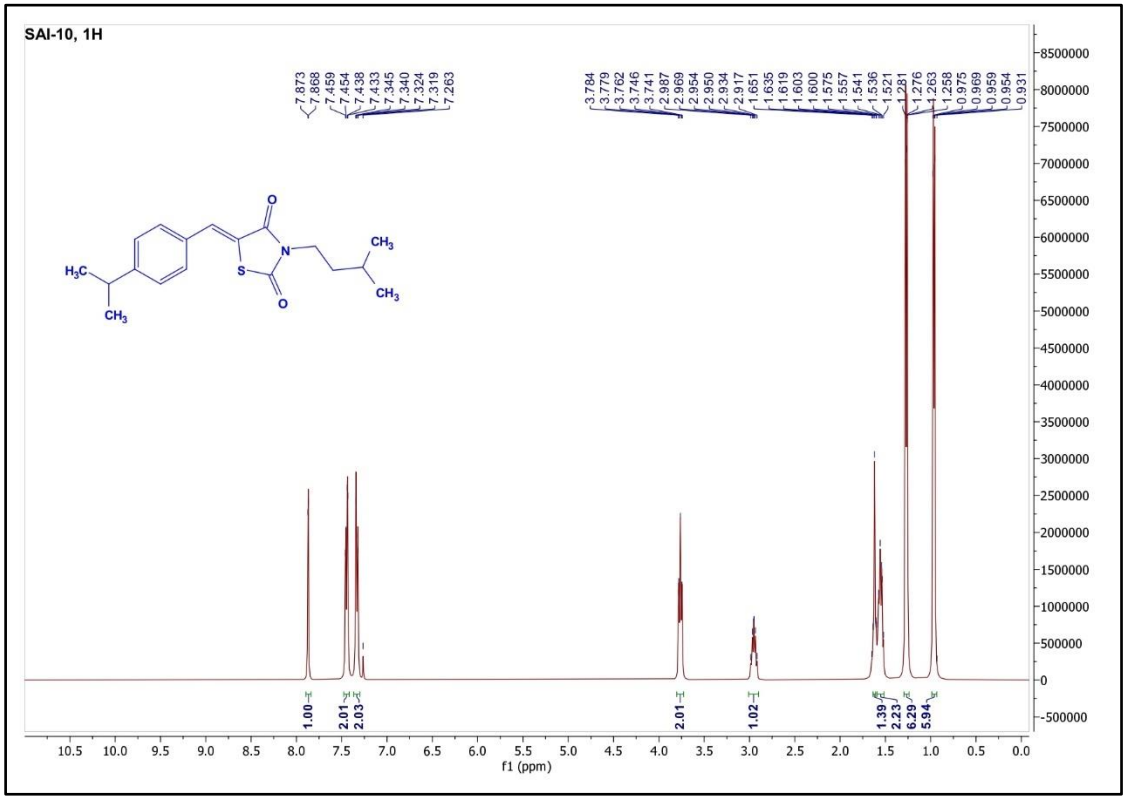

Figure 30: ^{1}H NMR spectra of SAI-10.

12) SAI-11:

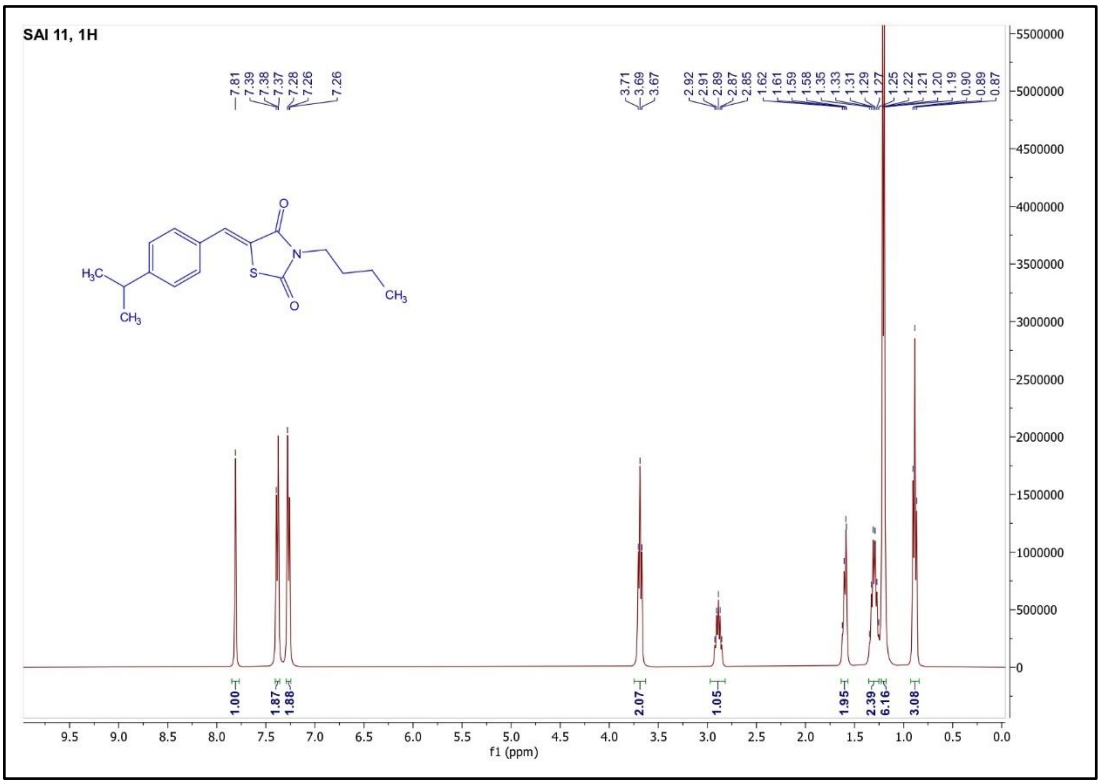

Figure 31: ^{1}H NMR spectra of SAI-11.

4.2.2. ^{13}C NMR spectra of the synthesized compounds:

1) SAI-1:

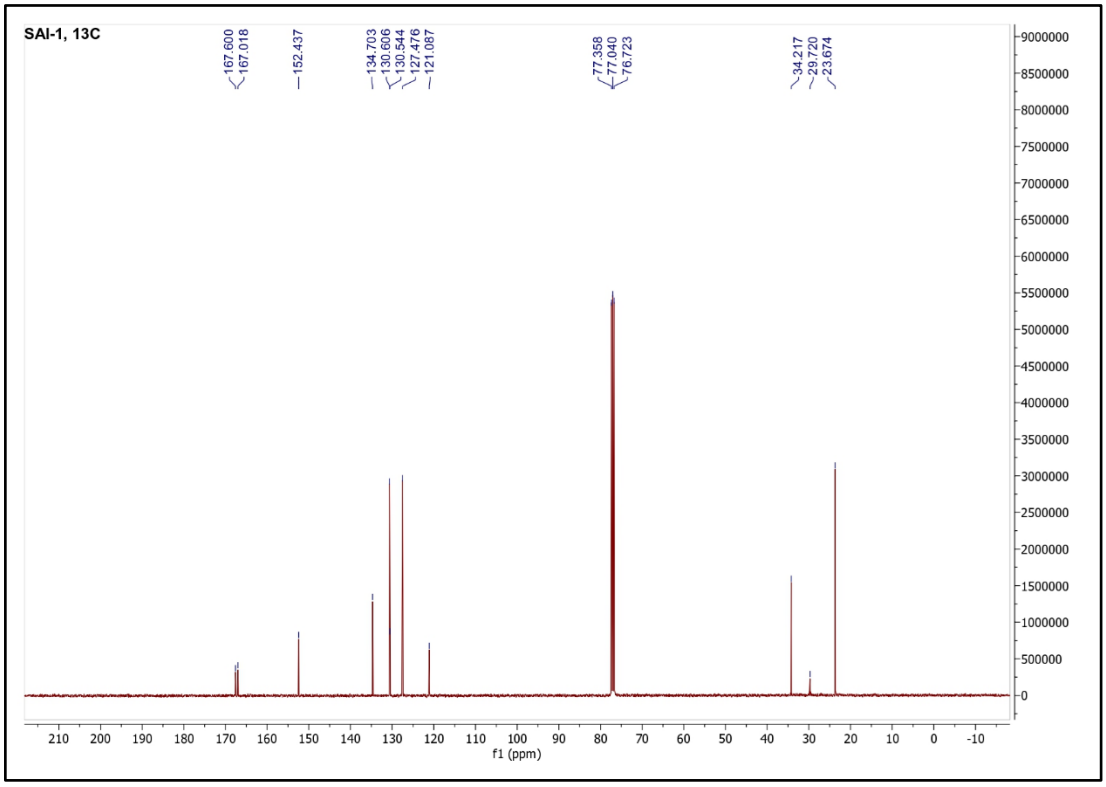

Figure 32: ^{13}C NMR spectra of SAI-1.

2) SAI-2:

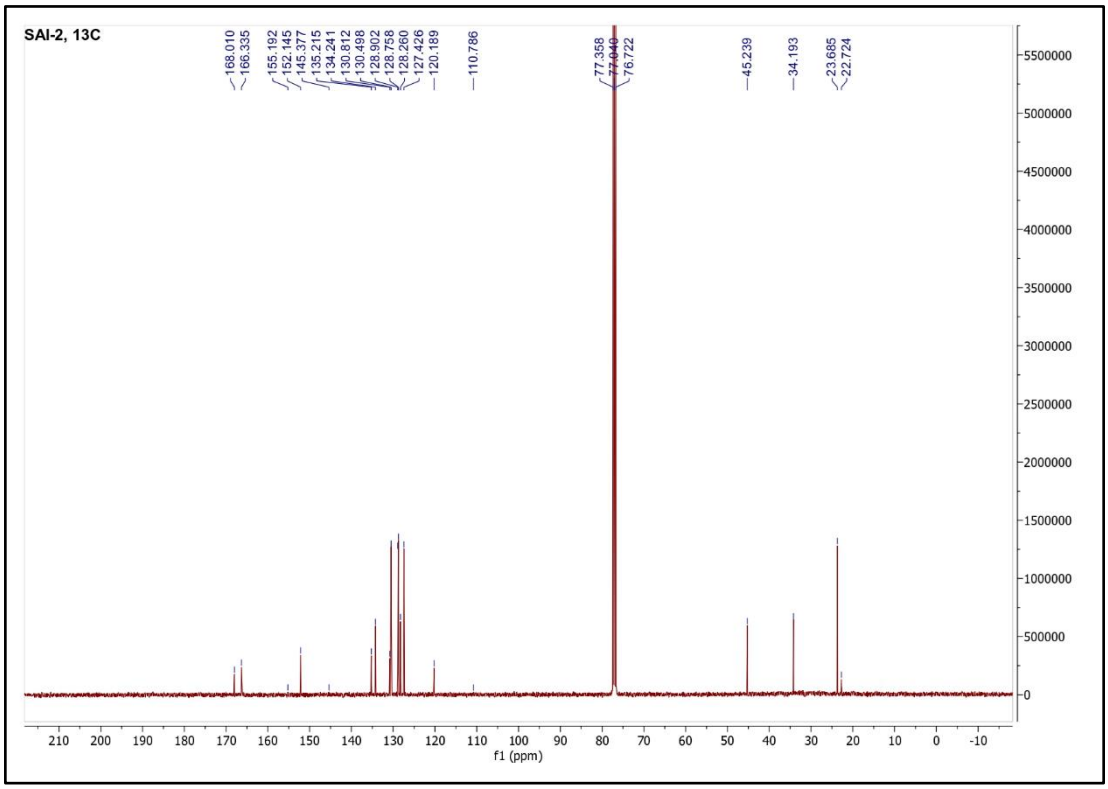

Figure 33: ^{13}C NMR spectra of SAI-2.

3) SAI-3:

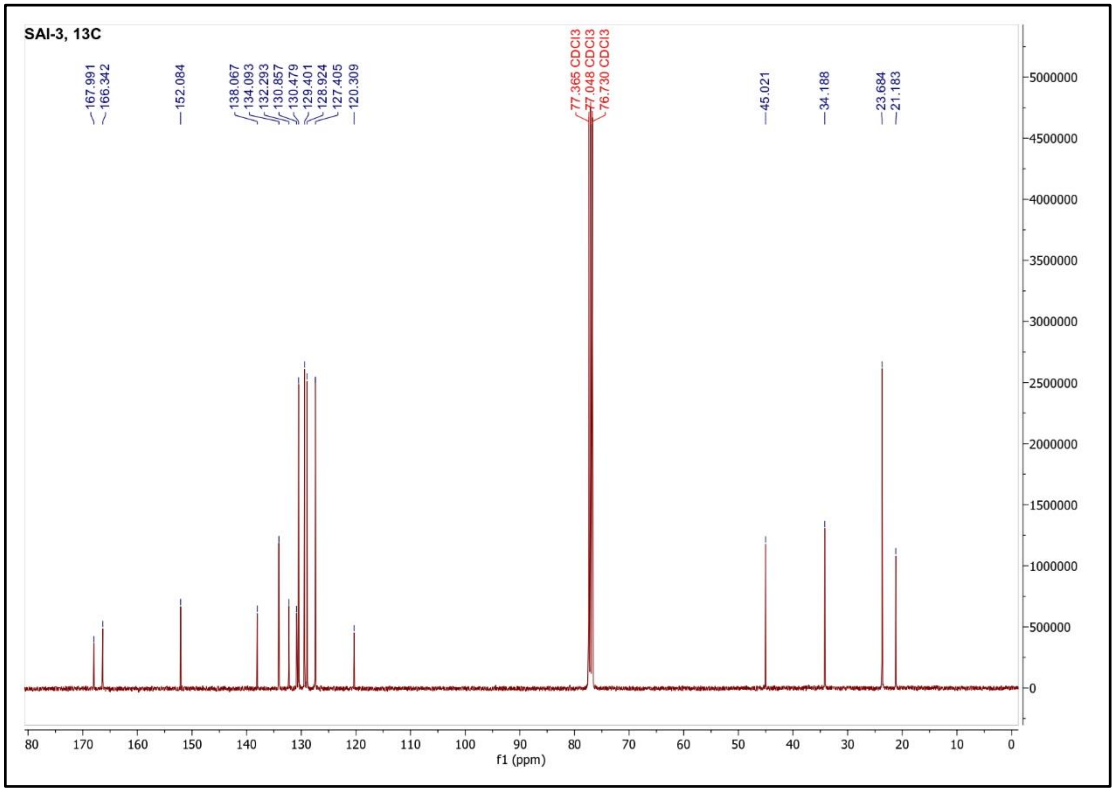

Figure 34: ^{13}C NMR spectra of SAI-3.

4) SAI-4:

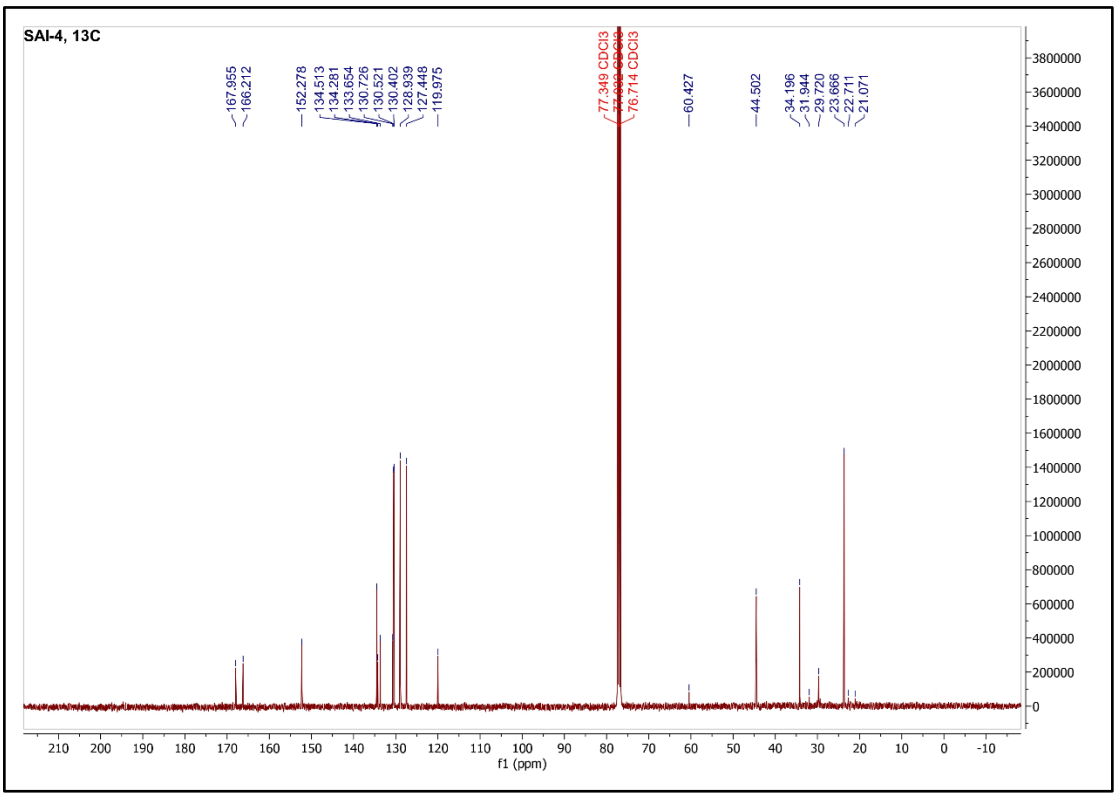

Figure 35: ^{13}C NMR spectra of SAI-4.

5) SAI-5:

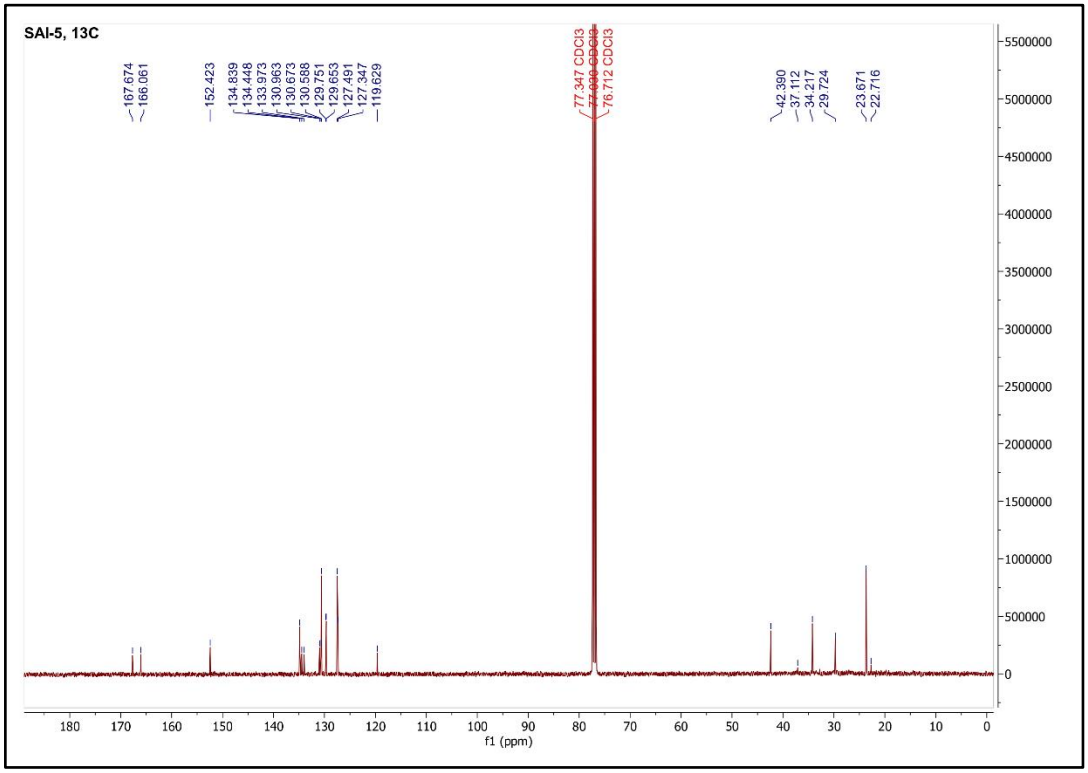

Figure 36: ^{13}C NMR spectra of SAI-5**.**

6) SAI-6:

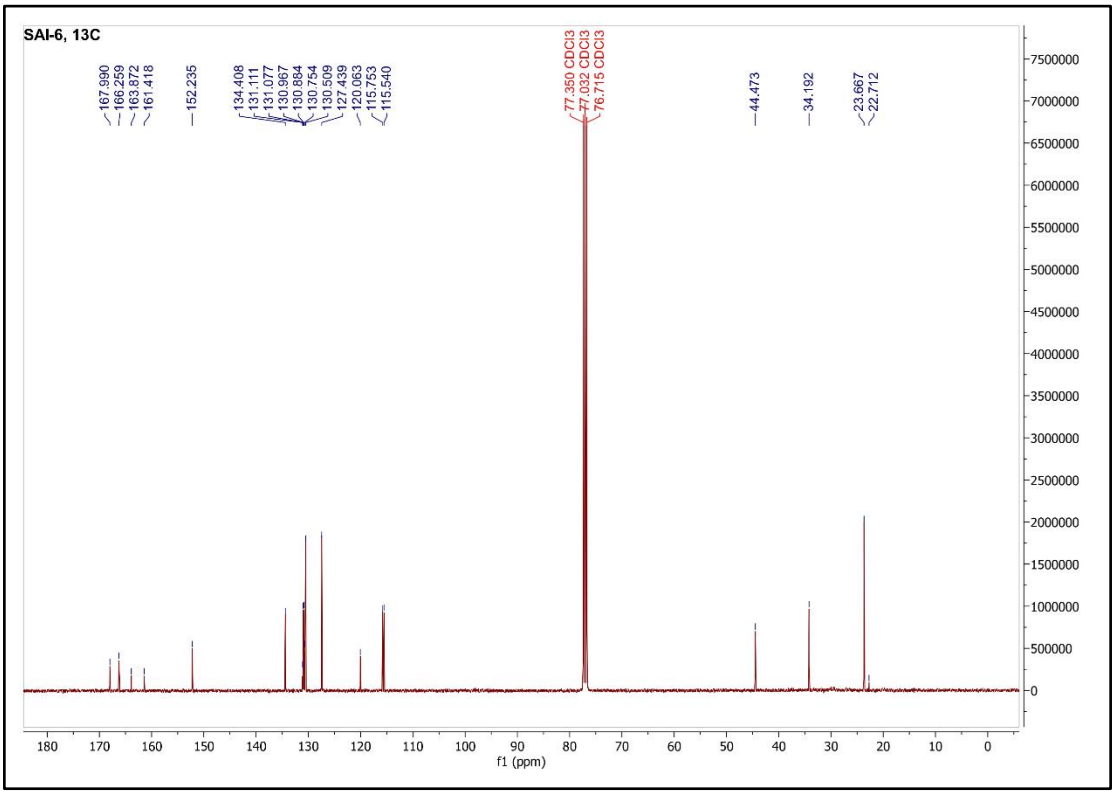

Figure 37: ^{13}C NMR spectra of SAI-6.

7) SAI-7:

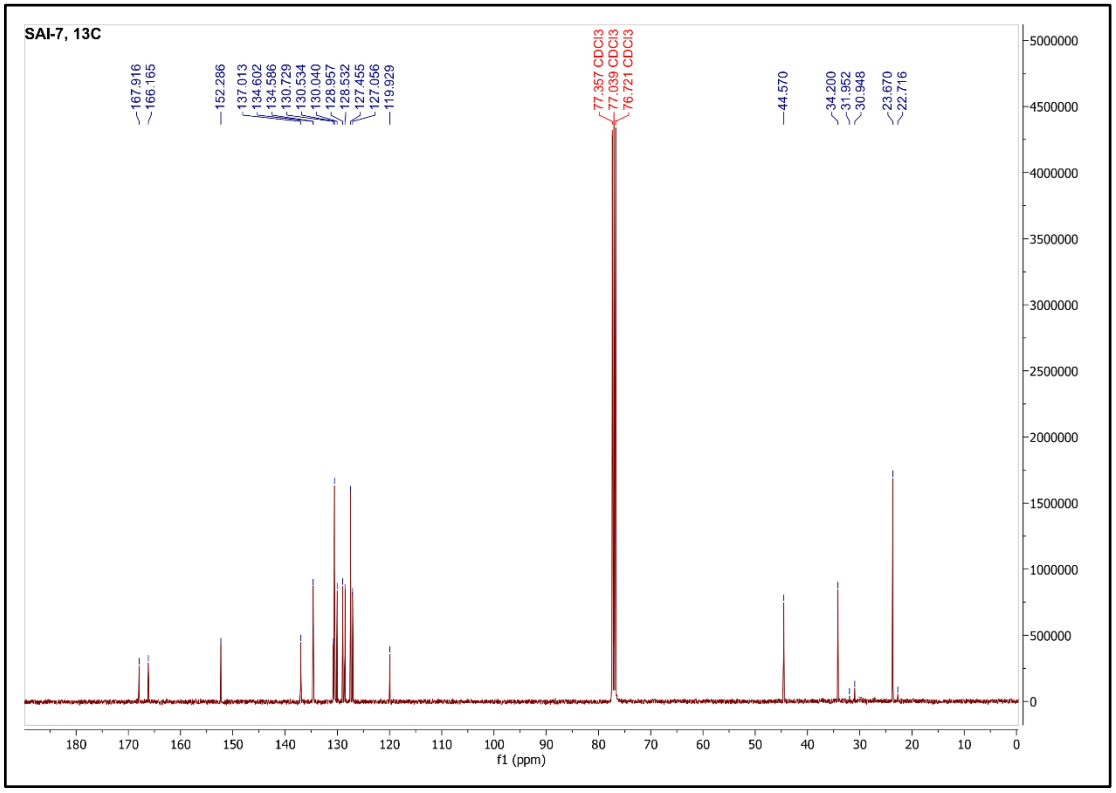

Figure 38: ^{13}C NMR spectra of SAI-7.

8) SAI-8:

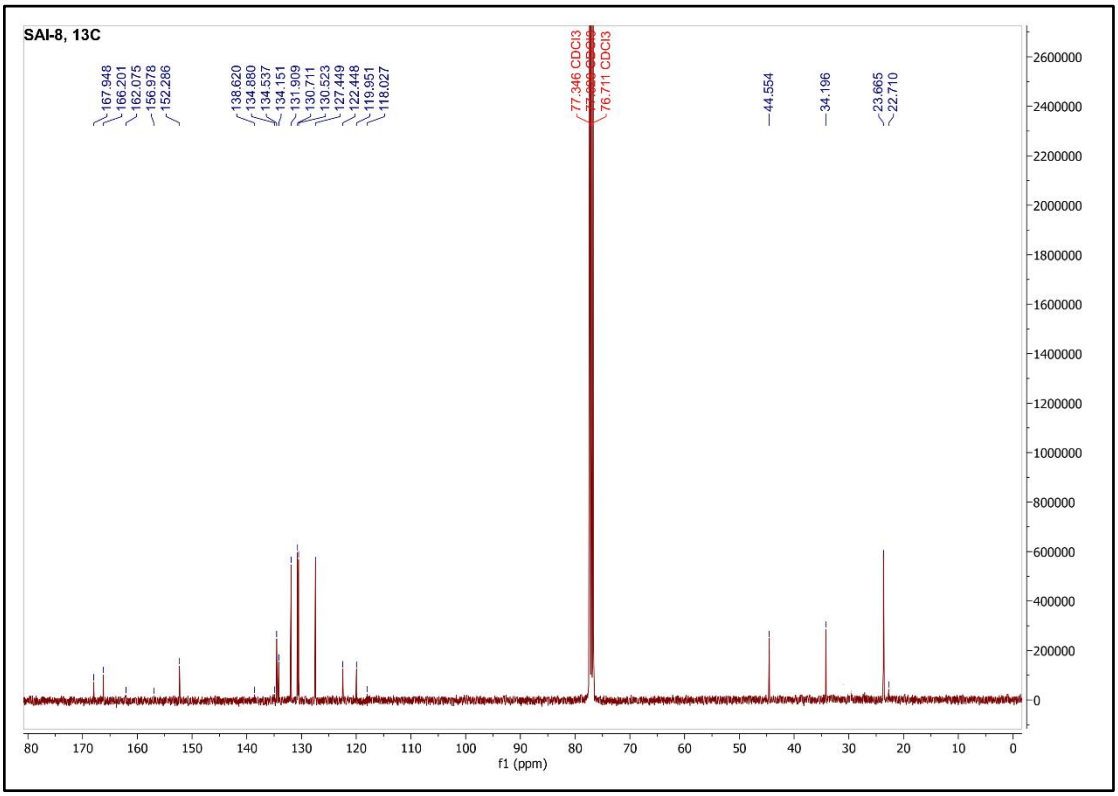

Figure 39: ^{13}C NMR spectra of SAI-8.

9) SAI-9:

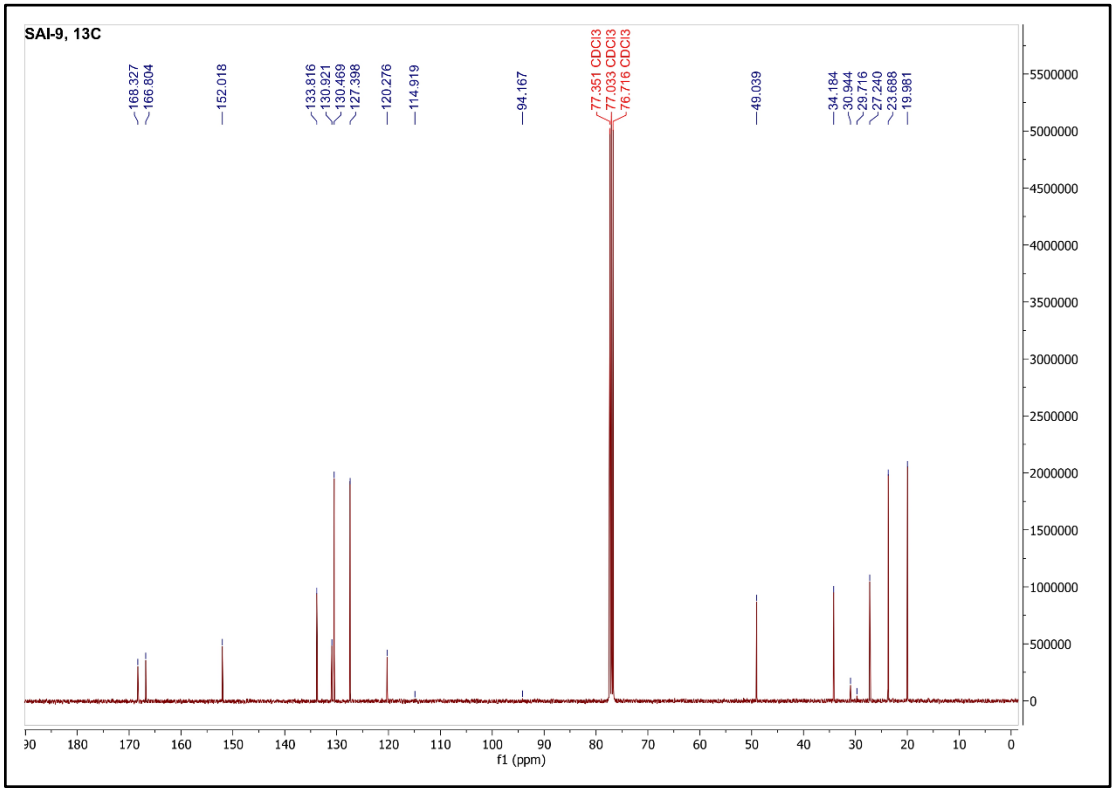

Figure 40: ^{13}C NMR spectra of SAI-9.

10) SAI-10:

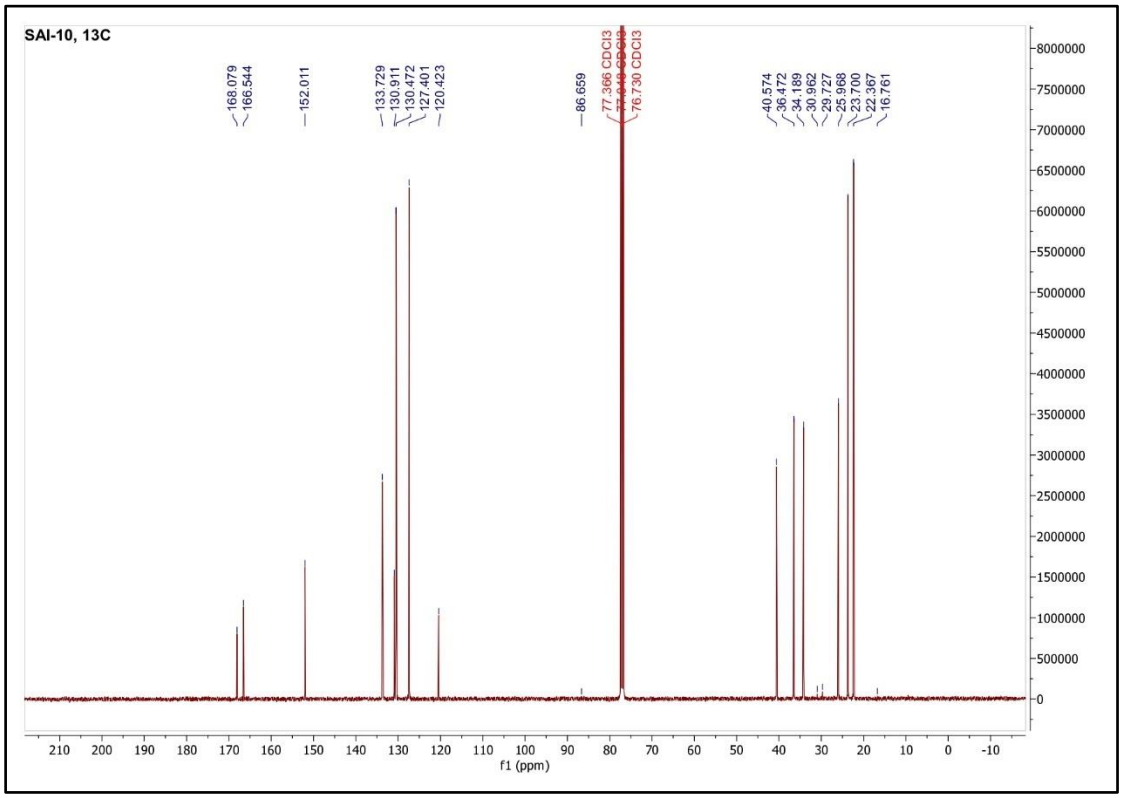

Figure 41: ^{13}C NMR spectra of SAI-10.

11) SAI-11:

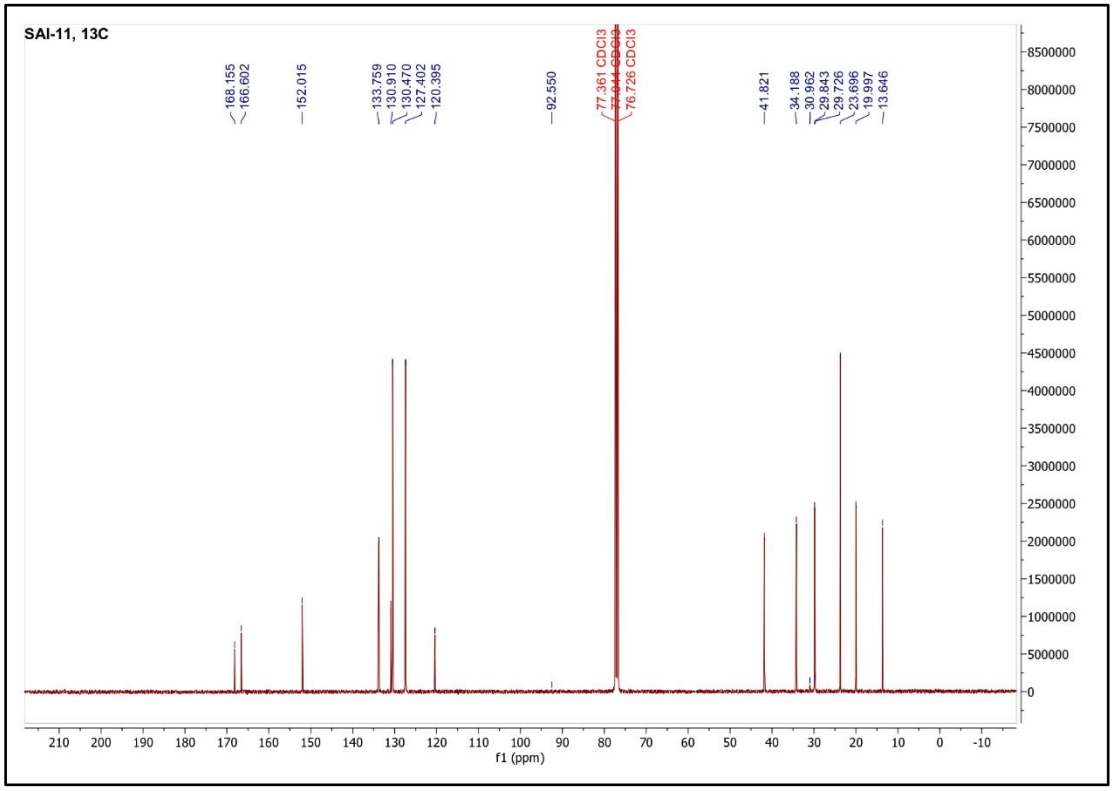

Figure 42: ^{13}C NMR spectra of SAI-11.

4.2.3. FT-IR spectra of the synthesized compounds:

1) Thiazolidine-2,4-dione (TZD):

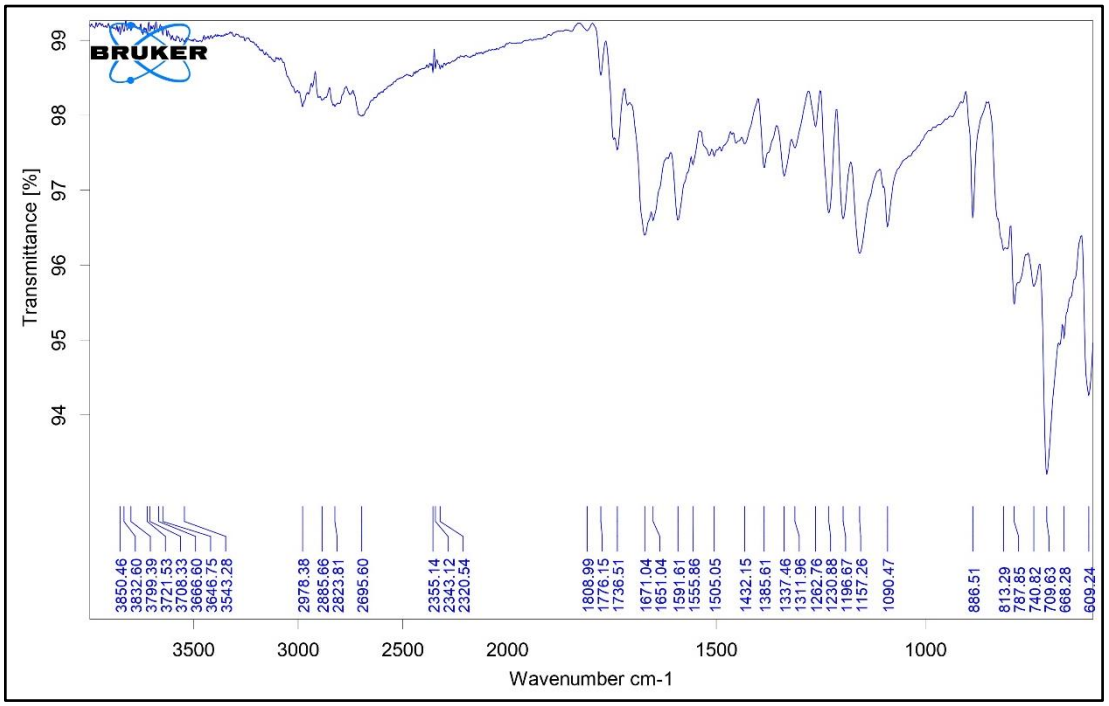

Figure 43: FT-IR spectra of TZD.

2) SAI-1:

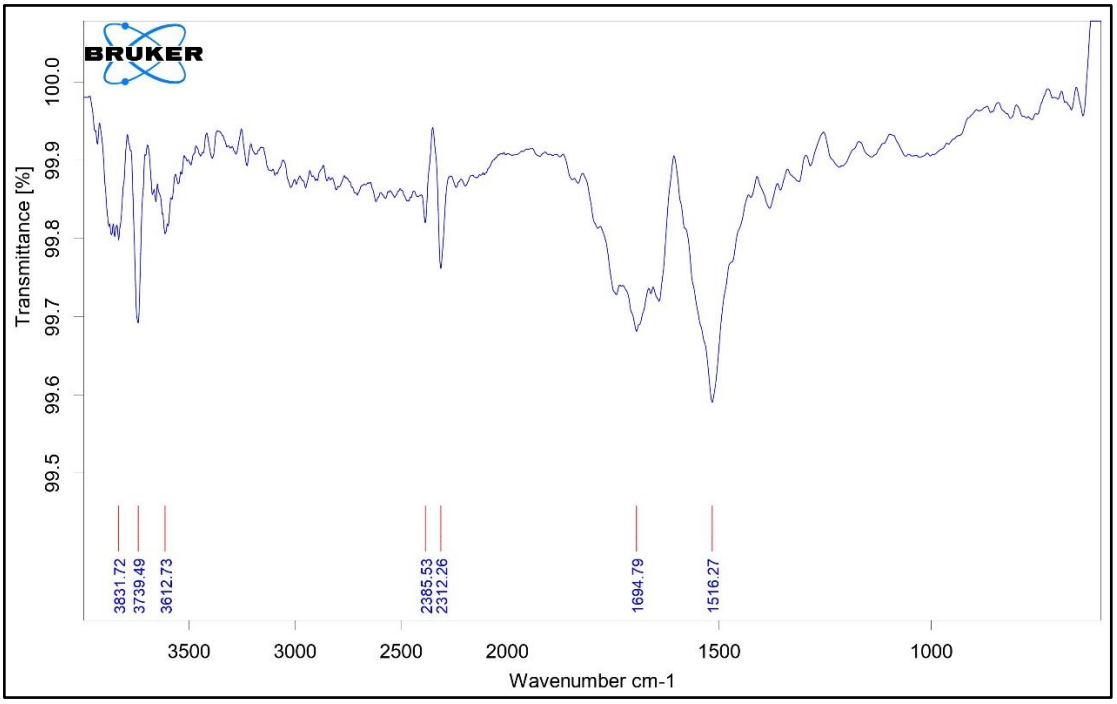

Figure 44: FT-IR spectra of SAI-1.

3) SAI-2:

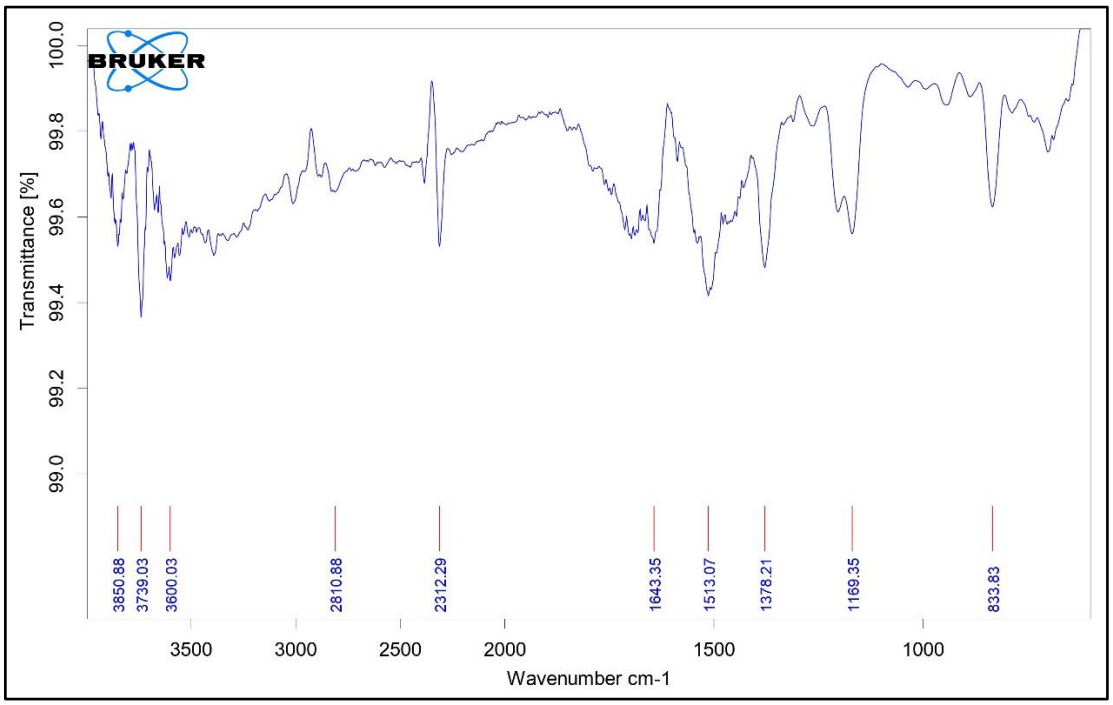

Figure 45: FT-IR spectra of SAI-2.

4) SAI-3:

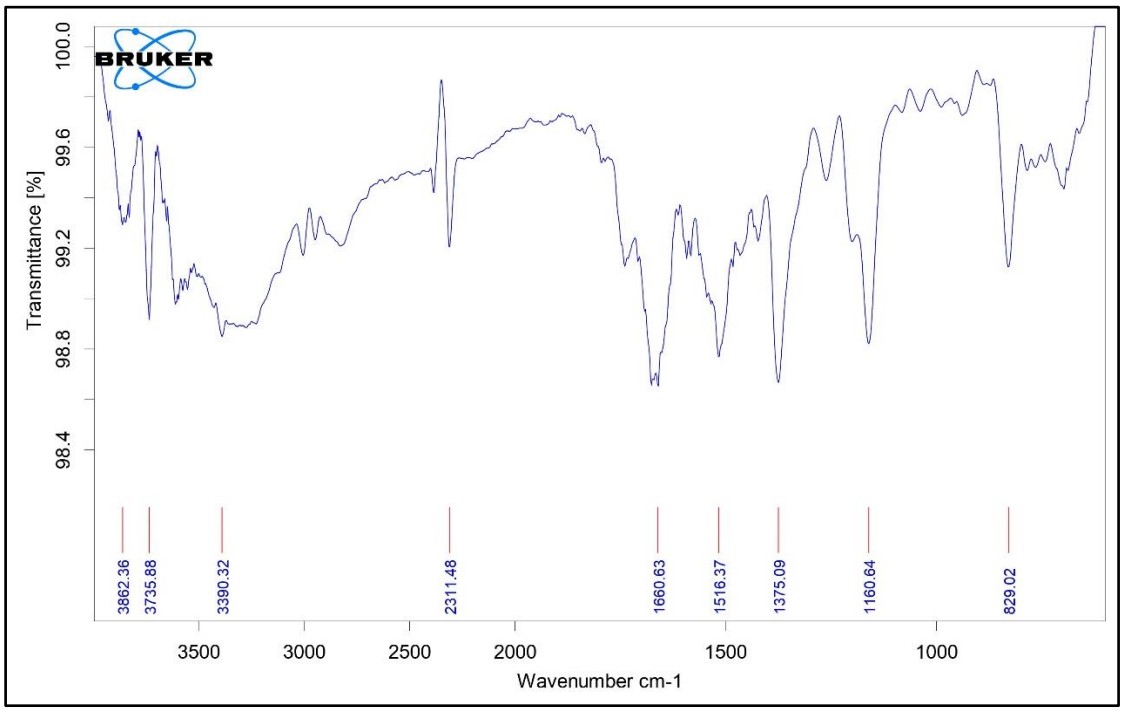

Figure 46: FT-IR spectra of SAI-3.

5) SAI-4:

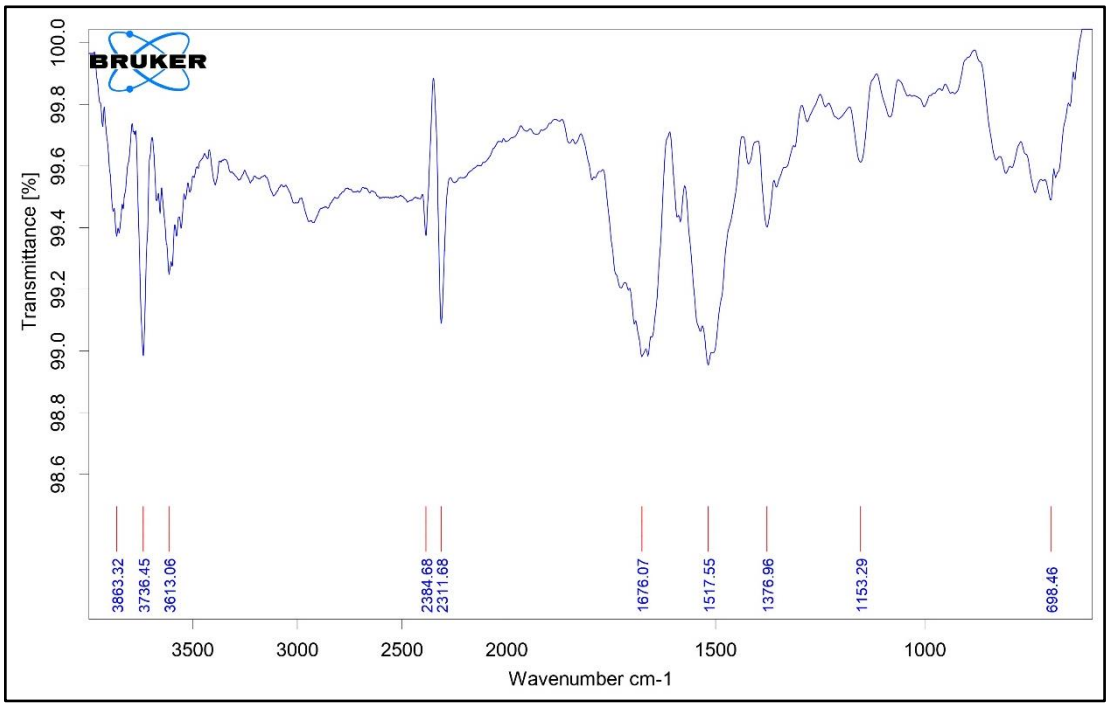

Figure 47: FT-IR spectra of SAI-4.

6) SAI-5:

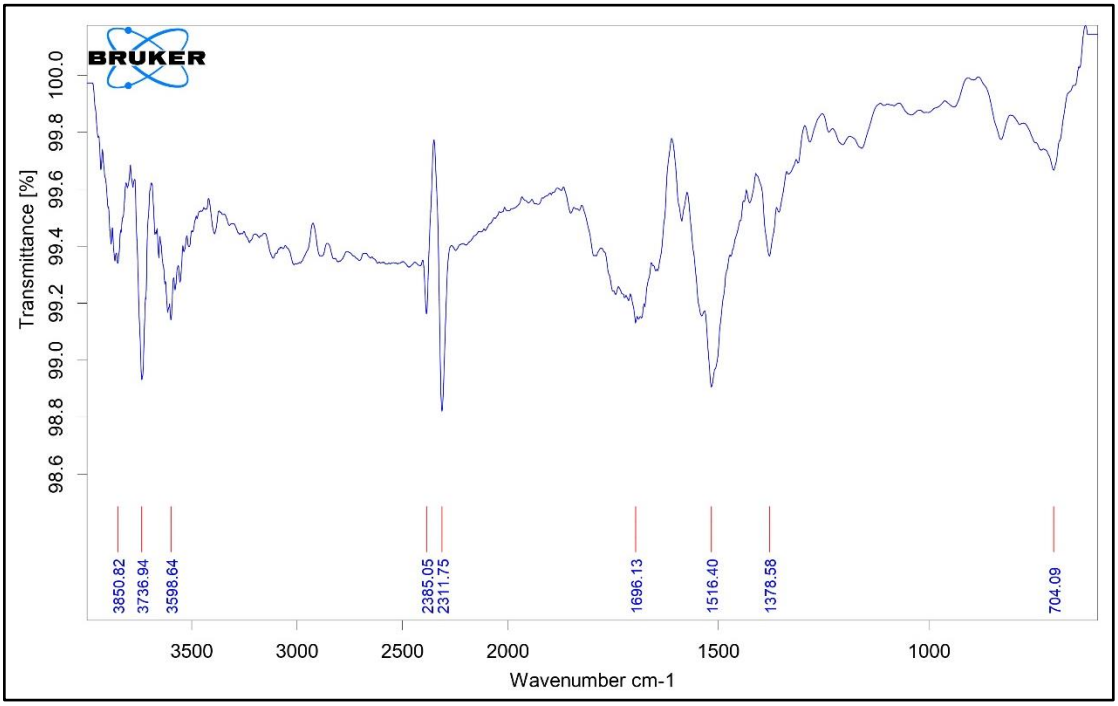

Figure 48: FT-IR spectra of SAI-5.

7) SAI-6:

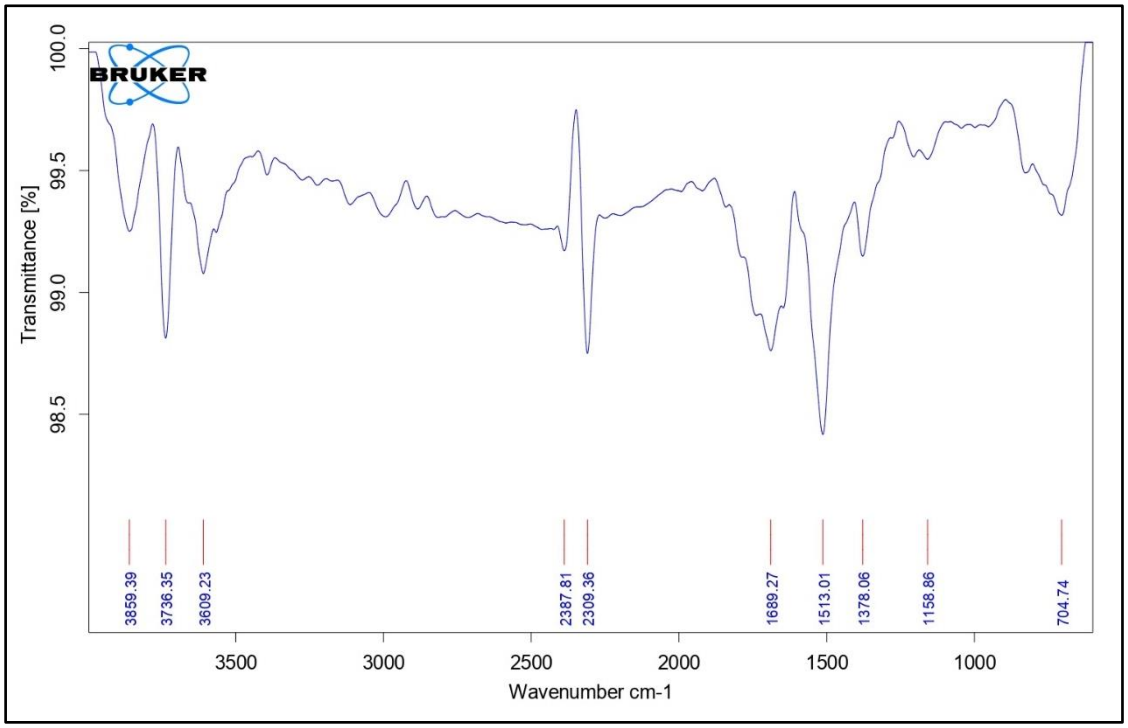

Figure 49: FT-IR spectra of SAI-6.

8) SAI-7:

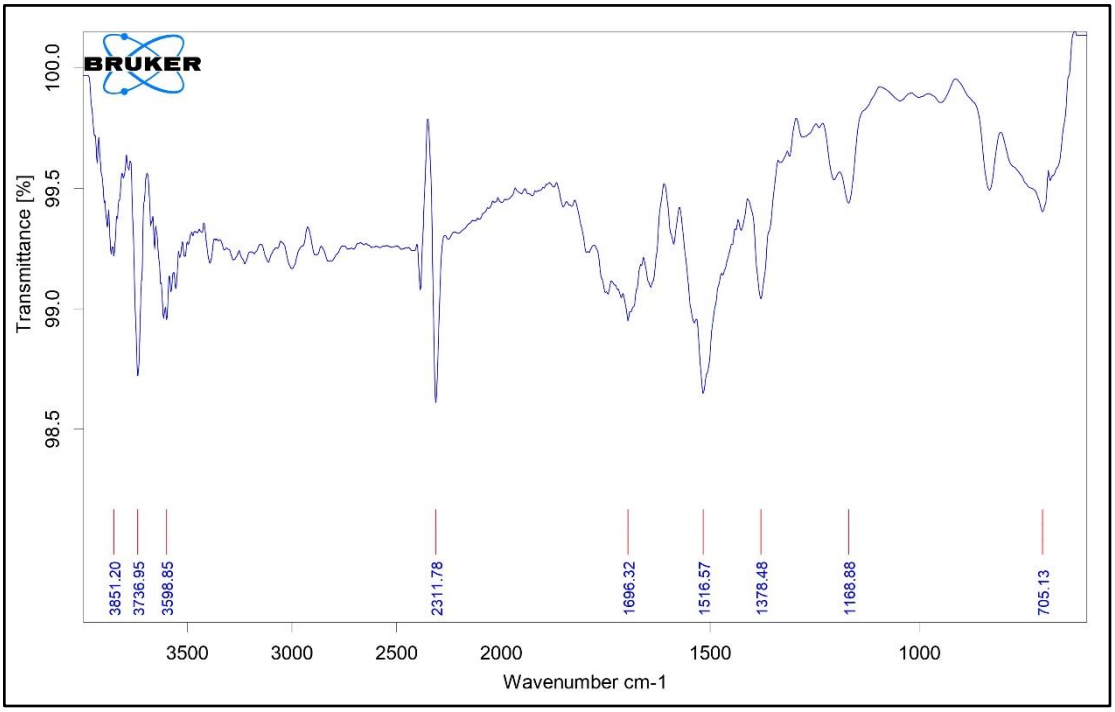

Figure 50: FT-IR spectra of SAI-7.

9) SAI-8:

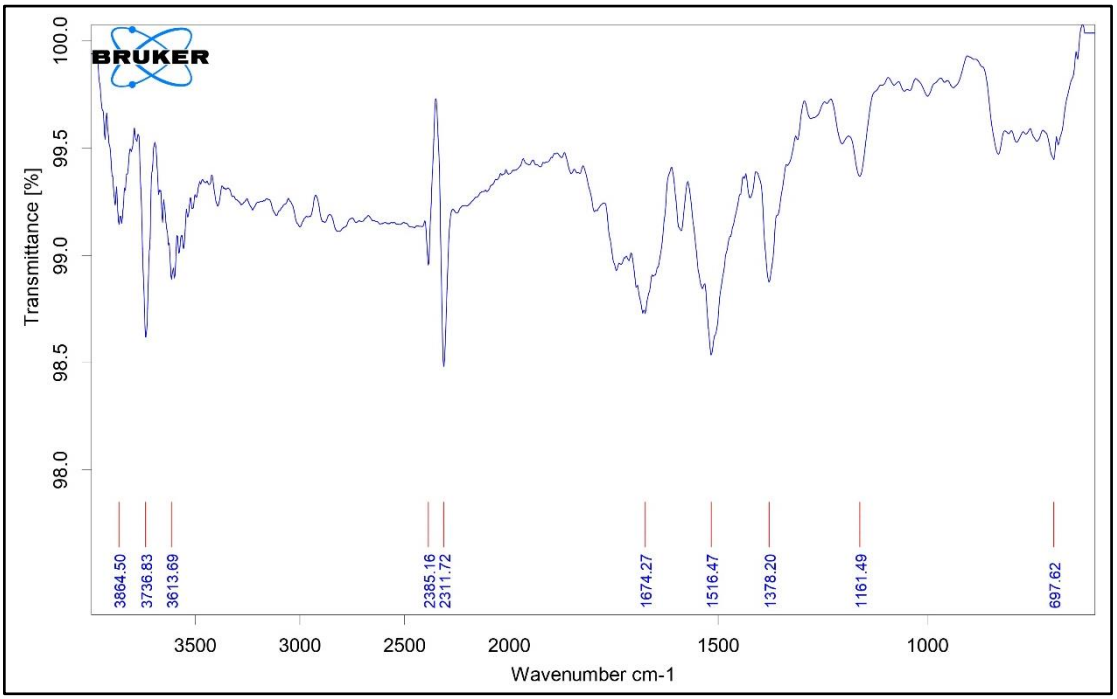

Figure 51: FT-IR spectra of SAI-8.

10) SAI-9:

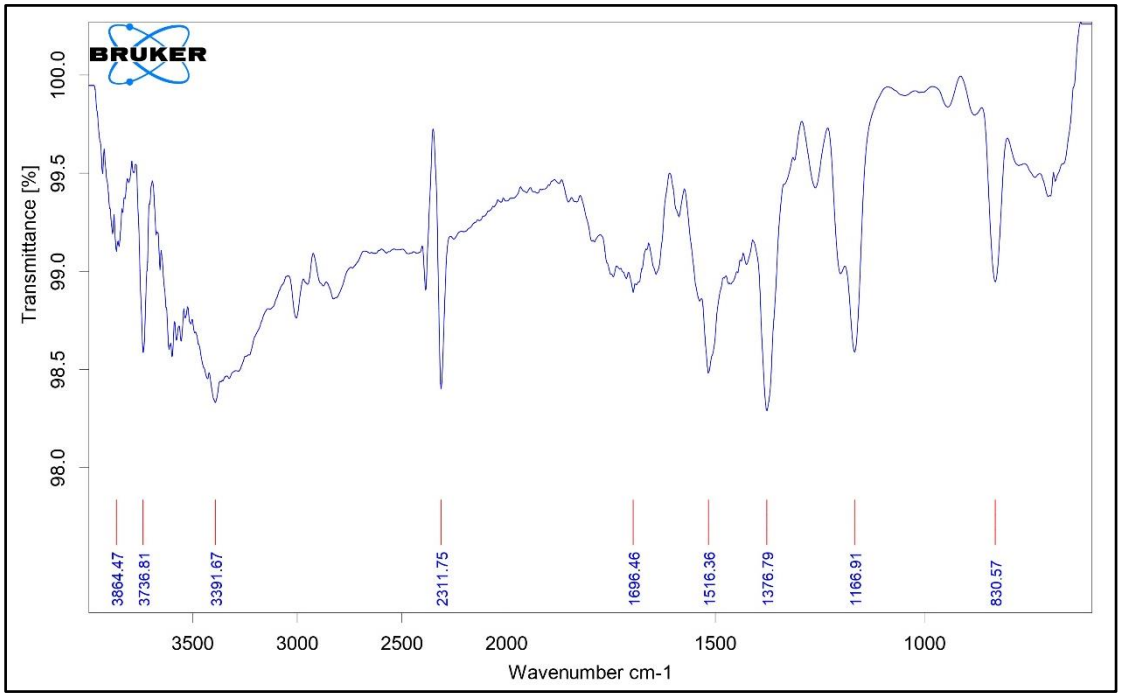

Figure 52: FT-IR spectra of SAI-9.

11) SAI-10:

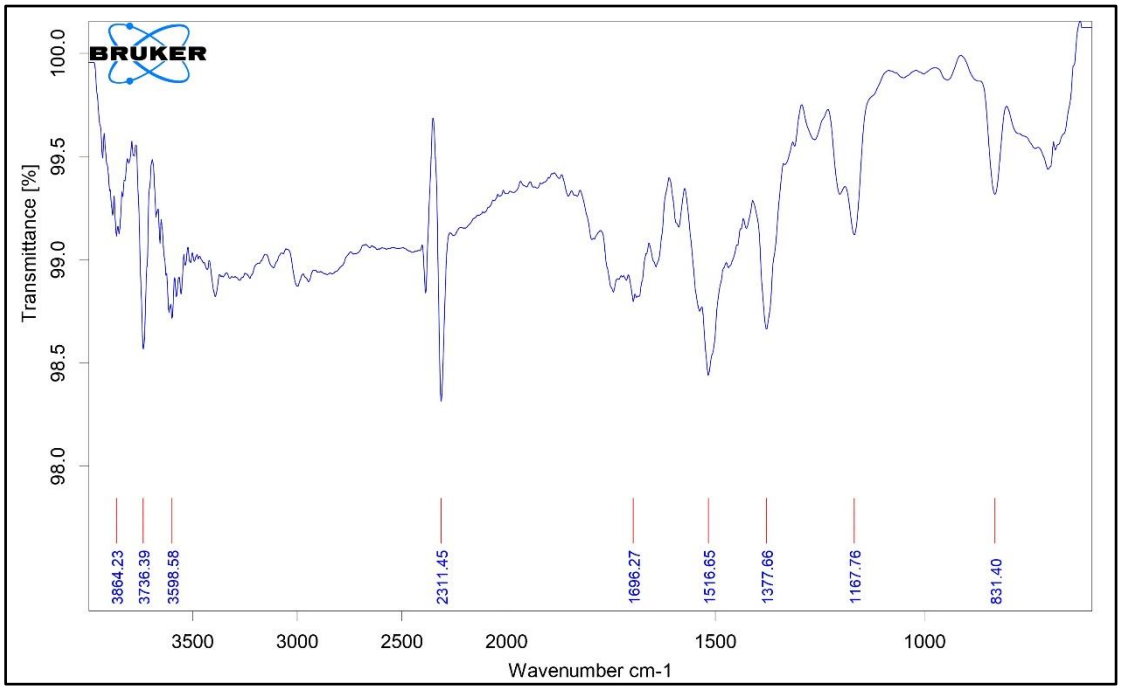

Figure 53: FT-IR spectra of SAI-10.

12) SAI-11:

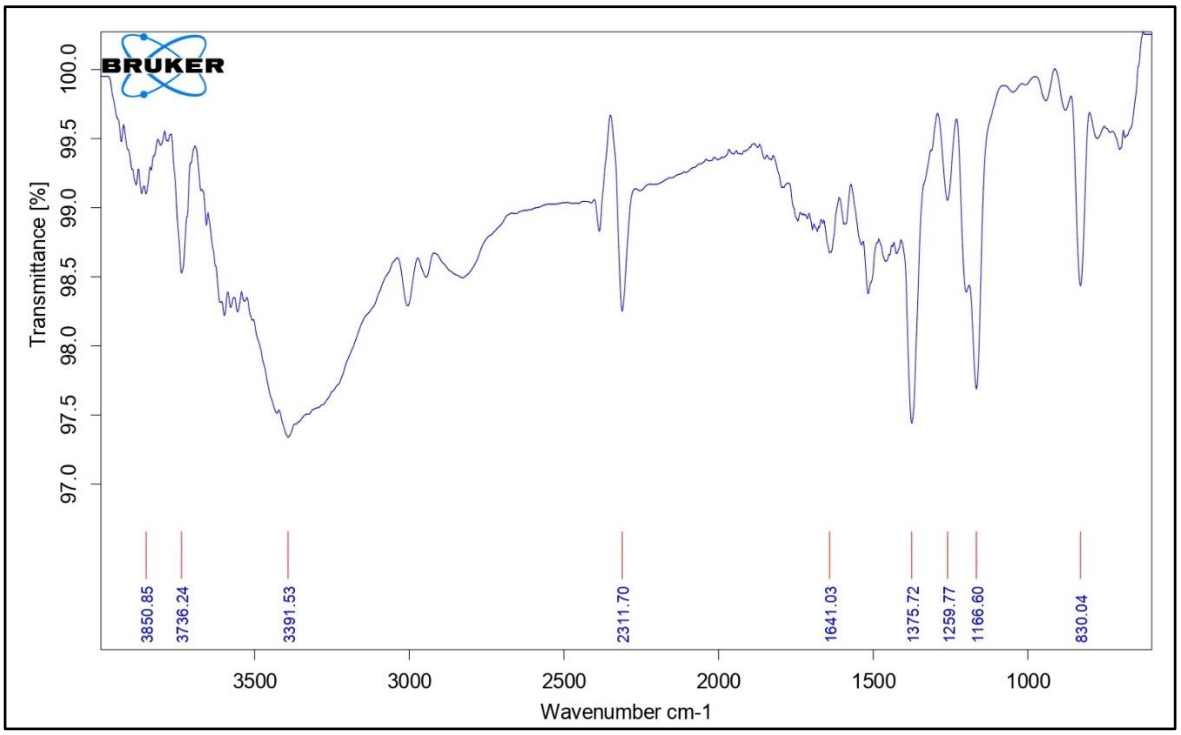

Figure 54: FT-IR spectra of SAI-11.

4.2.4. Mass spectrometry of the most potent compound:

1) SAI-9:

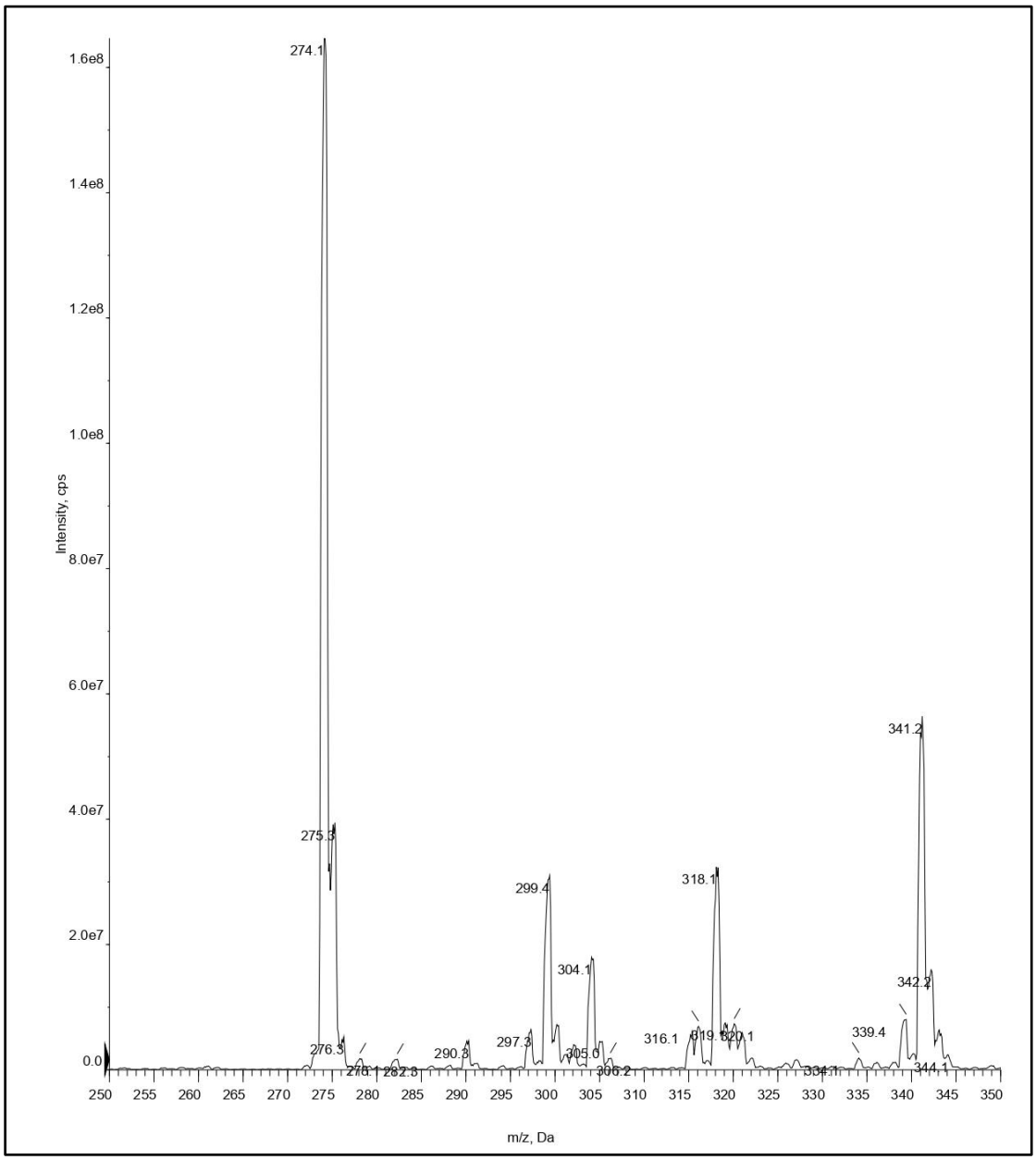

Figure 55: Mass spectra of SAI-9.

4.3. *In vitro* assay of α-glucosidase inhibitory activity:

The inhibitory ability of all the synthesized compounds was assessed against yeast α-glucosidase. Acarbose was used as the control medication in this investigation. The IC_{50} values of compounds are tabulated in **Table 2**. Several of the newly synthesized compounds

exhibited remarkable α-glucosidase inhibitory action. Among the all, **SAI-3**, **SAI-8**, **SAI-9**, and **SAI-10** showed good α- glucosidase inhibitory activity with IC_{50} values of 26.61 µg/ml, 28.67 µg/ml, 9.494 µg/ml, 36.94 µg/ml respectively. **SAI-9** displayed the most potent α-glucosidase inhibitory activity (IC_{50} = 9.494 µg/ml).

Table 2: The α-glucosidase inhibitory activity (IC_{50} values) *in vitro* of **SAI-1 to SAI-11**.

Sl. No.	Compound Name	R	IC_{50} (µg/ml)
1	SAI-1	-	48.66
2	SAI -2	**H**	>250
3	SAI -3	**4-methyl**	26.61
4	SAI -4	**4-chloro**	>250
5	SAI -5	**2,4-dichloro**	>250
6	SAI -6	**4-fluro**	>250
7	SAI -7	**3-chloro**	>250
8	SAI -8	**4-bromo**	28.67
9	SAI -9	**isobutyl**	9.494
10	SAI -10	**isopentyl**	36.94
11	SAI -11	**butyl**	>250
12	Acarbose	-	39.54

4.4. Molecular docking studies:

In the case of **SAI-3**, amino residue R315 interacts with methyl benzyl through alkyl and Pi-alkyl interaction in **Figure 56**. Amino acid F178 is involved in Pi-Pi T-shaped interaction with the 4-isopropyl benzylidene ring of the compound whereas V216 formed an alkyl bridge with the same scaffold. Additionally, amino residue D352 was involved in Pi-anion interaction with 4-isopropyl benzylidene ring and residue Y72 formed a Pi-sigma bond with

the isopropyl terminal. A conventional H-bond is formed between Q279 and the Ketone group of the thiazolidine ring.

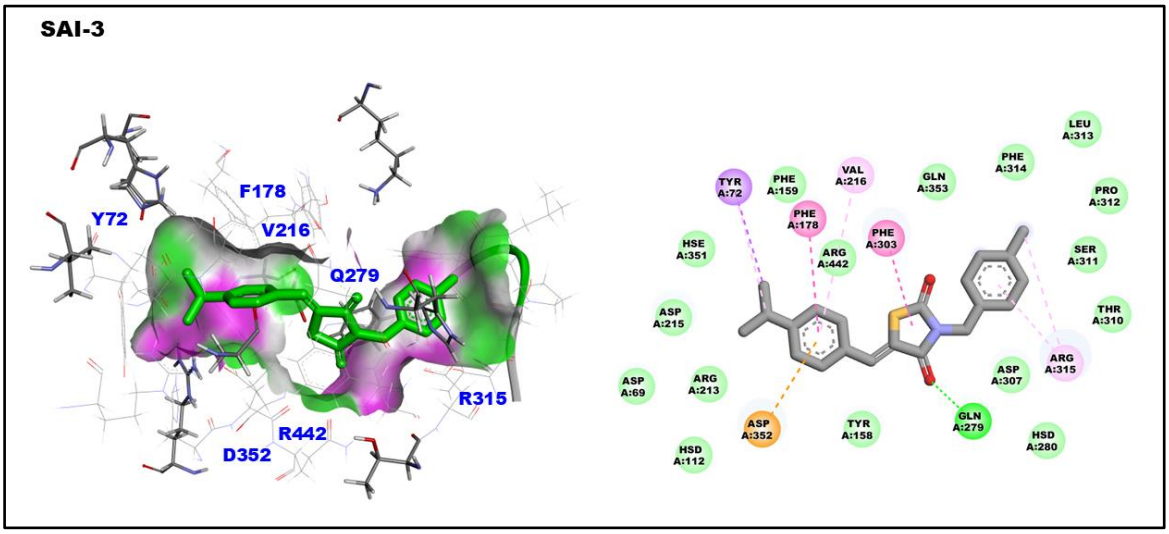

Figure 56: 3D & 2D binding interaction of SAI-3.

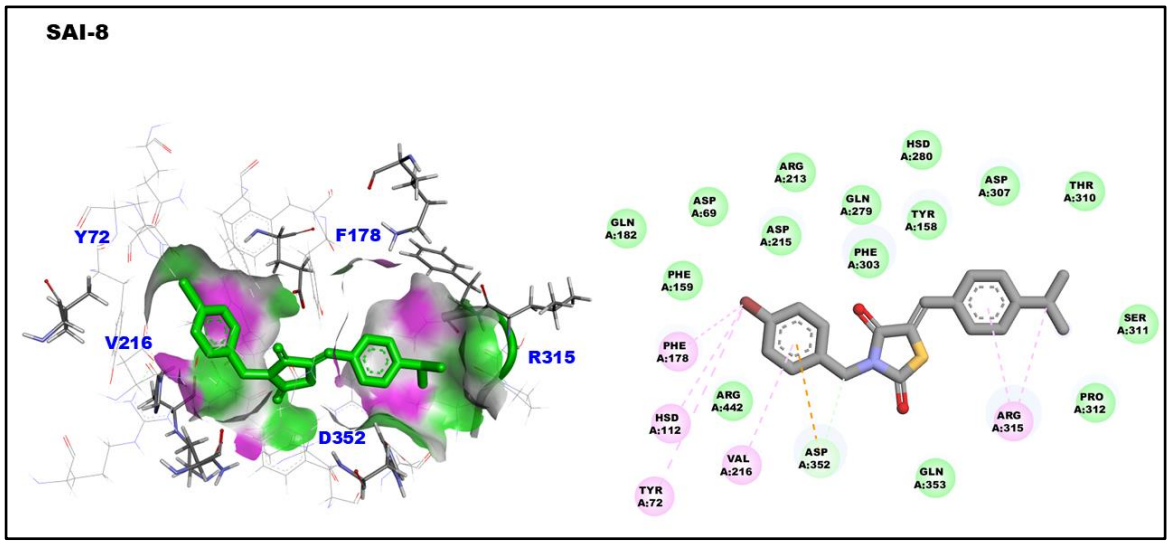

Figure 57: 3D & 2D binding interaction of SAI-8.

Furthermore, the docking interaction of **SAI-8** is nicely represented in **Figure 57.** Amino acids F178, V216, and, Y72 are involved in alkyl and Pi-alkyl bond formation with the bromobenzyl group of **SAI-8**. Whereas, amino residue D352 formed a Pi-anion bridge with the same ring scaffold. On the other hand, amino acid R315 interacts with the 4-isopropyl

benzylidene ring and isopropyl terminal separately through Alkyl and Pi-alkyl bond formation.

In **Figure 58,** amino acids R442 and R213 formed a conventional H bond with both sides' ketone group of thiazolidine of compound **SAI-9.** Whereas amino residue D352 interacts with thiazolidine via Pi-anion interaction and F178 is involved in Pi-sigma bond formation with isobutyl terminal. Additionally, amino acid Y72 interacts with the isobutyl terminal through Pi-alkyl interaction. There are several amino residues (F159, Y158, Q353, H280, and D307, etc.) involved in weak interaction (e.g. van der Waals interaction) with all three compounds (**SAI-3, SAI-8,** and **SAI-9**)

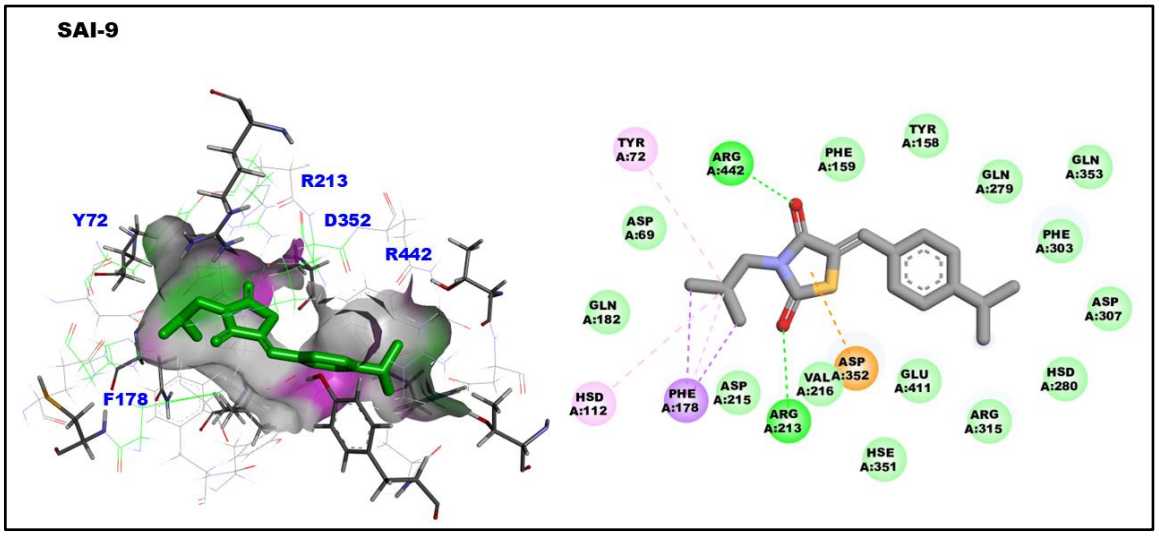

Figure 58: 3D & 2D binding interaction of SAI-9.

4.5. *In silico* ADMET predictions:

The synthesized compounds were studied *in silico* for their drug-like characteristics. The predicted physicochemical properties, pharmacokinetics (absorption, distribution, metabolism, excretion), drug-likeness, and toxicity of the synthesized compounds are presented in **Table 3 (a, b, c)** which shows the excellent bioavailability and drug-like characteristics of all the compounds.

Table 3(a): ADME prognosis using *SwissADME* ((MW = Molecular Weight, TPSA = total polar surface area, Consensus Log P = average of all predicted Log Po/w).

Compound Name	MW (g/mol)	#Heavy atoms	#Rotatable bonds	#H-bond acceptors	#H-bond donors	TPSA	Consensus Log P	Ghose #violations	Veber #violations	Egan #violations	Muegge #violations	Bioavailability Score	Synthetic Accessibility
SAI-1	247.31	17	2	2	1	71.47	2.69	0	0	0	0	0.55	3.03
SAI-2	337.44	24	4	2	0	62.68	4.23	0	0	0	0	0.55	3.52
SAI-3	351.46	25	4	2	0	62.68	4.56	0	0	0	1	0.55	3.63
SAI-4	371.88	25	4	2	0	62.68	4.79	0	0	0	1	0.55	3.5
SAI-5	406.33	26	4	2	0	62.68	5.28	1	0	0	1	0.55	3.56
SAI-6	355.43	25	4	3	0	62.68	4.55	0	0	0	1	0.55	3.5
SAI-7	371.88	25	4	2	0	62.68	4.77	0	0	0	1	0.55	3.52
SAI-8	416.33	25	4	2	0	62.68	4.85	0	0	0	1	0.55	3.53
SAI-9	303.42	21	4	2	0	62.68	3.92	0	0	0	0	0.55	3.51
SAI-10	317.45	22	5	2	0	62.68	4.23	0	0	0	1	0.55	3.56
SAI-11	303.42	21	5	2	0	62.68	4.01	0	0	0	0	0.55	3.45

Table 3(b): Drug-likeness prediction of synthesized compounds from the *SwissADME* server.

Compound Name	GI absorption	BBB permeant	Pgp substrate	CYP1A2 inhibitor	CYP2C19 inhibitor	CYP2C9 inhibitor	CYP2D6 inhibitor	CYP3A4 inhibitor	log Kp (cm/s)
SAI-1	High	Yes	No	Yes	Yes	Yes	No	No	-5.45
SAI-2	High	Yes	No	No	Yes	Yes	No	Yes	-4.81
SAI-3	High	Yes	No	No	Yes	Yes	No	Yes	-4.64
SAI-4	High	Yes	No	No	Yes	Yes	No	Yes	-4.57
SAI-5	High	No	No	No	Yes	Yes	No	Yes	-4.34
SAI-6	High	Yes	No	Yes	Yes	Yes	No	No	-4.85
SAI-7	High	Yes	No	Yes	Yes	Yes	No	Yes	-4.57
SAI-8	High	Yes	No	No	Yes	Yes	No	Yes	-4.8
SAI-9	High	Yes	No	Yes	Yes	Yes	No	No	-4.71
SAI-10	High	Yes	No	Yes	Yes	Yes	No	Yes	-4.55
SAI-11	High	Yes	No	Yes	Yes	Yes	No	No	-4.77

Table 3(c): Toxicology predictions. Information was retrieved via the *Deep-PK* database.

Compound Name	AMES Mutagenesis	Biodegradation	Carcinogenesis	Liver Injury I	Maximum Tolerated Dose	Liver Injury II	hERG Blockers	NR-PPAR-gamma	T. Pyriformis	Rat (Acute)	Rat (Chronic)	Fathead Minnow	Skin Sensitisation
SAI-1	Safe	Safe	Safe	Toxic	1.13	Toxic	Safe	Safe	3.16	2.23	2.05	4.2	Toxic
SAI-2	Safe	Safe	Safe	Toxic	0.9	Toxic	Safe	Safe	2.64	2.11	1.89	4.75	Toxic
SAI-3	Safe	Safe	Safe	Toxic	0.74	Toxic	Toxic	Safe	1.94	2.11	1.97	4.86	Toxic
SAI-4	Safe	Safe	Safe	Toxic	0.81	Toxic	Toxic	Safe	2.15	2.16	1.86	4.93	Toxic
SAI-5	Safe	Safe	Safe	Toxic	0.76	Toxic	Toxic	Safe	1.31	2.2	1.69	5.13	Toxic
SAI-6	Safe	Safe	Safe	Toxic	1.03	Toxic	Toxic	Safe	1.95	2.14	1.93	4.83	Toxic
SAI-7	Safe	Safe	Safe	Toxic	0.84	Toxic	Toxic	Safe	2.22	2.13	1.83	4.91	Toxic
SAI-8	Safe	Safe	Safe	Toxic	0.86	Toxic	Toxic	Safe	2.27	2.23	1.8	4.97	Toxic
SAI-9	Safe	Safe	Safe	Safe	0.82	Toxic	Safe	Safe	3.9	2.11	1.88	4.5	Toxic
SAI-10	Safe	Safe	Safe	Safe	0.76	Toxic	Safe	Safe	3.89	2.07	1.85	4.52	Toxic
SAI-11	Safe	Safe	Safe	Safe	0.79	Toxic	Safe	Safe	3.86	2.12	1.91	4.43	Toxic

CHAPTER: 5

CONCLUSION AND FUTURE PERSPECTIVES

5. Conclusion and future perspectives:

In this research work, we have designed and synthesized, a series of cuminaldehyde-thiazolidinedione hybrids and characterized the compounds through elemental analysis such as TLC, and melting points. All the recrystallized products were characterized and analyzed by FT-IR, ^{1}H NMR, ^{13}C NMR, and mass spectroscopy (summarized in Chapter 4). In addition, we carried out *in vitro* assessments to determine the inhibitory activity of all the synthesised compounds against α-glucosidase. The *in vitro* inhibitory study result revealed that the **SAI-9** with an isobutyl side chain on the 3rd position of the thiazolidinedione ring exhibited the most potent against α-glucosidase enzyme, with an IC_{50} values of 9.494 µg/ml. Similarly, molecular docking investigations of **SAI-9, SAI-3, and SAI-8** with α-glucosidase enzyme also showed better interactions which provided valuable information for the further development of α-glucosidase inhibitors. Furthermore, we have predicted *in silico* pharmacokinetics and toxicity characteristics for all the synthesized compounds and found that the potential compound (**SAI-9**) possessed good bioavailability, drug-like characteristics, and permissible toxicity toward the liver and skin.

During our work, we learned that synthesis with TZD is simple and versatile. The TZD scaffold can be modified by substituting different moieties at the third (-N) and fifth ($-CH_2$) positions to create unique TZD molecules. If we explore the third and fifth positions with different heterocyclic rings and substitute those with various other moieties viz $-OCH_3$, $-NO_2$, etc. may result in large no. of compounds increasing the chemical space TZD derivatives enormously.

In the future, we want to investigate these synthesized molecules' anti-diabetic properties against other targets such as α-amylase, aldose reductase, PTP1b, etc. On the other hand, enzyme kinetics, fluorescence quenching, and circular dichroism spectroscopy need to be studied to understand enzyme inhibition with protein folding changes. Similarly, *in vivo,*

anti-diabetic activity and toxicity will be evaluated and compared to the data derived from the *in silico* ADMET studies indicating drug-likeness nature. These findings will lead to the identification of the most promising compound, with minimal toxicity and maximum potency, for the treatment of type 2 diabetes.

CHAPTER: 6

List of Publications

List of Publications

1. Abhik Paul, **Sai Satyaprakash Mishra**, Avik Maji, Ajeya Samanta, Sourin Nahar, and Tapan Kumar Maity. "Exploring the Therapeutic Potentials of Cuminaldehyde: A Comprehensive Review of Biological Activities, Mechanisms, and Novel Delivery Systems". In **Phytochemistry Reviews**. Springer Science and Business Media LLC (**PHYT-D-24-00060**). 2024. (**IF:7.3**) ……..……...…**1st Revision submitted**
2. **Sai Satyaprakash Mishra**, Ajeya Samanta, Abhik Paul, Avik Maji, and Tapan Kumar Maity. "Unveiling the Anti-cancer Potential of Oxadiazole Derivatives: A Comprehensive Exploration of Structure-Activity Relationships and Chemico-Biological Insights". In **Medicinal Chemistry**. Bentham Science Publishers Ltd (**BMS-MC-2024-HT14-5343-16**). 2024 (**IF: 1.9**) ……..……..……. **Accepted**
3. Ajeya Samanta, Avik Maji, Abhik Paul, **Sai Satyaprakash Mishra**, Sourin Nahar, and Tapan Kumar Maity. "1,3,4-Oxadiazole Based EGFR Inhibitors as Anticancer Therapeutics: SAR Study, Binding Mode of Interaction Analysis, and in silico ADMET predictions" (**EJMCRP-D-24-00290**). 2024 (**IF: 4.0**) …… **Under review**

Book Chapters

1. Therapeutic Advancement of Betulinic Acid in the Treatment of Type 2 Diabetes Mellitus in **Nova Science Publisher** (2023) …… **Under Review**
2. Therapeutic Approaches to Newer Classes of Drugs and Treatments for Type 2 Diabetes Mellitus in **CRC Press** (2024) ……..……...……. **Under Production**
3. Recent Development of Natural Glucokinase Activators for the Treatment of Type 2 Diabetes in **Bentham Science** (2024) ……...……. **Under Review**
4. Potential Application of Secondary Metabolites in Cancer in **Elsevier** (2024) ……. **Proposal accepted**